University of Sheffield

The chemistry & properties of new thermally reversible adhesives

Jonathan Gregg

A thesis submitted in partial fulfilment of the requirements for the degree of Doctor of Philosophy

The University of Sheffield

Faculty of Science

Department of Chemistry

September 2023

Declaration

I, Jonathan Gregg, confirm that the thesis is my own work. I am aware of the University's Guidance on the Use of Unfair Means (www.sheffield.ac.uk/ssid/unfair-means). This work has not been previously been presented for an award at this, or any other, university. All the work is the original work of the author, except where acknowledged.

Signature: 

Jonathan Gregg September 2023

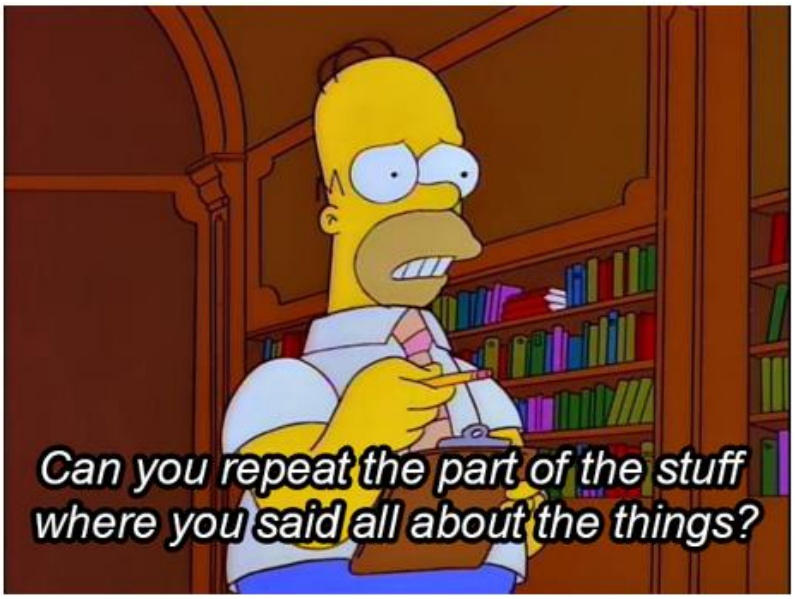
Can you repeat the part of the stuff
where you said all about the things?

Acknowledgements

I will begin with a massive thank you to the Slark Squad. The biggest goes to James; the support you provided throughout my whole project was above and beyond, not to mention the uplad. I owe a lot to the original Slark Boiz Simon and Xander who were there to welcome me into the group and enjoy many jamborees, bonanzas, and galas together. Neil, an acknowledgement with a warning; nobody speaks to me like that. Not gonna lie Jenny, you've been a right laugh to be fair. And what can I say about Tom...? Finally the big man himself, Andrew. I can't imagine having a better supervisor, you helped me achieve my best and I'm really proud of the research we have done together.

Probably more of a negative influence but worthy of an acknowledgement nonetheless, my two favourite people to go goblin-mode with, Josh and Tom. Reuben, I really admire your character. Alongside me the whole time was my housemate/colleague/friend Millie. Seeing all your hard work inspired me and I have no doubt you will go far in the future.

Thanks to everyone down at Scott-Bader who assisted my project and made me feel welcome on my placement, in particular Steven, Dean, and Stefan. And the extra funding was nice. Big appreciation to the UKRI for their funding too.

Finally a shoutout to my parents for guiding me my whole life up until this point. Seems to have worked so far.

Contents

List of figures

List of schemes

List of tables

List of abbreviations

1-C	One-component
2-C	Two-component
ABS	Acrylonitrile butadiene styrene
AROP	Anionic ring-opening polymerisation
BFCE	Bifunctional chain extender
BHMF	Bishydroxymethylfuran
BMI	*N,N'*-(4,4'-methylene diphenyl) bismaleimide
CAN	Covalent adaptable network
CHDM	Cyclohexanedimethanol
COSY	Homonuclear correlation spectroscopy
CROP	Cationic ring-opening polymerisation
DA	Diels-Alder
DA1	Diels-Alder network
DEG	Diethylene glycol
DEPT	Distortionless enhancement by polarization transfer
$Đ_M$	Dispersity
DMSO	Dimethyl sulfoxide
DP	Degree of polymerisation
DSC	Differential scanning calorimetry
ETA	Ethanolamine
F1	Trifurfuryl 1,3,5-benzenetricarboxylate
FTIR	Fourier-transform infrared
G	Gibbs free energy
H	Enthalpy
HEMI	*N*-(2-hydroxyethyl)maleimide
HMDIT	Hexamethylene diisocyanate trimer
HMTF	Trifuran hexamethylene trimer carbamate
HOMO	Highest occupied molecular orbital
IPDF	Difuran isophorone carbamate
IPDI	Isophorone diisocyanate
LUMO	Lowest unoccupied molecular orbital

m/z	Mass-to-charge ratio
M_0	Molecular weight of the monomer unit
M1	Bismaleimidocaproyl C_{36} dimerate
MALDI-TOF	Matrix-assisted laser desorption/ionisation-time of flight
MDF	Difuran methylene diphenyl carbamate
MDI	4,4'-methylenediphenyl diisocyanate
MMA	Methyl methacrylate adhesive
M_n	Number average molecular weight
M_w	Weight average molecular weight
N	Number of monomers at the time of measurement
N_0	Number of monomers at the start of the reaction
NCO	Isocyanate
NIPU	Non-isocyanate polyurethanes
NMR	Nuclear magnetic resonance
p	Extent of the reaction
PBC	Poly(butylene citraconate)
PBM	Poly(butylene maleate)
PET	Poly(ethylene terephthalate)
PG	1,2-propylene glycol
PPC	Poly(propylene citraconate)
PPF	Poly(propylene fumarate)
PPFPS	Poly(propylene fumarate-*co*-propylene succinate)
PPI	Poly(propylene itaconate)
ppm	Parts per million
PPM	Poly(propylene maleate)
PU	Polyurethane
PVC	Poly(vinyl chloride)
rDA	retro Diels-Alder
ROCOP	Ring-opening copolymerisation
ROMP	Ring-opening metathesis polymerisation
ROP	Ring-opening polymerisation
RROP	Radical ring-opening polymerisation
S	Entropy
SEC	Size exclusion chromatography

TBD	1,5,7-triazabicyclo[4.4.0]dec-5-ene
$T_{deg5\%}$	5% mass degradation temperature
TFCE	Trifunctional chain extender
T_g	Glass transition temperature
TGA	Thermogravimetric analysis
T_m	Crystallinity melting temperature
T_{rDA}	Retro Diels-Alder temperature
X_n	Degree of polymerisation
ΔH_{rDA}	Retro Diels-Alder enthalpy change

Abstract

Most adhesives today are irreversibly cross-linked, which presents many difficulties when it comes to recycling composite materials at their end-of-life. This thesis aims to tackle such problems by suggesting an alternative; covalent adaptable networks which can debond on demand, allowing for easy separation of materials.

In **Chapter 2**, a model system containing maleimide and furan Diels-Alder (DA) adducts was used to test the viability using such materials in adhesive applications. High bond strength was achieved, and the bond could be healed using the same material with little loss of bond strength. Then, in **Chapter 3**, chain extenders containing DA adducts were synthesised, for the novel application of cross-linking moisture-curing polyurethanes to add reversibility to a material that would otherwise become a thermoset.

In **Chapter 4**, unsaturated polyesters (UPEs) were considered for use as a thermally reversible adhesive, and six materials from two polyesters and three cross-linkers were synthesised and examined. Diels-Alder bonds between the unsaturation in the polyester and the furan cross-linkers were successfully formed to generate a network. One material displayed good tensile strength, and others were improved with the addition of a comonomer.

During this testing it was discovered that networks made with poly(propylene maleate) were more thermally stable than those made with poly(propylene fumarate), however synthesising PPM is difficult as the high temperatures involved in the polyesterification causes isomerisation to fumarate. **Chapter 5** shows that this could be limited by the glycol choice, with rigid or long chain primary diols retaining the most maleate content.

Finally, in **Chapter 6**, UPEs were functionalised with furan groups *via* the thiol-ene Michael addition onto the alkene. This gave the polyester the ability to form DA linkages with unreacted sites of unsaturation on other UPE chains in either a one-component or two-component DA system.

1 Introduction and aims

Arguably the most pressing issue in the world today is the negative impact the human race is having on the environment. Since their invention, plastics have seen widespread use as a material for many applications, from food packaging to clothing. In its current state, the lifecycle of plastic is far from circular. It is so cheap and readily available, that for the end user it is much more convenient to discard the product after a single life cycle rather than reusing or recycling it. This issue is so prevalent in modern culture that "single-use" was named 2018 word of the year by Collins Dictionary.[1] Global plastics production has doubled in the past 20 years, reaching 460 million tonnes (Mt) in 2019, and plastic waste has more than doubled at 353 Mt.[2] Almost two thirds of this waste comes from applications with lifespans of less than 5 years. Statistics after this date are skewed, as lockdowns and low economic activity reduced plastic use. However, single-use plastic waste still increased as a result of widespread protective personal equipment use.

Although accounting for 25.8 Mt of waste in Europe annually, the potential for recycling plastic remains largely unexploited; less than 30% of this waste is collected for recycling.[3] The UK Plastics Pact is a collaborative initiative striving towards a circular economy for plastics, with a key target that all plastic packaging will be reusable, recyclable or compostable by 2025. The 68 members signed up are responsible for 80% of plastic packaging sold in UK supermarkets. Since 2018, there has been an 84% reduction in single-use plastics.[4] Reuse strategies have been shown to be useful, for example, after the introduction of the 5p plastic bag charge in 2015, plastic bag sales dropped by 86%,[5] contributing to a 50% reduction in plastic bag marine litter.[6] It is quite clear that recycling benefits the planet in a multitude of ways, reducing the demand for raw materials and energy for the production of new items, reducing waste, and protecting wildlife.

One difficulty in recycling end-of-life plastic is that our systems are currently only equipped to handle monomaterials and not composites. For example, multi-layered materials account for around 17% of all world film production.[7] Multi-layered films are much more attractive than single-layered films due

to their ability to combine desired properties of different materials to create a tailor-made property profile. Specific properties can include oxygen or moisture barriers, high mechanical strength and good sealability, making them prime candidates for use in food packaging. Moreover, much less material is required to make a multi-layered film than a single-layered film that performs the same function. It is often the case that the polymers in each layer are immiscible and unless they are separated, they are unable to be recycled since different polymers have different properties and processing characteristics. As a result, tonnes of non-biodegradable material is currently being sent to landfill or released into the atmosphere through incineration.[8]

Disposal is also an issue for larger scale items that are in longer term use. For example, wind turbines from the 1990s are reaching the end of their 25-year working lives, and the problems with disposing them in an environmentally friendly way are now being realised. The carbon fibre or glass fibre composite blades are built to withstand hurricane-force winds, rendering them extremely difficult to recycle as they cannot be crushed easily and nothing short of a diamond-encrusted industrial saw is suitable to cut a turbine blade into small enough pieces to be hauled away. The current "solution" is to bury them at landfill sites where they will be interred in stacks that reach 30 feet under (**Figure 1.1**). Evidently, a much more sustainable solution must be reached.

Figure 1.1 – A “wind turbine graveyard” in Wyoming, the final resting place for 1,000 blades. Photo from BBC News.

One approach is to bond the individual components with an adhesive that enables easy separation at the end of the product’s lifetime without compromising performance in use. Previously, the use of permanently cured adhesives made the separation of substrates unfeasible. However, there is now a growing interest towards thermally reversible adhesives that provide high performance during use, but experience a significant loss in modulus at high temperatures to facilitate separation of components. Furthermore, an adhesive that regains its structural properties on cooling would allow it to be used elsewhere, eliminating the need for raw materials to create fresh adhesive thus providing a circular life cycle for the adhesive and well as the components it’s applied to. These two ideas form the key aims of my research.

To develop an adhesive that:
a) Can debond in response to external stimuli such as heat
b) Regenerate its bond strength after multiple heat cycles

1.1 Thermoplastics and thermosets

Polymers can be classified into two groups by how they are processed, as a thermoplastic or a thermoset.

Thermoplastics achieve their shape by a physical process brought about by cooling or evaporation of solvent. They comprise high molecular weight polymer chains, tangled together and attracted to one another by non-covalent intermolecular forces, such as van der Waals forces and hydrogen bonds. The chains are susceptible to solvents and the weak forces can be easily overcome by heating. Above their melting temperature, the chains untangle, allowing the material to deform reversibly and macroscopically to flow like a viscoelastic liquid. In this state, they can be processed using conventional techniques, such as injection moulding and extrusion. In principle, they can be melted and recast in this way almost indefinitely, making them mechanically recyclable and ideal for uses including drinks bottles and sports equipment. A downside of this is that thermoplastics have inferior mechanical properties and solvent or temperature resistance in comparison to thermosetting polymers and thus, are unsuitable for intensive uses that require durability.

Thermosets avoid these limitations by cross-linking the polymer chains to form a permanent three-dimensional network. These links make them stronger than the chemically independent polymer chains of thermoplastics, with the chains chemically linked together by strong covalent bonds. These cross-links make the chains insoluble and inhibit chain mobility, enabling thermosets to be useful for applications requiring solvent resistance and high mechanical strength, *e.g.* structural adhesives. The mechanical strength, resistance to heat degradation & chemical attack all improve with cross-link density.[9] The thermoset will be applied as a viscous liquid prepolymer, that will irreversibly harden during the curing process as strong covalent bonds are made between the individual chains. The cross-linking is irreversible, so the thermoset must be cured in the desired shape and location and cannot be recycled for the same purpose after use. The polymer chains can be linked in various ways. For example, sites of unsaturation along the backbone can be linked by copolymerisation with

unsaturated monomer diluents, as seen in polyesters.[10] Epoxy-functional resins can ring-open and polymerise in the presence of a catalyst and heat, with highly functionalised resins resulting in highly branched cross-linked structures.[11] Polyurethanes are made from the nucleophilic addition of polyisocyanates and polyols, with the degree of cross-linking determined by the functionality and ratio of the reagents.[12] Thermosets are commonly seen in electrical insulators,[13] coatings[14] and sealants.[15]

1.2 Polyurethanes

As the name suggests, the urethane group is the major repeating unit in polyurethane, but the chain often contains a number of other groups, such as ethers, esters and urea. First invented by Otto Bayer in 1937,[16] they were initially developed as an alternative for rubber during World War II, but the versatility of these materials means they are still one of the most common and researched materials in the world. The variety of sources from which polyurethanes can be synthesised, and the intimate structure-property relationship, means that the final material can be fine-tuned for very specific and contrasting applications. Because the properties of different polyurethanes can be so varied, they are often separated into several different classes, some major ones being rigid PU foams, flexible PU foams, and thermoplastic PUs.[17]

1.2.1 Synthesis

The urethane group is generated *via* a step growth mechanism between isocyanate and hydroxyl groups. (**Scheme 1.1**).

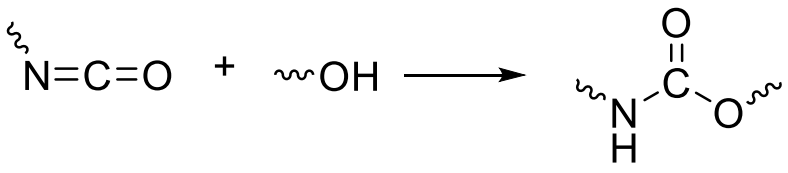

Scheme 1.1 - Formation of a urethane linkage from a hydroxyl group and an isocyanate.

In a typical polymerisation, long chain polyols (normally a polyester or polyether diol) undergo addition with a bifunctional isocyanate linking monomer, such as 4,4'-methylenediphenyl diisocyanate

(MDI), followed by the addition of a small diol chain extender. This results in an alternating block copolymer of two incompatible segments: the long elastomeric soft segment comprising the long chain diol, and the hard segment comprising the small isocyanate linker and chain extender (**Figure 1.2**). Due to the highly reactive nature of the isocyanate, this occurs with relative ease, but care needs to be taken to avoid unwanted side-reactions.

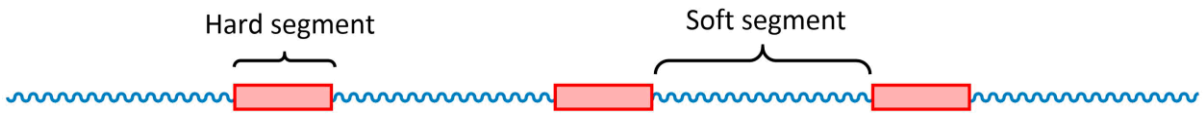

Figure 1.2 - A simple diagram of a polyurethane comprising hard and soft segments.

The polymerisation can be done in two ways; the prepolymer (two-pot) method and the one-pot method. The prepolymer method has two steps; the first stage of the addition involves excess diisocyanate being reacted with the long chain diol, to form telechelic urethane prepolymers terminated with reactive NCO groups. In the second stage, a chain extender, such as ethylene glycol, diethylene glycol, 1,4-butanediol or a diamine, reacts with the reactive termini of the prepolymer and remaining isocyanate monomer. If using stoichiometrically equivalent reactants, the final product will be a high molecular weight alternating copolymer of the two hard and soft segments seen previously. The prepolymer method is typically used for the manufacture of polyurethane elastomers, coatings, sealants, and flexible foams.

The one-pot method involves very efficient mixing of all the raw materials in “one-pot.” For simplicity, a premix of components that do not react with each other is made, containing polyol, chain extender, and other desired components such as blowing agents, catalysts, flame-retardants and fillers. This is then mixed with the isocyanate component to create a rigid polyurethane product that is a consequence of the very efficient contact between the isocyanate and polyolic components. The one-pot process is the most direct and economical method, as the time and effort involved in creating the

prepolymer is eliminated. However, the prepolymer method allows for a much more controlled polymerisation in terms of polymeric structure and physical properties.

Side reactions occur when moisture is present in the system (**Figure 1.3a**). The NCO group will react readily with water to give an amine and carbon dioxide through a carbamic acid intermediate, and this competes with the desired reaction between the isocyanate and polyol.[18,19] Nevertheless, this alternative reaction does have its uses; it is used extensively in moisture-curing systems.[20] NCO-terminated prepolymers can react with atmospheric water to give the amine, which can then react with another NCO-terminated prepolymer and form a urea link (**Figure 1.3b**).

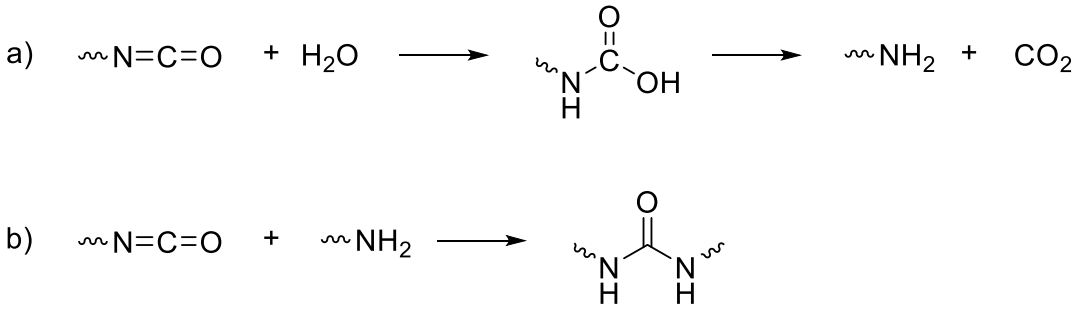

Figure 1.3 - a) The competing side reaction involving water to generate an amine. b) The formation of a urea link using an isocyanate and amine.

The final polymer is influenced by the choice and stoichiometry of starting materials, which will affect the ratio of hard segment to soft segment in the bulk composition. Using a large amount of long chain polyols will result in large proportion of soft segment to obtain an elastomeric polymer. It follows that using shorter chain polyols and chain extenders, will increase the amount of hard segment, resulting in a rigid or glassy polymer. A foam can be generated by utilising reactions that evolve gas, such as adding water to form urea linkages that release CO_2.

1.2.2 Hard and soft segments

Phase separation is commonplace in polyurethane elastomers composed of multi-block copolymers $(H\text{-}E)_n$. The soft phase (E) is typically made up of polymer segments with a sub-ambient glass transition

temperature. They are amorphous (or semi-crystalline) and can be fluid at room temperature, providing flexibility to the system. The hard phase (H) typically comprise short polymer segments, with more rigid functionalities like urethanes and phenyl rings. It is a crystalline with a high melting point and provides the system its strength by preventing the soft phase from flowing under stress.

The separation is thermodynamically driven by the difference in polarity between the polar hard segments and non-polar soft segments. Despite the dramatically increased entropy upon mixing two segments together, the absence of favourable enthalpic interactions between the two unlike segments typically results in mutual immiscibility.[21] At high temperatures, the two segments will be miscible if the free energy of mixing is negative ($\Delta_{mix}G < 0$), where $\Delta_{mix}G = \Delta_{mix}H - T\Delta_{mix}S$. As the polymer cools, the hard segments associate to form hydrogen bonded clusters, these are immiscible with the soft segment and will trigger spinodal decomposition leading to phase separation. The degree of phase mixing can be controlled by the compatibility between the segments.

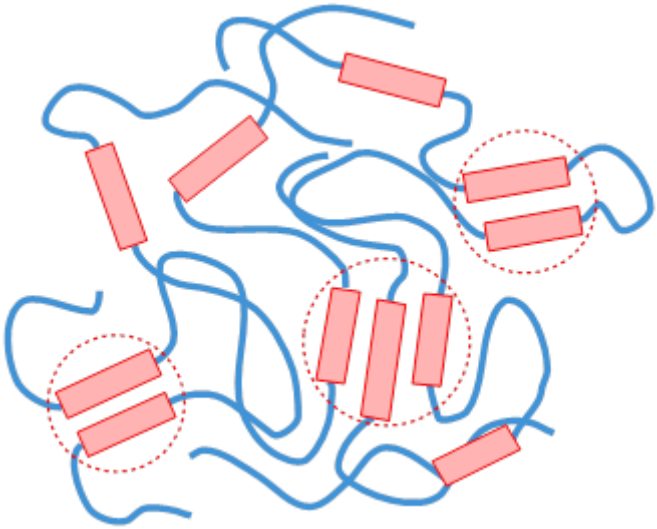

Figure 1.4 - Morphology of a thermoplastic elastomer illustrating how the hard segments (red blocks) of independent chains arrange to from regions of hard phase.

At room temperature, the hard segments act as physical cross-links by forming regions of crystallinity interspersed within the amorphous regions of the soft segment (**Figure 1.4**). A single chain can often traverse several hard regions. Under stress, the chains can reorient and extend in the direction of the

force but will be prevented from stretching too far by the unaffected hard segment. When the hard regions are melted or dissolved in solvent, the polymer can flow, classifying it as a thermoplastic.

The individual glass transition temperature (T_g) and/or crystallinity melting point (T_m) of each phase is often retained despite being combined. This gives rise to three distinct regions on a chart of modulus as a function of temperature (**Figure 1.5**), namely the glassy plateau, the rubbery plateau and the viscous fluid.

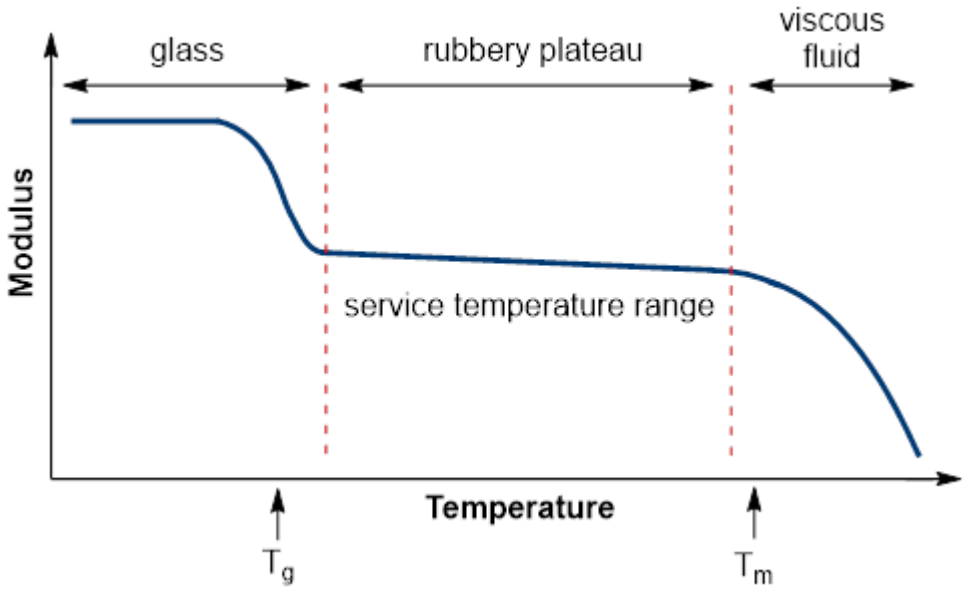

Figure 1.5 - Graph showing how the modulus of a typical thermoplastic changes with temperature.

Below the T_g of the soft segment, the material is brittle. Above the T_g/T_m of the hard segment, both phases are fluid. In between these two transition temperatures is what is known as the service temperature range, sometimes described as the rubbery plateau owing to the relatively constant modulus. In this range, the material exhibits the desired properties of the thermoplastic elastomer. Most polymers are required to function over a large temperature range, such as in automobile engine parts, so it is vital to have a large service temperature range that encompasses the whole operating temperature of the component.

1.2.3 Applications

The huge variety of starting materials available means that polyurethanes can be made with a multitude of different properties, which is the reason polyurethanes are ubiquitous in all sectors of manufacturing today. For example in a car, the firm, yet low-density foam in the seating is made of polyurethanes. Similarly, the sealant and adhesives used to bond core structures, such as bumpers, lights and glass windscreens are also polyurethanes. The insulation for refrigerated vehicles transporting food is a polyurethane rigid foam. In fact, a typical 1000 kg car contains 100 kg of plastics, of which 15 kg are polyurethanes.[22] The rapid growth of the automotive industry impelled the demand for polyurethane adhesives and this is likely to continue in the coming years.

Developed between 1955 and 1960, polyurethanes were the first thermoplastic elastomers to be commercialised and now the global polyurethane adhesives market is valued at $9.6 billion and predicted to expand at a compound annual growth rate of 6.1% from 2022-2032. This formed around 15% of the global adhesives and sealants market worth $62.3 billion in 2021.[23]

1.3 Polyesters

Polyesters are another widely used class of polymers today, beginning with the work of Carothers in the 1930s. Discouraged by their low melting point (<100 °C) and susceptibility to hydrolysis, Carothers never completed his work on polyesters, focusing instead on polyamides, such as nylon. It was not until the 1940s, when British scientists Whinfield and Dickson continued the work and patented poly(ethylene terephthalate) (PET) that polyesters became commercially viable.[24] In 1950, the first commercial articles began to appear under the brand name Terylene®; a derivation of terephthalic acid and ethylene glycol. Sales were phenomenal due to its silky appearance, whilst being much stronger and having good crease, shrink and stretch resistance, making it excellent for use in textiles. Whinfield carried out his own durability test on a polyester shirt by wearing it daily on two trips around the world and washing it 750 times before it needed repair.[25] Polyesters are now one of the most economically important classes of polymers, with PET being the most common. Its biggest application

is in fibres but its high strength and chemical resistance means it's widely used to make plastic bottles. Polyesters, such as PET, are classified as thermoplastic resins as they consist of polymer chains containing no chemical cross-links that makes them easy to recycle. Mechanical recycling is the simplest and most cost-efficient method currently, which consists of obtaining clean PET flakes that are used directly or mixed with virgin polymer to obtain other end products. Chemical recycling is the other process, wherein PET undergoes glycolysis, methanolysis or hydrolysis, with the aim of depolymerising PET back into base chemicals and chemical feedstocks, supplying virgin-quality raw materials back into the supply chain.[26]

1.3.1 Synthesis

Step growth

The most facile and common method of synthesising polyesters is through a step growth polymerisation, typically between a dicarboxylic acid and a diol (or their functional derivatives). The reaction between the carboxylic acid and alcohol generates the ester linkage, whilst liberating water (**Scheme 1.2**). Polycondensations often require high temperatures of over 200 °C and increased pressure.[27,28]

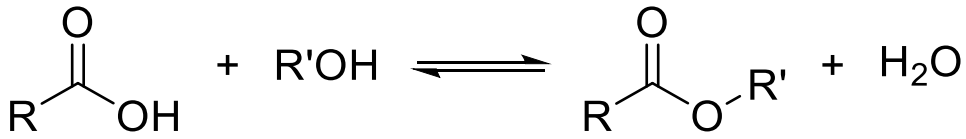

Scheme 1.2 - Formation of an ester linkage from a carboxyl group and an alcohol.

In a general step-growth polymerisation, the monomers must have at least two functional groups capable of reacting with each other. In each reaction, two monomers react to form a dimer. The dimer then reacts with another monomer to form a trimer. Eventually longer chains, or oligomers, react with each other, leading to a large increase in molecular weight (**Figure 1.6a**). This is why the chain growth is exponential, and towards the end of the reaction there is a rapid increase in molecular weight

(**Figure 1.6b**). The process continues until all of the monomers have reacted and a polymer chain has been formed. The extent of the reaction, p, can be calculated by the equation:

$$p = \frac{N_0 - N}{N_0}$$

Where N_0 is the number of monomers at the start of the reaction and N is the number of monomers at the time of measurement. The Carothers equation can then be used to calculate the degree of polymerisation, $\bar{X}_n$. For the reaction of two monomers in equimolar quantities:

$$X_n = \frac{1}{1-p} \qquad \text{The Carothers equation}$$

This equation highlights how important the extent of the reaction is to the degree of polymerisaiton. A *p* of 98% would result in $\bar{X}_n$ = 50, and a small increase of *p* to 99% doubles this to $\bar{X}_n$ = 100. Using the molecular weight of the monomer unit, M_0, the number average molecular weight, M_n, and weight average molecular weight, M_w, can be found:

$$M_n = M_0 \frac{1}{1-p}$$

$$M_w = M_0 \frac{1+p}{1-p}$$

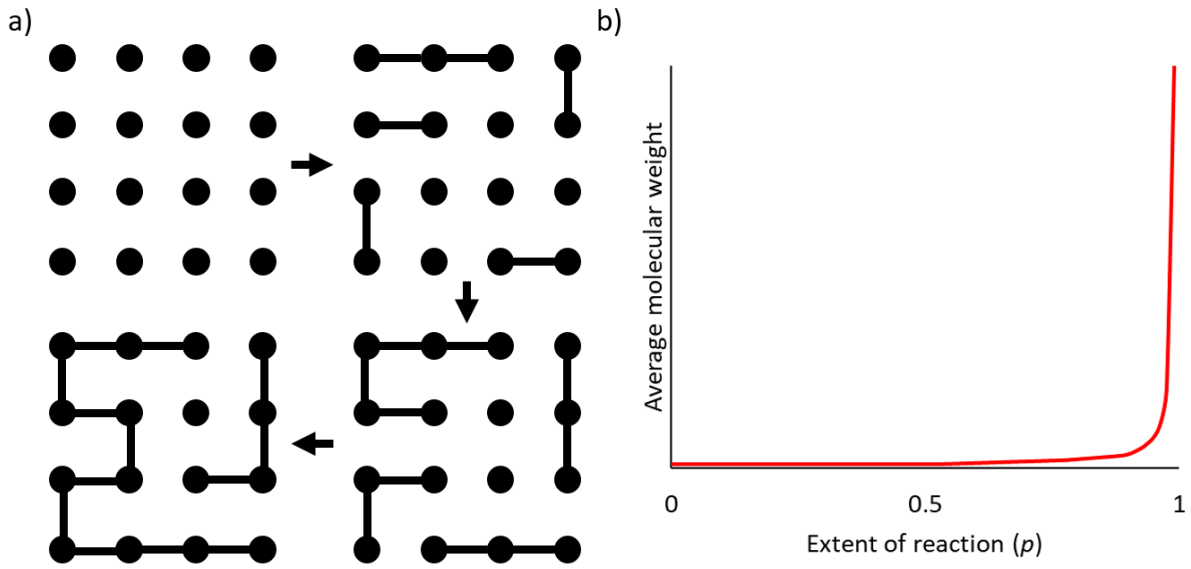

Figure 1.6 - Formation of dimers, then trimers and finally oligomers that causes a rapid increase in molecular weight towards the end of the reaction.

The physical properties of the polymer are determined by the molecular weight and chemical composition. A high molecular weight is essential for the polymer to have sufficient thermal and mechanical properties to be useful. For the synthesis of a high molecular weight linear polymer to be successful, the following criteria must be met:

- High reaction conversions (>99.9%) as predicted by the Carothers equation,
- Monomer functionality of 2,
- Functional group stoichiometry of 1,
- Absence of side reaction that remove monomer functionality,
- Efficient removal of condensates,
- Accessibility of mutually reactive groups.[29]

Ring-opening polymerisation

Polyesters can also be synthesised *via* ring-opening polymerisation (ROP), or copolymerisation (ROCOP). This technique is much more involved, and it is yet to be scaled up appropriately to be

industrially viable. Despite this, it does have its benefits. Higher polymer molecular weights can be more easily achieved (100,000–300,000 g mol^{-1}), and no by-product formation. ROP is a type of chain-growth polymerisation, where one polymer chain has a reactive centre on its terminus that reacts with a cyclic monomer, that ring-opens to form a longer polymer chain (**Scheme 1.3**).

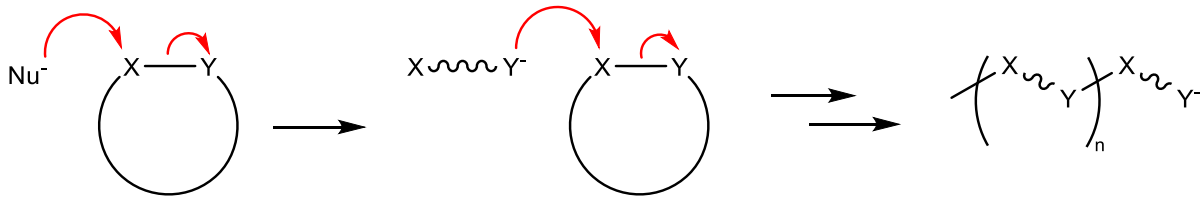

Scheme 1.3 - An example of ROP, initiated by a nucleophile.

The driving force behind the reaction is steric repulsions and ring strain.[30] The loss of enthalpy associated with the loss of ring strain counteracts the loss of entropy occurring as a consequence of the polymerisation, which is why strain-free 5-membered rings generally do not polymerise. The cyclic monomers typically contain alkenes or heteroatoms in the ring. The ring-opening can proceed through a number of mechanisms; radical ROP (RROP),[31] cationic ROP (CROP),[32] anionic ROP (AROP),[33] and ring-opening metathesis polymerisation (ROMP).[34]

1.4 Covalent adaptable networks

Covalent adaptable networks (CANs) potentially offer the performance advantages of thermosets whilst maintaining the reprocessing, recycling, self-healing, and reshaping functions of thermoplastics. They are chemical networks with dynamic covalent bonds that allow the network to change its topology as a response to external stimuli.[35] There has been ample research into preparing CANs using suitable groups that respond to various stimuli such as temperature (*e.g.* Diels-Alder adducts,[36] alkoxyamines,[37] urethanes/urea,[38,39] triazolinediones,[40] 1,2,3-triazoliums,[41] and aniliniums);[42] light (*e.g.* coumarin dimers,[43,44] trithiocarbonates,[45] disulfides,[46] and diarylbibenzofuranone derivatives)[47] and chemicals (*e.g.* boronic esters,[48,49] disulfides,[50,51] acylhydrazones,[52,53] imines,[51,54] and acetals).[55] After

exposure to the external stimulus, the dynamic nature of the covalent bonds make the CAN available for reprocessing.

The exchange mechanism can be associative or dissociative (**Figure 1.7**). In an associative mechanism, a new bond is made to the dynamic covalent cross-link before the original cross-link is broken, enabling covalent bond rearrangement with no significant decrease in cross-link density, thus preventing depolymerisation. This is characterised physically by a gradual decrease in viscosity and retention of insolubility during the bond exchange mechanism.

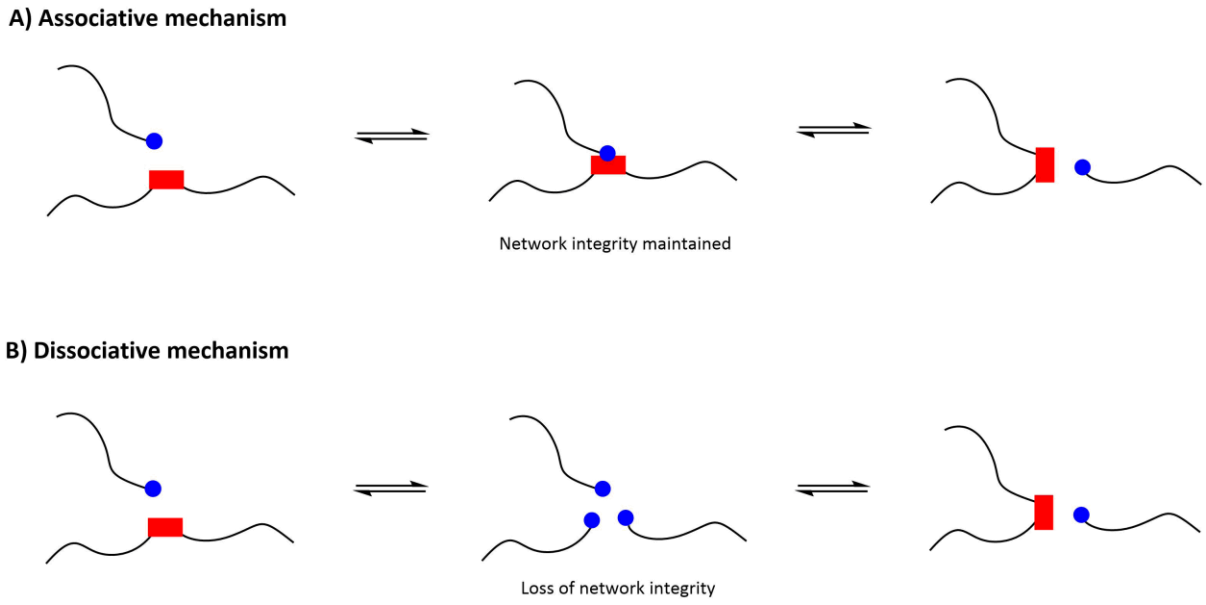

Figure 1.7 - CANs are divided into two groups depending on their exchange mechanism, either A) associative or B) dissociative.

In 2011, Leibler *et al*. took this concept and applied it to polyester materials cross-linked with epoxy acid/anhydride units.[56] At elevated temperatures, the associative transesterification takes place, and the epoxy network can be reprocessed without losing network integrity (**Scheme 1.4**). The networks displayed behaviour similar to vitreous silica and were hence named "vitrimers."[57]

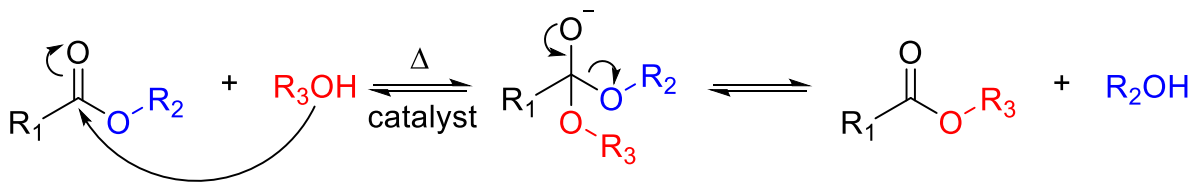

Scheme 1.4 - Associative transesterification mechanism.

In a dissociative mechanism, the opposite occurs; the cross-links dissociate before being remade. This causes a dramatic change in macromolecular structure, shown by a sudden drop in viscosity and loss of solvent resistance whilst the bond exchange mechanism takes place. These two features make dissociative CANs perfect candidates for the starting point for an adhesive that can be removed easily in response to an applied stimulus. Networks cross-linked by Diels-Alder bonds are chemical systems that match this description.

1.5 Self-healing

In recent decades, self-healing materials have garnered significant attention due to their diverse array of properties, including prolonged lifespan, heightened security, and environmental compatibility.[58] Taking inspiration from the regenerative abilities of living organisms, a multitude of investigations have been conducted into self-healing mechanisms. Two primary avenues, extrinsic and intrinsic strategies, have been developed to create self-healing materials.

The extrinsic strategy depends on external healing agents within carriers such as microcapsules,[59] and vascular networks.[60] These agents are released upon material damage. While this method is commonly employed, it possesses certain limitations. Notably, the self-healing capability diminishes once the agents are depleted. Consequently, researchers have shifted their focus towards intrinsic strategies, aiming to achieve repeated healing of coatings. The intrinsic approach to mending damage entails incorporating functional groups capable of non-covalent interactions or covalent reactions.

Non-covalent or physical interactions encompass hydrogen bonding,[61] ionic bonding,[62] and chain entanglement. Conversely, covalent reactions manifest through mechanisms like disulfide bonding,[63]

boronic ester exchange,[64] and Diels-Alder (DA) reactions.[65] Among these, DA reactions stand out due to their unique merits, including mild reaction conditions devoid of catalysts, a wide range of flexible monomer options, thermal reversibility, and a shape-memory effect.

1.6 Diels-Alder bonds

Introduced to the world by Otto Diels and Kurt Alder in their landmark paper in 1928,[66] the Diels-Alder (DA) reaction is now one of the most well studied reactions in organic chemistry, and the pair were awarded the Nobel Prize in Chemistry in 1950 for their efforts. It involves a pericyclic reaction between a conjugated diene and dienophile to give a cyclohexene derivative (**Figure 1.5**).[67]

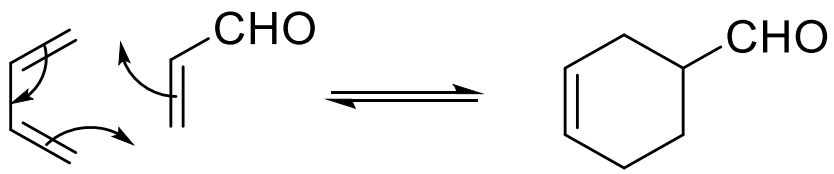

Scheme 1.5 - The Diels-Alder mechanism between the diene (left) and dienophile (right) to give the cyclohexene derivative

In the reaction, three π-bonds are broken and two σ-bonds and a new π-bond are formed in a concerted mechanism. Taking part are the four π-electrons of the diene and two π-electrons of the dienophile, which is denoted as a [4+2] cycloaddition. The formation of the more energetically stable σ-bonds drives the reaction, which happens rapidly because of the perfect alignment of the p-orbitals involved. The rearrangement is concerted and takes place with no intermediates; only a transition state with six delocalized π-electrons, thus benefitting from aromatic stabilization. The reaction often falls into a category termed “click” chemistry, referring to a group of reactions that are rapid, simple to use, easy to purify, versatile, regiospecific, atom economic and give high product yields.[68,69]

The reaction can proceed with numerous different dienes or dienophiles containing appropriate substitution, but there are certain prerequisites. Firstly, the diene can be open-chain or cyclic, but it must be conjugated; otherwise the electrons cannot delocalise and participate in the reaction.

Secondly, it must be able to form an s-*cis* conformation. A Diels-Alder reaction is impossible with an s-*trans* diene as the two ends are too far away to both react with the dienophile. In a molecule such as butadiene, the s-*cis* conformation is disfavoured because the close proximity of terminal CH_2 groups leads to some Van Der Waals repulsion. Since the barrier to rotation around a central σ-bond is small (30 kJ mol^{-1}) and the energy difference between conformations is small (≈2-5 kcal mol^{-1}), meaning there is often plenty of s-*cis* isomer to react (**Scheme 1.6**). It is possible to lock cyclic dienophiles in the s-*cis* conformation, making them ideal for this reaction, cyclopentadiene being a prime example.

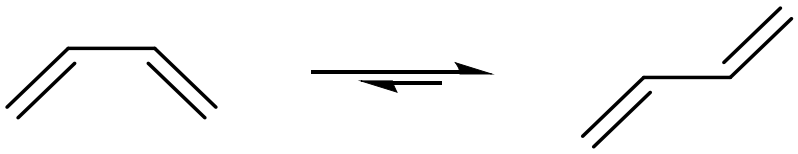

Scheme 1.6 - Two different conformations of butadiene. Left: s-*cis*, disfavoured but can undergo DA. Right: s-*trans*, favoured but unable to undergo DA.

The dienophile is usually an alkene but can also be an alkyne, often accompanied by an adjacent electron-withdrawing group to provide extra conjugation. The conjugation can be in the form of carbonyl compounds, nitro compounds, nitriles, sulfones, *etc.* and help the reaction by activating the alkene. This becomes clear when we consider the molecular orbital description of the reaction.[70]

The new σ-bonds are formed from combining the highest occupied molecular orbital (HOMO) of the diene with the lowest unoccupied molecular orbital (LUMO) of the dienophile (**Figure 1.8**). This happens very successfully because the HOMO of the diene (ψ_2) and the LUMO of the dienophile (π*) have matching symmetry and good overlap (**Figure 1.9)**. The formed σ-bonds are much lower in energy too, making them more stable and preferred. Introducing an electron-withdrawing substituent to the dienophile will cause the alkene to be electron deficient and lower its LUMO, narrowing the energy gap between itself and the diene's HOMO. The smaller the gap, the better the overlap and rate of reaction. This reduction in the energy gap is what is meant by activating the dienophile.

There is also correct symmetry and overlap for a transition between the LUMO of the diene and HOMO of the dienophile, but the energy gap is larger, so this doesn't normally occur. By adding electron-withdrawing substituents to the diene and electron-donating substituents to the dienophile the energy gap can be altered enough to make this preferred. This is known as the inverse electron demand Diels-Alder reaction.[71]

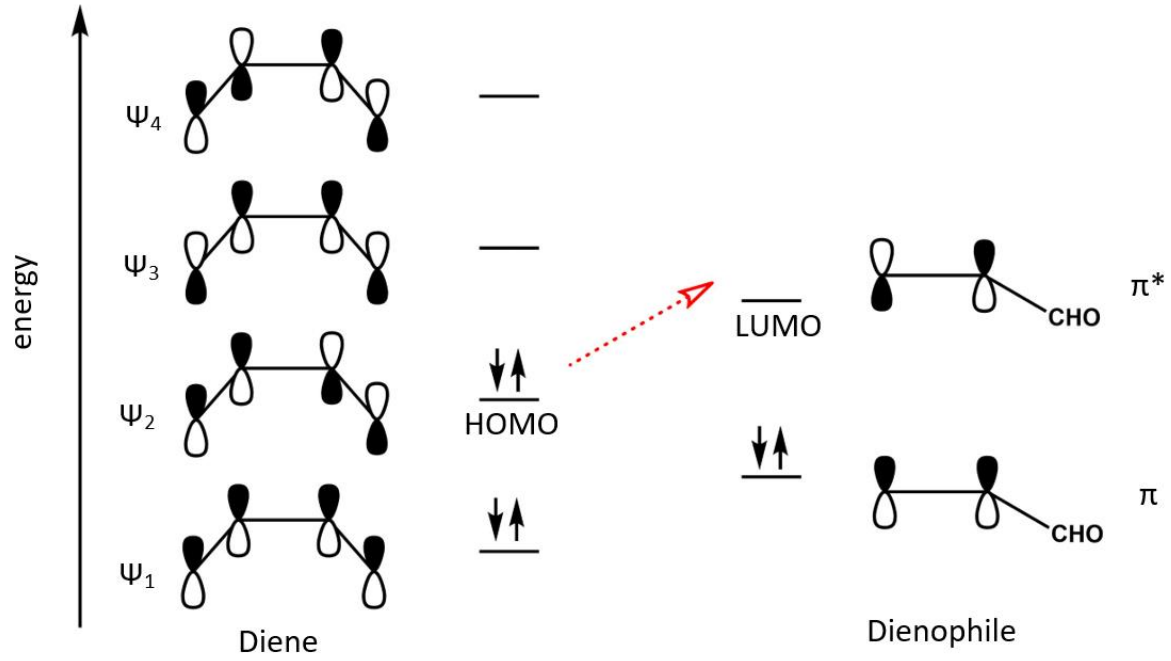

Figure 1.8 - Molecular orbital diagram showing the thermally allowed transition from the diene's HOMO to the dienophile's LUMO.

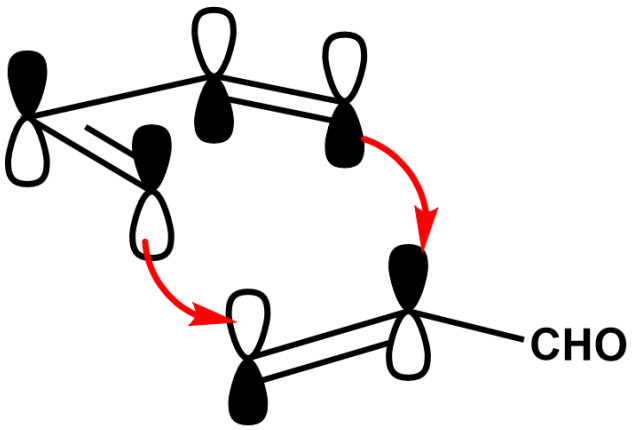

Figure 1.9 - The p orbitals are aligned perfectly and have matching symmetry.

At every temperature, the process exists as a dynamic equilibrium, such that at low temperatures the cycloadducts form predominantly, and at high temperatures the equilibrium favours dissociation. When using certain reactants, this process is reversible under heat, has fast reaction kinetics and high conversion at ambient temperatures, making Diels-Alder linkages a very attractive way to form thermally reversible adhesives. Commercial adhesives today are typically thermosets, meaning they are permanently cross-linked once cured, whereas thermally reversible adhesives have the potential to be debonded on command simply by heating to an appropriate temperature. In their dissociated state at high temperature, they are likely to exhibit improved flow (wetting of small features or rough substrates) due to the reversible decrease in molecular weight, whilst being cross-linked, producing high mechanical performance and solvent resistance at room temperature. Diels-Alder bonds have been extensively researched for creating mendable polymer networks ever since its inception by Chen *et al.* in 2002.[36] Throughout literature, the use of maleimide and furan derivatives as the moieties for the DA reaction has by far been the most common, as a consequence of its high yields with minimal side reactions under mild conditions (**Figure 1.7**).[72–74]

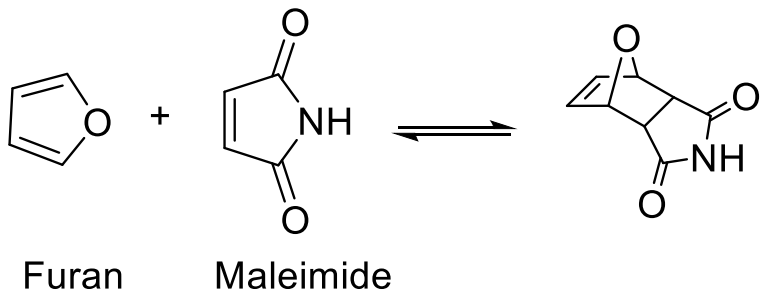

Scheme 1.7 - Furan and maleimide moieties react to yield a Diels-Alder product.

Materials incorporating such linkages have already been shown to have mechanical properties equalling those of commercial epoxy resins, and the mildly exothermic (20-40 kJ mol^{-1}) linkages can be dissociated by heating above 120 °C allowing for very fast topology rearrangements. The network can then be restored at room temperature without the need for a catalyst, additional monomer or

special treatment. The self-healing capabilities are understood, but knowledge of the adhesive capabilities after multiple heating cycles is limited.[75]

A very interesting recent article by Das *et al.* detailed the synthesis of a random graft copolymer with furfuryl moieties added to the branches post-polymerisation. These groups were then linked through the cycloaddition of a bismaleimide. Factors such as monomer stoichiometry and cooling rate after application were altered to see the effect on tensile strength.[76] Reattached specimens were tested a further two times and retained 88% and 95% of their initial strength.

Anthracene derivatives could be a suitable alternative for furan group as the diene. The anthracene-maleimide adducts are much more thermally stable, requiring temperatures exceeding 250 °C for the retro Diels-Alder (rDA) reaction.[77] While a higher rDA temperature (T_{rDA}) means the material is much more appropriate for use in hot environments, it would be more difficult to recycle at its end of life since the forward reaction also requires high temperatures (>100 °C) which poses potential challenges for the initial curing and subsequent self-healing. So far, research into the mending behaviour of these materials has not been successful. Cut pieces that have been healed by spending 3 days at 100 °C in contact with each other showed only an average recovery rate of 27% in tensile strength and 55% in elongation at break.[78] This slow mending rate appears to be a major drawback for this material.

Work by Wudl's group has used cyclopentadiene as both the diene and dienophile to create a linear polymer possessing dicyclopentadiene moieties.[79] The polymers underwent two healing treatments of a 120 °C for 20 hours in an argon atmosphere, with fracture testing performed after each heal. The average recovered strength after each test was only 46%, which limits the material's potential as a reusable adhesive.

1.7 Adhesives

Adhesives are used to join two substrates together through attractive forces acting across the interfaces (**Figure 1.10**). There are two important regions in the adhesive where different forces are

found. In the bulk of the adhesive known as the cohesion zone (coloured blue), cohesive forces govern the strength of the internal polymer network and hold the adhesive together. At the interface, there are adhesive forces that bind the adhesive to the substrate surface. Between the cohesion zone and the interface exists the interphase, an intermediate region where the composition, structure and properties vary across the region.

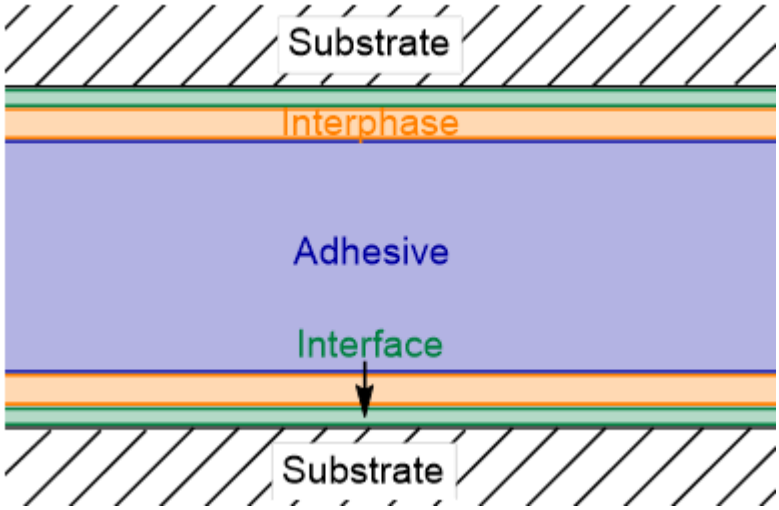

Figure 1.10 - Cross-section of the two substrates bonded by an adhesive.

The two dominant mechanisms taking place at the interface to bring about successful adhesion are mechanical and dispersive.

Mechanical interlocking occurs when the adhesive fills in the pores on the surface of the substrate. This is known as wetting the surface and relies on favourable thermodynamic surface energies that encourage intimate contact of the adhesive and substrates being bonded. Low viscosity adhesives are the most efficient as their molecular mobility means the polymer can flow more easily into and conform to the shape of the pores and maximise surface contact. Lowering the viscosity will negatively affect the cohesion, so a compromise between wetting and bond strength must be carefully reached. The geometry of the pores also determines how well the adhesive penetrates the surface. Mechanical roughening, such as the grit-blasting of aluminium, can increase bond strength by introducing pores and removing weakly bound surface layers.

Dispersive attraction is when the two materials are attracted by intermolecular interactions, namely van der Waals forces, between molecules of each material. It is widely regarded as the most important mechanism as it is prevalent in every type of adhesive system. At any given moment, the electrons around an atom are spread unevenly, giving rise to areas of delocalisation. Regions of opposite charge will attract each other, and this will happen between the adhesive and the substrate. Individually, these interactions are very low energy, but when combined over the bulk of the whole material they become significant.

1.7.1 One component and two component adhesives

The transition of a chemically hardening adhesive from an applicable liquid to a solid is known as curing and there are a variety of mechanisms available *via* single component (1-C) or two-component curing (2-C).

Single component adhesives are already premixed and stored in such a way that prevents premature curing. When these adhesives are exposed to certain conditions, they are activated, and the adhesive will begin curing. Examples of 1-C curing methods are:

1. Anaerobic – Cure under the absence of oxygen.[80] Dimethacrylate monomers are kept in half-filled air-permeable plastic bottles, which allows oxygen to maintain contact with the adhesive thus inhibiting curing. Once placed in a bond line, accessibility to oxygen is lost and the adhesive cures.

2. Cyanoacrylates – Also known as “Super Glue,” this adhesive will bond almost instantly to any surface by undergoing rapid anionic polymerisation in the presences of a weak base, such as water.[81]

3. Moisture – The curing mechanism in these systems are triggered by moisture and are typically non-volatile urethane prepolymers.[82]

4. Radiation – The adhesive is irradiated after application, commonly by ultraviolet (UV) or electron beam (EB) radiation.[83]

Two component adhesives are supplied as a resin and a hardener, which are combined at the point of application to the substrate. The prescribed ratio of resin to hardener is very specific in order to obtain the desired cure and physical properties of the adhesive. The curing begins immediately, and at room temperature, so it is vital that application is as fast as possible before the increased viscosity of the adhesive diminishes the wetting of the substrate. Full curing can take from minutes to weeks but can be accelerated by heat to fulfil the energy requirement to cure, generally resulting in the highest strength. When applied successfully, the result is a tough and rigid bond with good temperature and chemical resistance. The major 2-C adhesives are:

1. Epoxies are the most common structural adhesives, and are used to bond metal, plastic, fibre-reinforced plastic and glass.[84] They are based on the reaction between epoxies and amines. They cure quickly, with a worklife of 2-5 minutes, to give a rigid but brittle bondline.

2. Urethanes adhesives are made from polyols and isocyanates.[85] They are the most versatile as they can be formulated to be hard, soft, rigid or flexible. Their flexibility makes them especially useful in bonding two substrates with different thermal coefficients of expansion.

3. Methyl methacrylate adhesives (MMAs) have a faster strength build-up than epoxies and are more resistant to oil.[81] They are used to bond plastic to each other or to metals, making them useful in the automotive industry. They are supplied as a resin and catalyst that triggers the polymerisation of the monomer molecules, creating a polymer or copolymer of methyl methacrylate.

1.8 Bibliography

1 Collins 2018 Word of the Year Shortlist, https://blog.collinsdictionary.com/language-lovers/collins-2018-word-of-the-year-shortlist/, (accessed 1 September 2023).

2 OECD, *Global Plastics Outlook: Economic Drivers, Environmental Impacts and Policy Options*, OECD Publishing, 2022.

3 European Commission, *A European Strategy For Plastics In A Circular Economy*, 2018.

4 The UK Plastics Pact, *The UK Plastics Pact Annual Report 2021-22*, 2022.

5 GOV.UK, Plastic bag sales in 'big seven' supermarkets down 86% since 5p charge, https://www.gov.uk/government/news/plastic-bag-sales-in-big-seven-supermarkets-down-86-since-5p-charge.

6 T. Maes, J. Barry, H. A. Leslie, A. D. Vethaak, E. E. M. Nicolaus, R. J. Law, B. P. Lyons, R. Martinez, B. Harley and J. E. Thain, *Science of The Total Environment*, 2018, **630**, 790–798.

7 Z. Tartakowski, *Resour Conserv Recycl*, 2010, **55**, 167–170.

8 K. Kaiser, M. Schmid and M. Schlummer, *Recycling*, 2017, **3**, 1.

9 S. H. Goodman and H. Dodiuk-Kenig, *Handbook of Thermoset Plastics*, Willia Andrew, 3rd edn., 2013.

10 T. J. Mao, *Journal of Polymer Science: Polymer Letters Edition*, 1978, **16**, 201–201.

11 B. Ellis, in *Chemistry and Technology of Epoxy Resins*, Springer Netherlands, 1993, pp. 1–36.

12 G. Oertel, *Polyurethane Handbook*, Hanser, Munich, 2nd edn., 1993.

13 M. Amin, M. Ali and A. Khattak, *Science and Engineering of Composite Materials*, 2018, **25**, 753–759.

14 F. Aguirre-Vargas, in *Thermosets: Structure, Properties, and Applications: Second Edition*, Elsevier, 2018, pp. 369–400.

15 L.-H. Lee, in *Applied Polymer Science: 21st Century*, Elsevier, 2000, pp. 273–301.

16 O. Bayer, *Angewandte Chemie*, 1947, **59**, 257–272.

17 J. O. Akindoyo, M. D. H. Beg, S. Ghazali, M. R. Islam, N. Jeyaratnam and A. R. Yuvaraj, *RSC Adv*, 2016, **6**, 114453–114482.

18 J. Bernardini, D. Licursi, I. Anguillesi, P. Cinelli, M. B. Coltelli, C. Antonetti, A. M. R. Galletti and A. Lazzeri, *Bioresources*, 2017, **12**, 3630–3655.

19 M. Modesti, N. Baldoin and F. Simioni, *Eur Polym J*, 1998, **34**, 1233–1241.

20 D. K. Chattopadhyay, P. S. R. Prasad, B. Sreedhar and K. V. S. N. Raju, *Prog Org Coat*, 2005, **54**, 296–304.

21 A.-V. Ruzette and A. Mayes, *Macromolecules*, 2001, **34**, 1894–1907.

22 ISOPA, 2011.

23 Future Market Insights, Polyurethane Adhesives Market Snapshot (2022-2032), https://www.futuremarketinsights.com/reports/polyurethane-adhesives-market, (accessed 4 September 2023).

24 Whinfield, J.R. and Dickson, J.T., 1941. Improvements relating to the manufacture of highly polymeric substances. *British Patent*, *578*, p.79.

25 *Journal of the Society of Dyers and Colourists*, 1992, **108**, 363–364.

26 K. Ghosal and C. Nayak, *Mater Adv*, 2022, **3**, 1974–1992.

27 Z. Sun, M. Chen, G. Xie, Z. Jiang and Z. Qiu, *Polymer (Guildf)*, 2023, **283**, 126300.

28 Z. Cai, Y. Wan, M. L. Becker, Y.-Z. Long and D. Dean, *Biomaterials*, 2019, **208**, 45–71.

29 M. E. Rogers, T. E. Long and S. Richard Turner, in *Synthetic Methods in Step-Growth Polymers*, 2003, pp. 1–16.

30 O. Nuyken and S. Pask, *Polymers (Basel)*, 2013, **5**, 361–403.

31 T. Endo and A. Sudo, 2015, pp. 19–50.

32 A. E. Neitzel, T. J. Haversang and M. A. Hillmyer, *Ind Eng Chem Res*, 2016, **55**, 11747–11755.

33 C. Mangold, F. Wurm and H. Frey, *Polym Chem*, 2012, **3**, 1714.

34 C. W. Bielawski and R. H. Grubbs, *Prog Polym Sci*, 2007, **32**, 1–29.

35 N. J. Van Zee and R. Nicolaÿ, *Prog Polym Sci*, 2020.

36 X. Chen, M. A. Dam, K. Ono, A. Mal, H. Shen, S. R. Nutt, K. Sheran and F. Wudl, *Science (1979)*, 2002, **295**, 1698–1702.

37 Y. Higaki, H. Otsuka and A. Takahara, *Macromolecules*, 2006, **39**, 2121–2125.

38 E. Delebecq, J. P. Pascault, B. Boutevin and F. Ganachaud, *Chem Rev*, 2013, 113, 80–118.

39 H. Ying, Y. Zhang and J. Cheng, *Nat Commun*, 2014, **5**, 1–9.

40 S. Billiet, K. De Bruycker, F. Driessen, H. Goossens, V. Van Speybroeck, J. M. Winne and F. E. Du Prez, *Nat Chem*, 2014, **6**, 815–821.

41 M. M. Obadia, B. P. Mudraboyina, A. Serghei, D. Montarnal and E. Drockenmuller, *J Am Chem Soc*, 2015, **137**, 6078–6083.

42 P. Chakma, Z. A. Digby, M. P. Shulman, L. R. Kuhn, C. N. Morley, J. L. Sparks and D. Konkolewicz, *ACS Macro Lett*, 2019, **8**, 95–100.

43 M. Nagata and Y. Yamamoto, *React Funct Polym*, 2008, **68**, 915–921.

44 D. Zhao, B. Ren, S. Liu, X. Liu and Z. Tong, *Chemical Communications*, 2006, 779–781.

45 Y. Amamoto, J. Kamada, H. Otsuka, A. Takahara and K. Matyjaszewski, *Angewandte Chemie International Edition*, 2011, **50**, 1660–1663.

46 B. D. Fairbanks, S. P. Singh, C. N. Bowman and K. S. Anseth, *Macromolecules*, 2011, **44**, 2444–2450.

47 K. Imato, M. Nishihara, T. Kanehara, Y. Amamoto, A. Takahara and H. Otsuka, *Angewandte Chemie International Edition*, 2012, **51**, 1138–1142.

48 A. E. Ivanov, H. Larsson, I. Y. Galaev and B. Mattiasson, *Polymer (Guildf)*, 2004, **45**, 2495–2505.

49 M. C. Roberts, M. C. Hanson, A. P. Massey, E. A. Karren and P. F. Kiser, *Advanced Materials*, 2007, **19**, 2503–2507.

50 N. V. Tsarevsky and K. Matyjaszewski, *Macromolecules*, 2005, **38**, 3087–3092.

51 A. W. Jackson and D. A. Fulton, *Macromolecules*, 2012, **45**, 2699–2708.

52 G. Deng, F. Li, H. Yu, F. Liu, C. Liu, W. Sun, H. Jiang and Y. Chen, *ACS Macro Lett*, 2012, **1**, 275–279.

53 G. Deng, C. Tang, F. Li, H. Jiang and Y. Chen, *Macromolecules*, 2010, **43**, 1191–1194.

54 P. Taynton, K. Yu, R. K. Shoemaker, Y. Jin, H. J. Qi and W. Zhang, *Advanced Materials*, 2014, **26**, 3938–3942.

55 Q. Li, S. Ma, S. Wang, W. Yuan, X. Xu, B. Wang, K. Huang and J. Zhu, *J Mater Chem A Mater*, 2019, **7**, 18039–18049.

56 D. Montarnal, M. Capelot, F. Tournilhac and L. Leibler, *Science (1979)*, 2011, **334**, 965–968.

57 W. Denissen, J. M. Winne and F. E. Du Prez, *Chem Sci*, 2016, 7, 30–38.

58 C.-H. Li, C. Wang, C. Keplinger, J.-L. Zuo, L. Jin, Y. Sun, P. Zheng, Y. Cao, F. Lissel, C. Linder, X.-Z. You and Z. Bao, *Nat Chem*, 2016, **8**, 618–624.

59 S. R. White, N. R. Sottos, P. H. Geubelle, J. S. Moore, M. R. Kessler, S. R. Sriram, E. N. Brown and S. Viswanathan, *Nature*, 2001, **409**, 794–797.

60 K. S. Toohey, N. R. Sottos, J. A. Lewis, J. S. Moore and S. R. White, *Nat Mater*, 2007, **6**, 581–585.

61 X. Dai, Y. Zhang, L. Gao, T. Bai, W. Wang, Y. Cui and W. Liu, *Advanced Materials*, 2015, **27**, 3566–3571.

62 Y. Guo, X. Zhou, Q. Tang, H. Bao, G. Wang and P. Saha, *J Mater Chem A Mater*, 2016, **4**, 8769–8776.

63 S.-M. Kim, H. Jeon, S.-H. Shin, S.-A. Park, J. Jegal, S. Y. Hwang, D. X. Oh and J. Park, *Advanced Materials*, 2018, **30**, 1705145.

64 O. R. Cromwell, J. Chung and Z. Guan, *J Am Chem Soc*, 2015, **137**, 6492–6495.

65 S. Yu, R. Zhang, Q. Wu, T. Chen and P. Sun, *Advanced Materials*, 2013, **25**, 4912–4917.

66 O. Diels and K. Alder, *Justus Liebigs Ann Chem*, 1928, **460**, 98–122.

67 R. B. Woodward and T. J. Katz, *Tetrahedron*, 1959, **5**, 70–89.

68 H. C. Kolb, M. G. Finn and K. B. Sharpless, *Angewandte Chemie - International Edition*, 2001, **40**, 2004–2021.

69 C. D. Hein, X. M. Liu and D. Wang, *Pharm Res*, 2008, **25**, 2216–2230.

70 R. Hoffmann and R. B. Woodward, *Acc Chem Res*, 1968, **1**, 17–22.

71 H. P. Figeys and A. Mathy, *Tetrahedron Lett*, 1981, **22**, 1393–1396.

72 X. Liu, P. Du, L. Liu, Z. Zheng, X. Wang, T. Joncheray and Y. Zhang, *Polymer Bulletin*, 2013, **70**, 2319–2335.

73 T. T. Truong, H. T. Nguyen, M. N. Phan and L.-T. T. Nguyen, *J. Polym. Sci., Part A: Polym. Chem*, 2018, **56**, 1806–1814.

74 Y. Fang, J. Li, X. Du, Z. Du, X. Cheng and H. Wang, *Polymer (Guildf)*, 2018, **158**, 166–175.

75 D. H. Turkenburg, H. van Bracht, B. Funke, M. Schmider, D. Janke and H. R. Fischer, *J Appl Polym Sci*, 2017, **134**, 1–11.

76 S. Das, S. Samitsu, Y. Nakamura, Y. Yamauchi, D. Payra, K. Kato and M. Naito, *Polym Chem*, 2018, **9**, 5559–5565.

77 M. Grigoras and G. Colotin, *Polym Int*, 2001, **50**, 1375–1378.

78 N. Yoshie, S. Saito and N. Oya, *Polymer (Guildf)*, 2011, **52**, 6074–6079.

79 E. B. Murphy, E. Bolanos, C. Schaffner-Hamann, F. Wudl, S. R. Nutt and M. L. Auad, *Macromolecules*, 2008, **41**, 5203–5209.

80 In *Handbook of Plastics Joining*, Elsevier, 2009, pp. 145–173.

81 A. V. Pocius, in *Polymer Science: A Comprehensive Reference*, Elsevier, 2012, pp. 305–324.

82 J. Comyn, *Int J Adhes*, 1998, **18**, 247–253.

83 C. E. Hoyle, *Radiation Curing of Polymeric Materials*, American Chemical Society, Washington, DC, 1990, vol. 417.

84 J. L. Massingill and R. S. Bauer, in *Applied Polymer Science: 21st Century*, Elsevier, 2000, pp. 393–424.

85 M. Dunky and A. Pizzl, in *Adhesion Science and Engineering*, Elsevier, 2002, pp. 1039–1103.

2 Maleimide and furan-based networks

2.1 Introduction

The Diels-Alder (DA) reaction between maleimide and furan groups has been used extensively in polymer chemistry to make a variety of polymer networks and architectures.[1] The earliest reports as far back as 1994 by Kuramoto, who performed a Diels-Alder polymerisation between difurfuryl adipate and bismaleimidodiphenylmethane to yield a linear polymer.[2] This is because their cycloaddition occurs at a high rate and conversion even at ambient temperatures, making the creation of a highly cross-linked network easy and efficient. The reverse reaction, retro-DA (rDA) uncoupling, begins to occur at about 110 °C. This relatively low temperature makes these materials extremely attractive for recyclable networks and self-healing materials, because the temperature is low enough that side reactions and thermal degradation are negligible, even after multiple cycles, which can allow the use of sequential Diels-Alder/ retro Diels-Alder reactions to repeatedly reprocess the materials. The landmark work by Wudl in 2001 reported the use of trifunctional maleimide and tetrafunctional furan monomers to form heat-healable networks.[3] There are some reports on reversible adhesives using maleimide and furan groups including epoxy,[4] acrylic[5–7] and polyurethane[8] matrices but most of these networks are formed using the monomer *N,N'*-(4,4'-methylene diphenyl) bismaleimide (BMI) in relatively high quantities. This aromatic, low molecular weight bismaleimide monomer is highly toxic and unsuitable for practical application in consumer or industrial applications.

The Diels-Alder reaction between maleimide and furan groups has also been used to make reversible non-isocyanate polyurethanes (NIPUs) for potential adhesive applications although no detail has been reported on their material/adhesive properties.[9,10] A recent study has highlighted that flexible packaging films bonded with cross-linked polyurethane adhesives can be separated effectively, however this requires immersion of the bonded laminates in hot dimethyl sulfoxide solvent to dissociate the maleimide-furan adducts.[11] Elegant work based on hetero Diels-Alder reactions between cyclopentadiene and thioesters in acrylic networks has shown that network degradation is

fast and “self-reporting” due to the colour change when network dissociation occurs.[12] However, the methodology used is unlikely to be sustainable or suitably facile for industrial applications considering the multi-step chemistry with low atom economy used to make the dienes/dienophiles and the likely thermal instability of the thioesters producing malodour and safety issues. In addition, re-use was not demonstrated; Lewis acids are required for the network to form at ambient temperature and need to be removed for the retro reaction to occur. The use of furan derivatives in polymeric applications is on the rise because the raw materials used to make them are bio-derived and renewable. For example, furfural is sourced from a variety of agricultural by-products like corncobs or oats and can be hydrogenated to make furfuryl alcohol, which is used in thermoset polymer matrix composites, cements, adhesives, casting resins and coatings.[13]

For these reasons, the first networks synthesised in this project involve these functionalities, to establish a proof of concept and develop an understanding of the behaviour of DA cross-linked systems and their feasibility to be used as thermoreversible adhesives. This knowledge can then be applied to other, less-studied systems, to create novel materials. The approach reported here involves a dissociative covalent adaptable network (CAN) made from a telechelic maleimides and polyfunctional furans. At ambient temperature, network formation is favoured *via* cycloaddition reactions between the maleimide and furan functional groups whereas at higher temperatures the equilibrium shifts to the dissociated prepolymers. The chemistry is relatively straightforward where maleimide and furan functional groups are attached to prepolymer backbones with remarkably high atom efficiency in high conversion and without the need for purification.[14] The polymer networks are prepared by applying a heated mixture of functional prepolymers in the bulk without solvents or monomers and allowing them to cross-link after cooling under ambient conditions.

2.2 Results and Discussion

2.2.1 Synthesis of a Diels-Alder-based CAN

To create a network cross-linked with Diels-Alder bonds, the furan cross-linker trifurfuryl 1,3,5-benzenetricarboxylate (F1), and the long chain bismaleimide bismaleimidocaproyl C_{36} dimerate (M1), both commercially available, were combined in a hot melt blend at 120 °C for 30 minutes (**Scheme 2.1**). The masses of linker and bismaleimide used were calculated to give an equimolar ratio of furan to maleimide. Once the mixture was homogenous, the melt was cast as a 250 µm film and allowed to cool to ambient temperature, at which point the Diels-Alder reaction between the furan and maleimide can take place to form the network DA1.

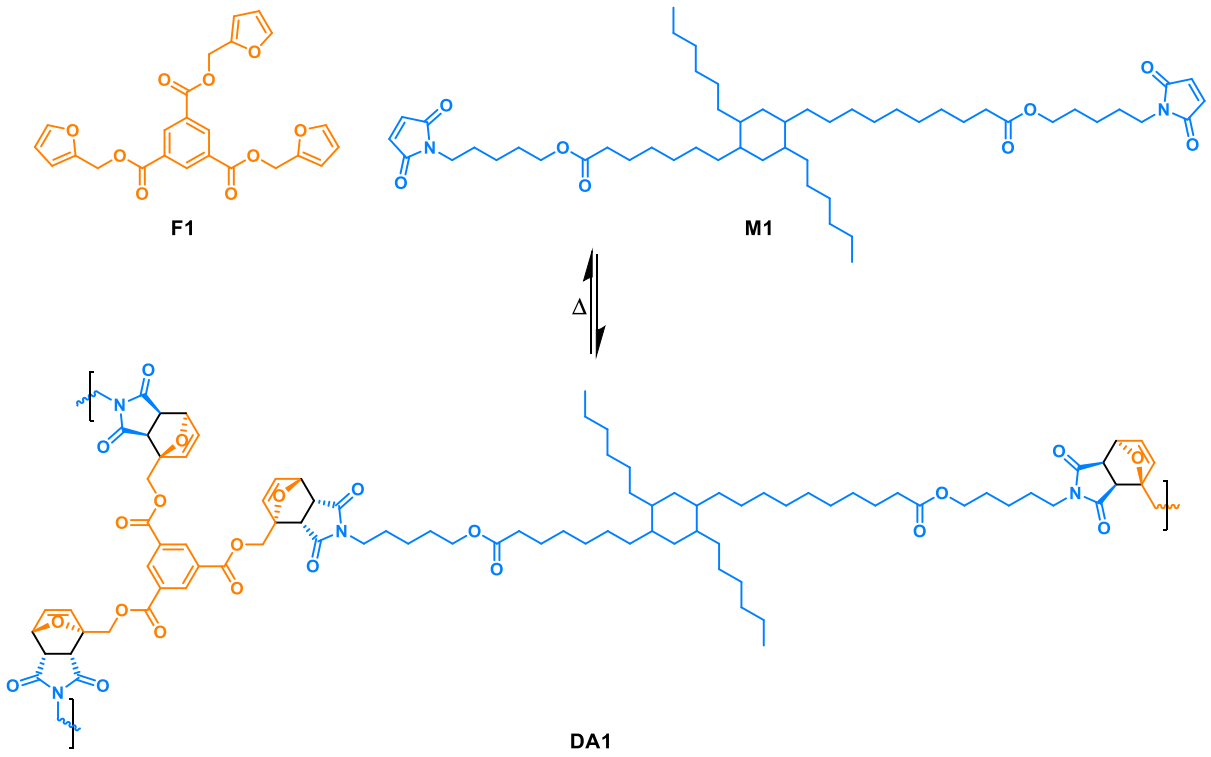

Scheme 2.1 – The trifunctional furan F1 and bismaleimide M1 reacting to generate the Diels-Alder network DA1.

This process was confirmed by analysing the materials before and after combination. The starting materials' structures were confirmed *via* ^{1}H nuclear magnetic resonance (NMR) spectroscopy (**Figure**

2.1, 2.2), in particular, the furan resonances (δ = 6.39, 6.50 and 7.45 ppm) and the maleimide resonance (δ = 6.68 ppm).

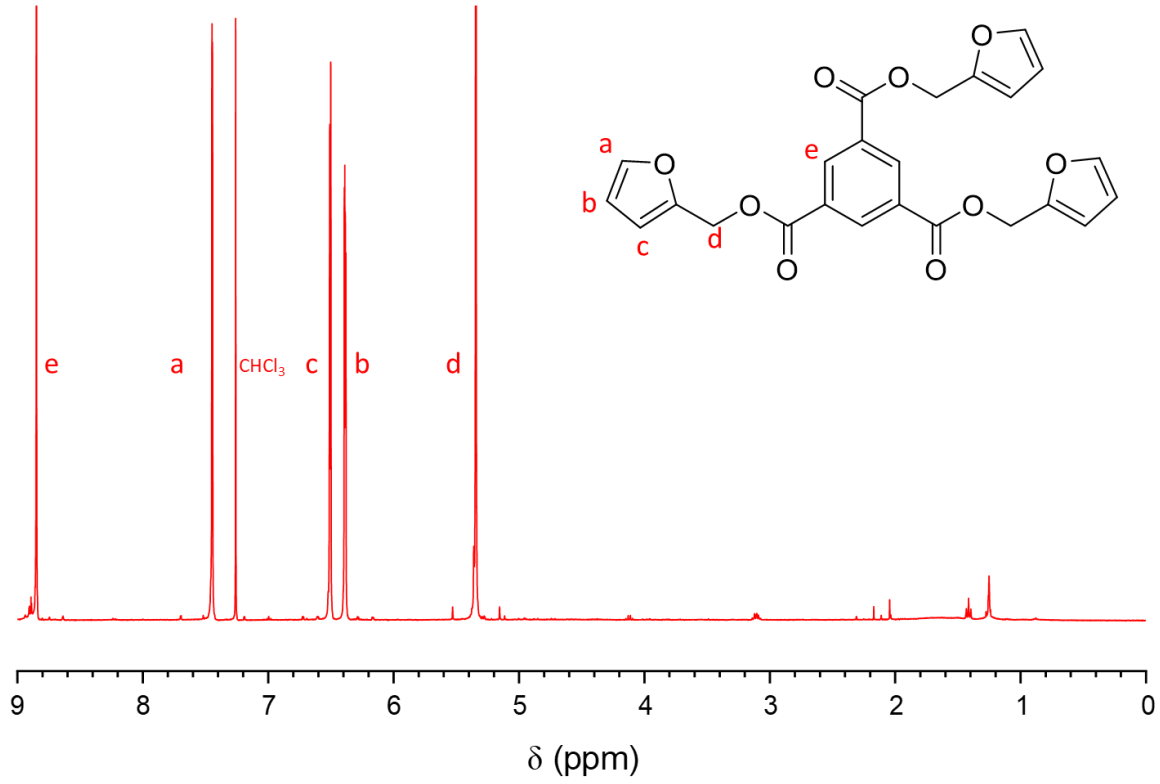

Figure 2.1 - ^{1}H NMR spectrum of the trifunctional furan (400 MHz, $CDCl_3$, 298 K).

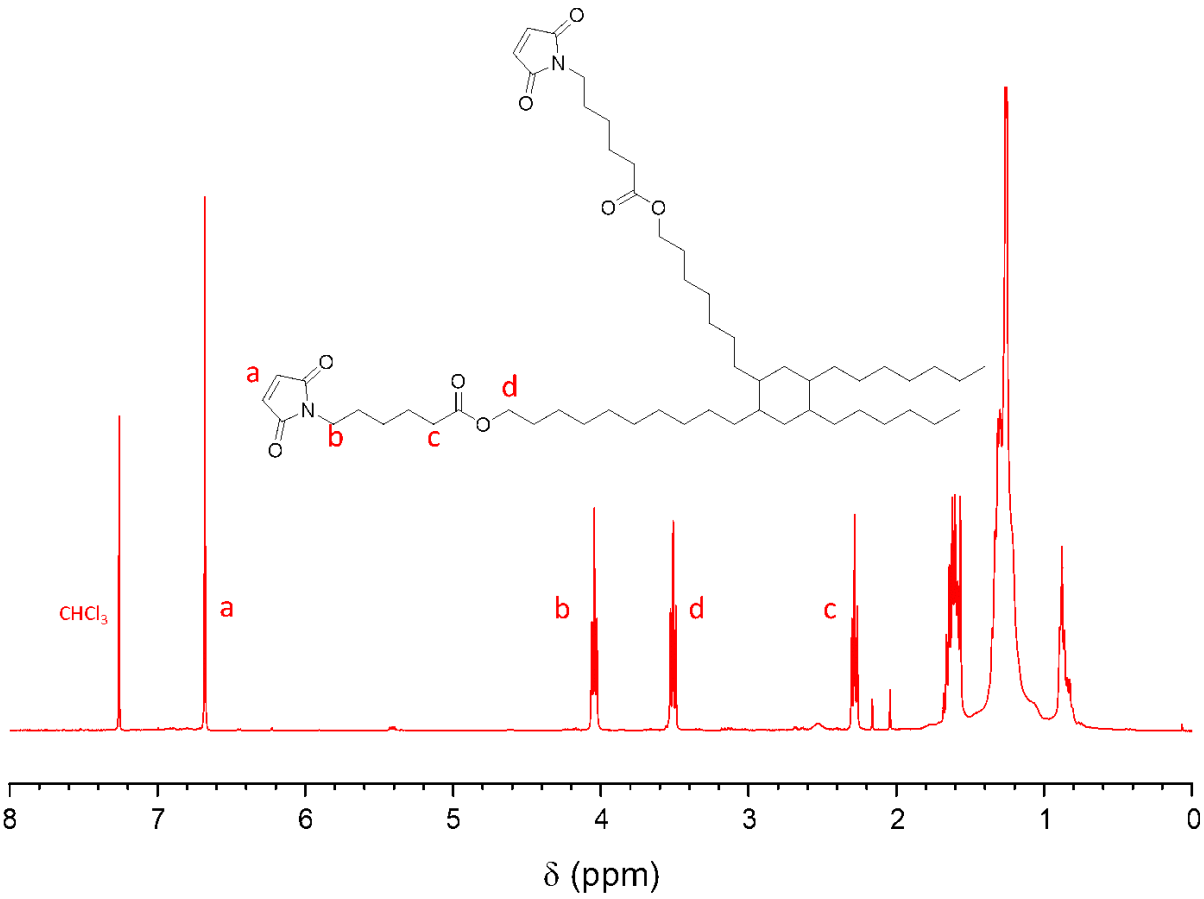

Figure 2.2 - ^{1}H NMR spectrum of the bismaleimide (400 MHz, $CDCl_3$, 298 K).

Fourier-transform infrared (FTIR) spectroscopy was used to determine any differences in the bonds present before and after network formation (**Figure 2.3**). The results showed that the network still contained the alkyl chain and the ester linkages from the bismaleimide, giving resonances at λ = 2923 cm^{-1} and 1695 cm^{-1}, respectively. The most important piece of information comes from the fingerprint region, namely the peak at 696 cm^{-1} in the bismaleimide spectrum corresponding to the maleimide B_1 antisymmetric ring deformation mode.[15,16] Once the maleimide associates with the furan, this vibration no longer occurs and the peak is not present in the spectrum.

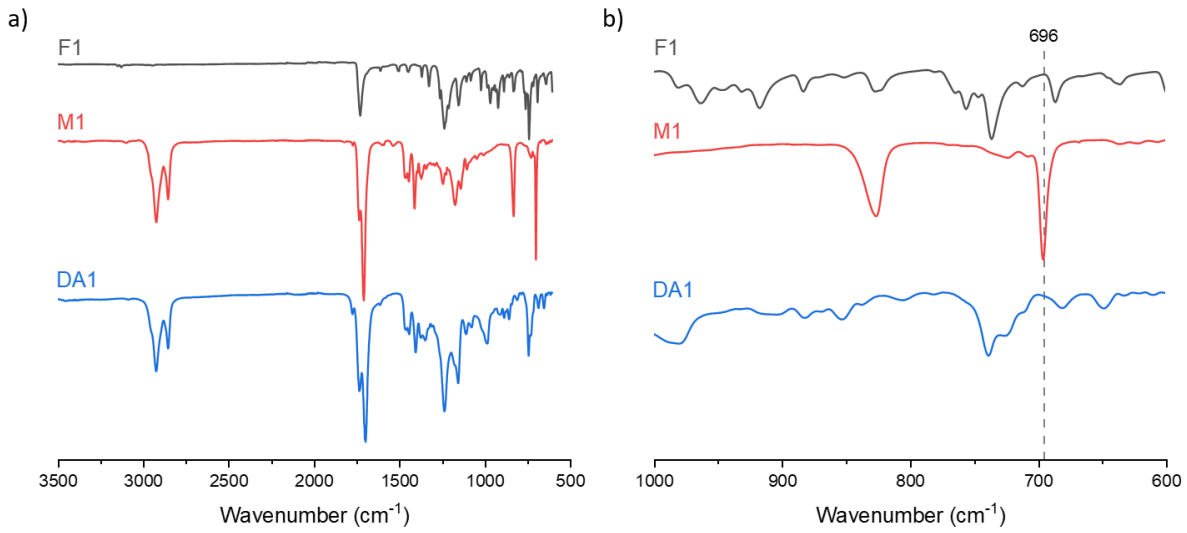

Figure 2.3 – a) Infrared spectra of F1, M1, and DA1 and b) an enlarged view highlighting the maleimide absorbance.

The three materials were then analysed using differential scanning calorimetry (DSC) (**Figure 2.4**). F1 is a highly crystalline compound, as shown by the sharp endotherm at 102 °C, the temperature at which the ordered structure melts. Conversely, M1 is an amorphous liquid with a low glass transition temperature (T_g) of -54 °C. Both of the observed transition temperatures for F1 and M1 are absent from the thermogram of the resultant network. The linker molecules are dispersed throughout the network, bonded to the bismaleimide, which prevents the crystalline structure from forming and hence, the sharp endotherm is not present. The T_g has increased to 19 °C as a result of the cross-linking hindering the molecular mobility of the bismaleimide chains. The emergence of a large endotherm that peaks at 152 °C can be attributed to the retro Diels-Alder reaction; where cycloreversion of the DA adducts occurs and thereby dissociates the network back into its separate components. At this temperature, the material becomes a low-viscosity fluid. In this state, the materials can be removed from substrates and reshaped, a key feature of its reusability.

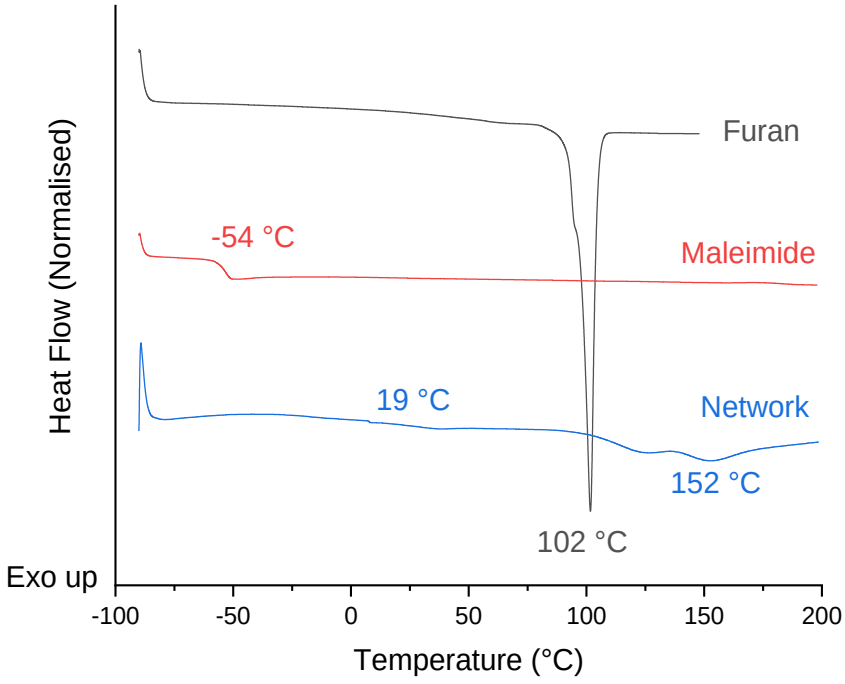

Figure 2.4 – DSC thermograms of the furan linker, bismaleimide, and the resultant network.

The rDA endotherm is separated into two peaks as a result of the adduct being able to have two different spacial arrangements requiring different energies in order to undergo rDA reversion. Depending on the initial suprafacial approach, the DA reaction can lead to the formation of two diastereoisomers, the *endo* and the *exo* (**Scheme 2.2**).[17]

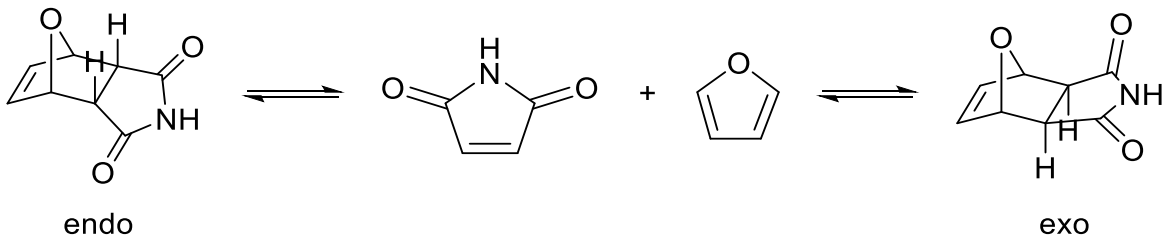

Scheme 2.2 - The two diastereoisomers formed from the furan-maleimide reaction.

The *endo* isomer forms when the diene is positioned above the electron-withdrawing group of the dienophile (**Figure 2.5**). The transition state is stabilised by secondary interactions between the

extended pi orbitals of the diene and dienophile. Therefore the *endo* isomer is formed faster due to the lower energy transition state, however it is less thermodynamically stable due to the steric hindrance it experiences. The *exo* isomer is formed from the opposite interactions, the heteroatom sides lie away from each other, so there are no secondary interactions to lower the activation barrier and increase the rate of reaction, but the final product is more thermodynamically stable as a result of less steric interaction.

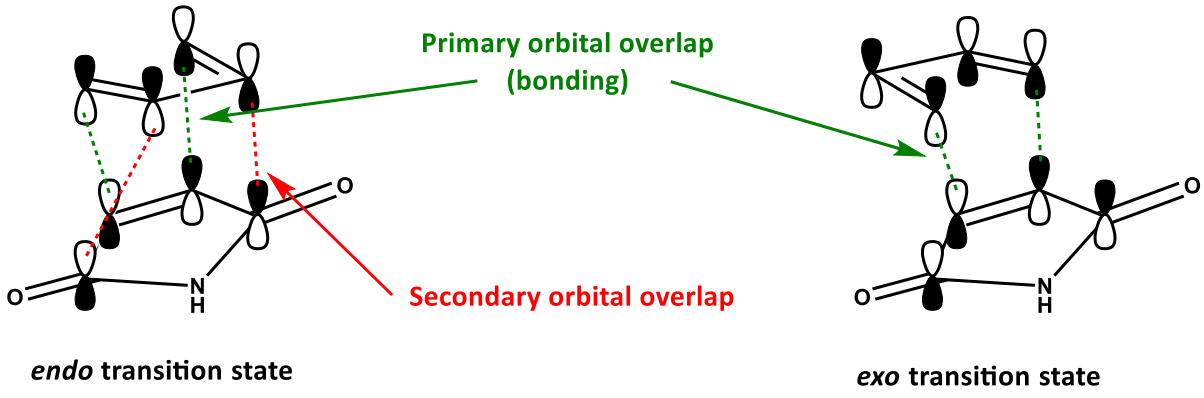

Figure 2.5 - Transition states leading to the *endo* and *exo* isomers.

The *exo* product will therefore require a higher activation energy to dissociate and consequently, a higher rDA temperature (T_{rDA}). To illustrate this, the network was fully dissociated with a 150 °C heat before returning to ambient temperature. The reforming network was then analysed *via* DSC over a period of days following the heating. The endotherm for the kinetic *endo* adduct, with the lower T_{rDA}, grew in magnitude over time, suggesting more *endo* adducts were forming, whereas the endotherm for the thermodynamic *exo* adduct stayed constant (**Figure 2.6**).

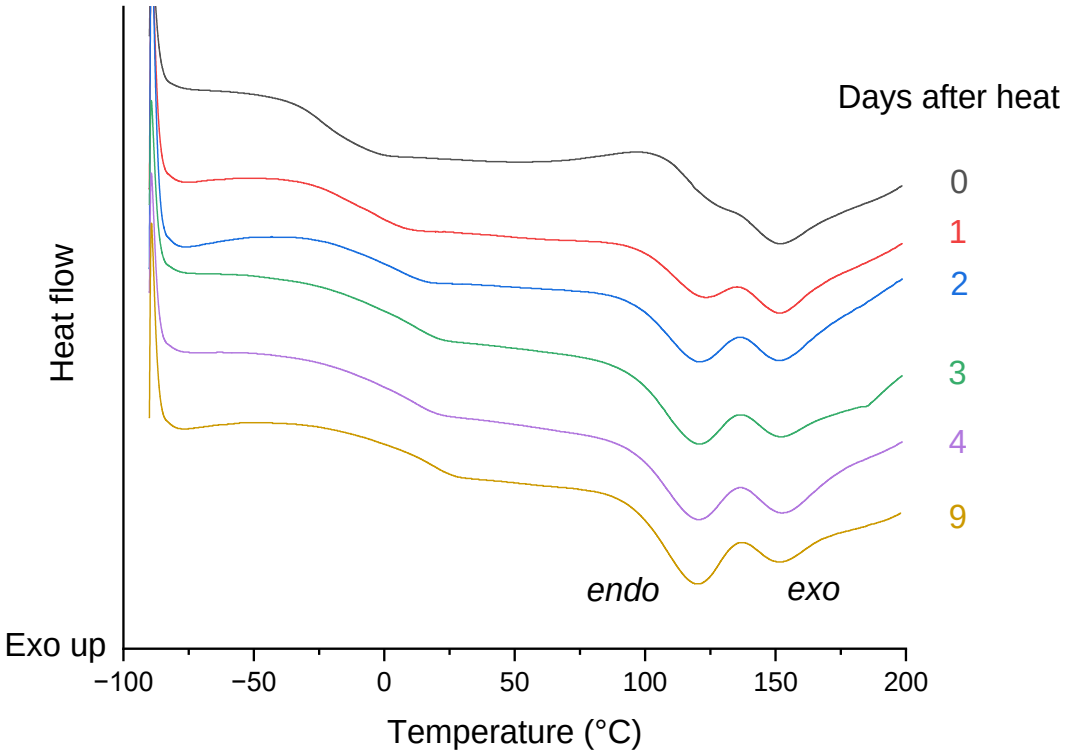

Figure 2.6 - The changes in the DSC thermogram of the network after being heated at 150 °C for 1 hour and then left at ambient temperature.

The increase in the *endo* isomer over the 9 days was a consequence of the DA reaction of unreacted furan and maleimide moieties, and not a rearrangement from the *exo* product. Ambient temperatures do not provide enough thermal energy for the *exo* product to form at an observable rate, so this endotherm stays constant. The *exo* endotherm is caused by the *exo* product that forms during the thermal window between the 150 °C heat and cooling to ambient, where sufficient thermal energy is available for this conformation to occur. The fast reaction kinetics of the DA reaction means it is unsurprising that there is a large conversion in this short space of time.

To evidence this, the sample was conditioned overnight at 50 °C, a temperature at which it would be able to overcome the larger energy barrier to form the thermodynamically favoured *exo* adduct. The *exo* peak increased relative to the *endo* peak, suggesting successful rearrangement (**Figure 2.7**). It

should be noted that this is not a direct isomerisation between adducts, as it needs to be preceded by the cycloreversion into the monomers.[18]

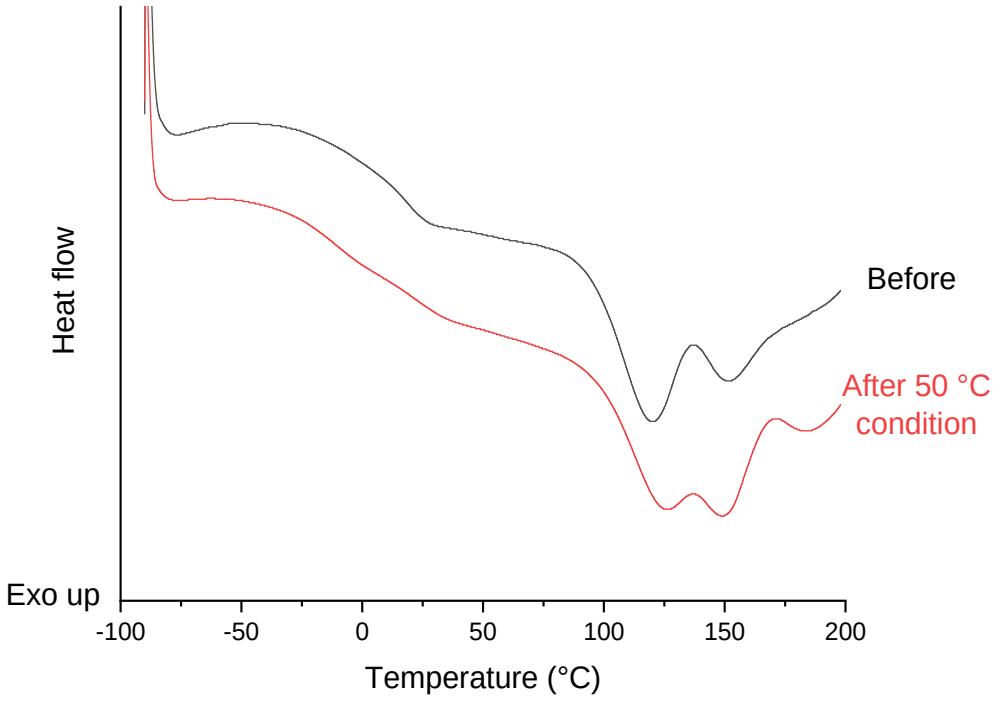

Figure 2.7 – The change in retro Diels-Alder enthalpy after a 50 °C condition overnight.

In the scope of adhesives, these findings show that curing the adhesive above ambient temperature (*e.g.* 50 °C) would be beneficial to preferentially form the *exo* isomer, which is more thermodynamically stable and thus more resistant to temperature. A higher curing temperature carries the added benefit of a faster cure, at the cost of a more onerous curing process.

2.2.2 The effect of heating rate on melt temperature

The T_{rDA} of DA1 was ascertained through DSC operating at the standard heating rate of 10 °C min^{-1}. Standard heating rates are useful when making comparisons between polymers but should be used with caution for practical purposes, as any differential scanning calorimeter will experience thermal

lag, so the true T_{rDA} value will be lower. This is because the sample temperature lags behind the furnace temperature as the heat must flow across a barrier (the sample pan) to reach the sample.[19] Furthermore, the sensor monitoring the sample temperature is not in contact with the sample itself, but rather a point nearby within the sample holder, introducing further delay. Thermal lag error is proportional to heat flow, heating rate, and to the mass of the sample/pan system.[19] Fast heating rates improve sensitivity and productivity, at the expense of temperature resolution and accuracy. The significance of thermal lag in the DSC results was investigated by systematically reducing the heating rate to 1 °C min^{-1} (**Figure 2.8**).

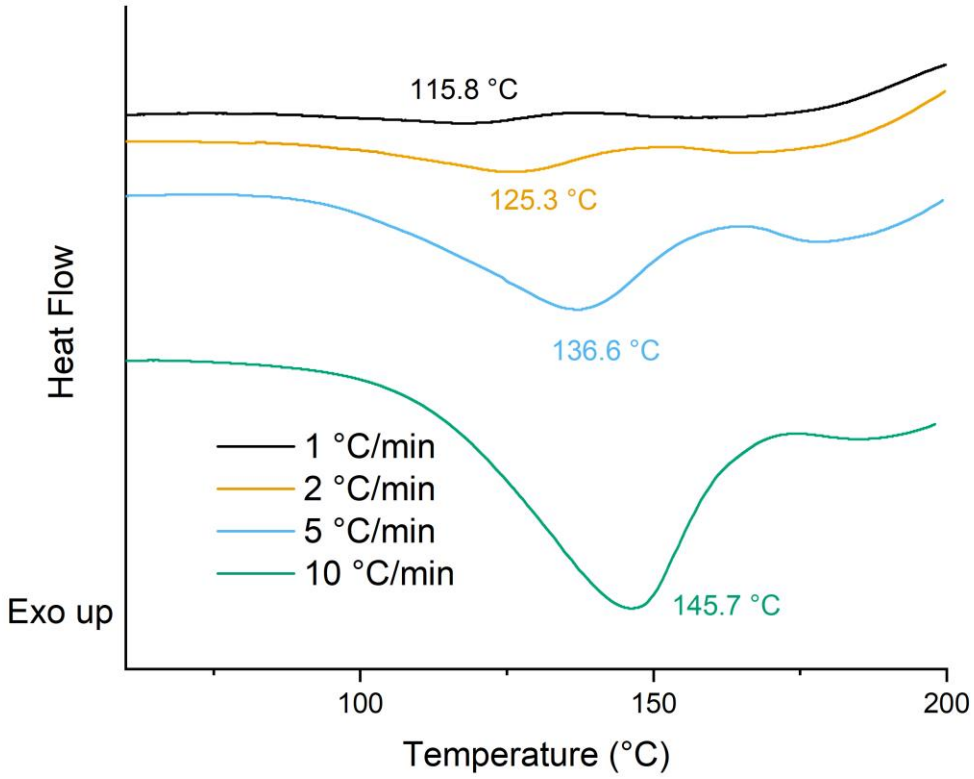

Figure 2.8 - The T_{rDA} of the network at different heating rates.

The results showed that a more realistic value for the network dissociation was 30 °C lower than given by the standard test, which is a substantial amount when planning real world applications. If the thermal lag in the experiment is not accounted for appropriately, the adhesive will fail much sooner than expected, to potentially catastrophic consequences.

2.2.3 Curing time

As seen in the previous section, the network continues to associate even after several days, and curing time is a key detail that needs to be considered in adhesives for certain applications. In a system based on DA cross-links, the rate of formation of these cross-links will directly correlate to the curing time, and so an experiment into the kinetics of this process was investigated. The network was heated beyond its T_{rDA} (150 °C for 1 hour) to dissociate the network and the rate of cross-linking was then monitored by measuring the decrease in maleimide absorbance by FTIR spectroscopy at ambient temperature over the course of 16 days (**Figures 2.9 and 2.10**). To prevent discrepancies caused by varying sample thicknesses across scans, the absorbance of the maleimide peak was measured relative to an adjacent, unchanging peak at 739 cm^{-1}. This reference peak is characteristic of out-of-plane bending from the arene ring in the furan linker.

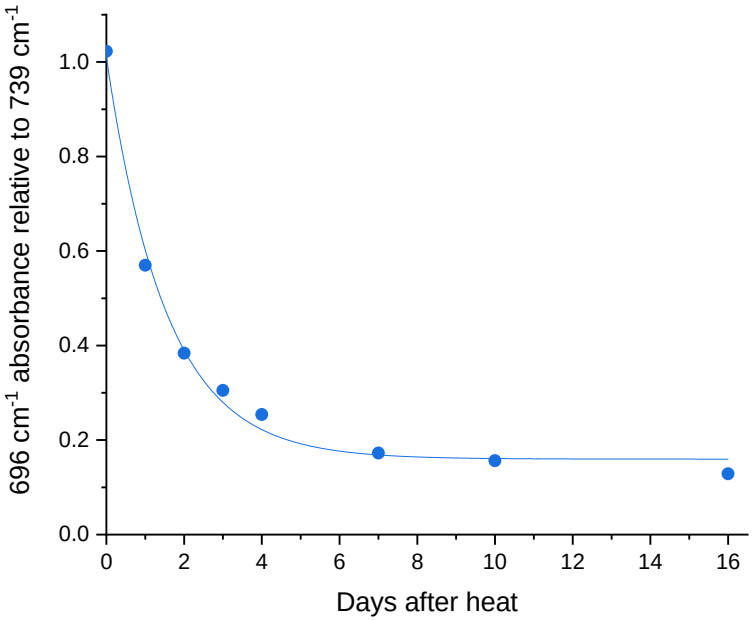

Figure 2.9 - A graph illustrating the disappearance of the 696 cm^{-1} peak at ambient temperature.

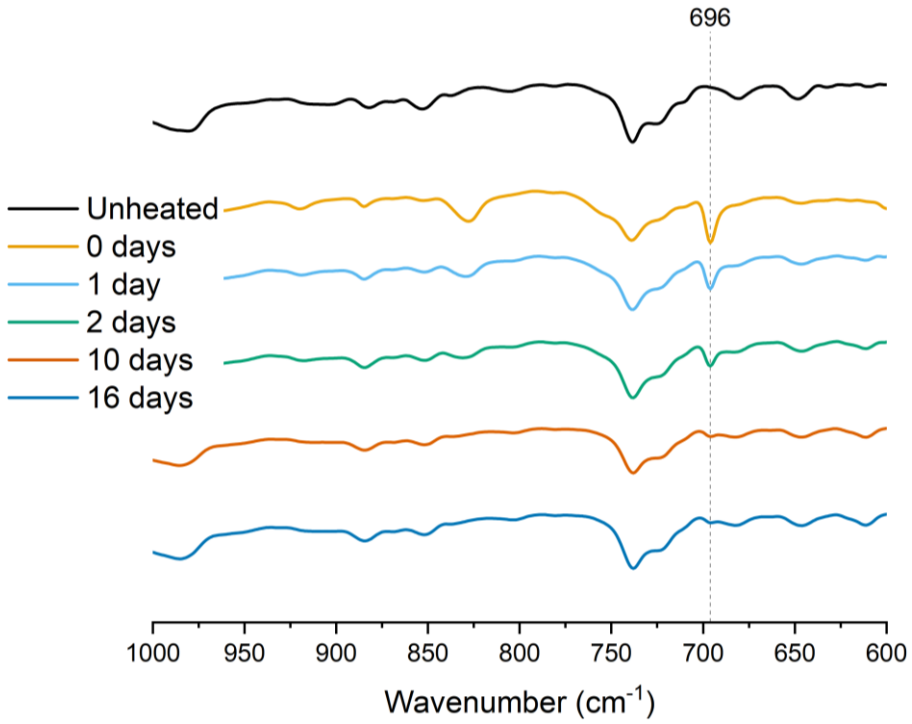

Figure 2.10 - A section of the IR spectra taken of the network before and after an hour-long heat at 150 °C and then left at ambient.

Directly after heating, the maleimide peak at 696 cm^{-1} appears, which suggests that the cross-links have successfully broken and the maleimide groups are now free to absorb. The film was left at ambient temperature over the course of 16 days and the peak rapidly decreased in intensity for the first two days before beginning to plateau, showing a very slow and constant decrease in intensity beyond 8 days. After 16 days, the maleimide peak was barely observable by FTIR spectroscopy.

Similar to other thermosets and vitrimers, the curing process can be accelerated by using an elevated temperature. An analogous experiment to the one above was set up, except the film was conditioned at 60 °C after the initial 150 °C heat. As expected, the curing process was accelerated significantly and the rate of decrease in absorbance began to plateau in a matter of hours (**Figure 2.11**).

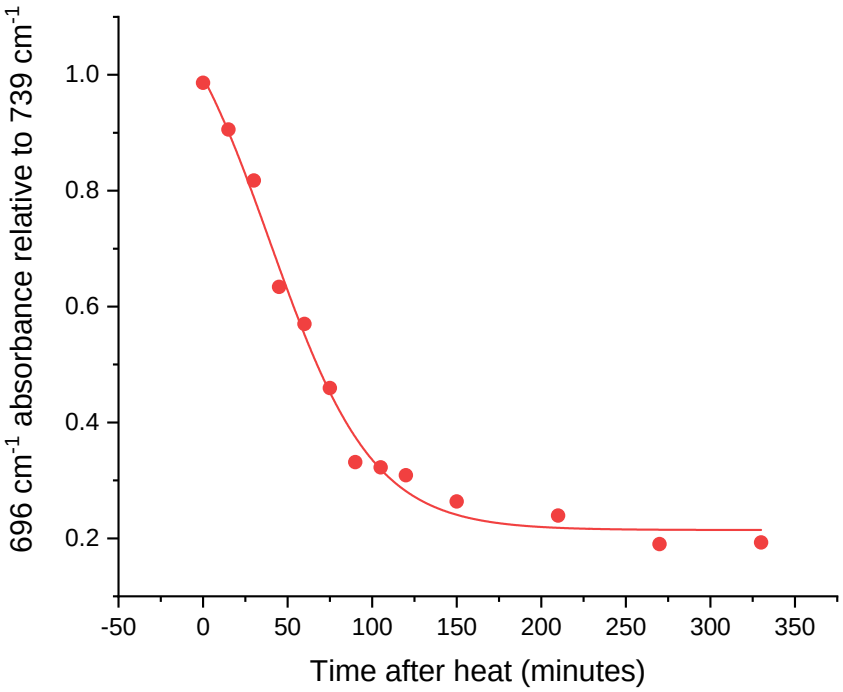

Figure 2.11 - A graph illustrating the disappearance of the 696 cm^{-1} peak at 60 °C.

The higher temperature provides more energy for the DA reaction to take place, and it maintains the mobility of the prepolymer chains for longer after heating, allowing the functional groups to migrate and react. At 60 °C, it took only 6 hours for the maleimide absorbance to decrease to a value that took 2 days at ambient temperature.

2.2.4 Repeated heating cycles of polyurethanes

A primary objective of this project is to develop an adhesive that can be reused multiple times. As such, it is vital for them to maintain their properties throughout multiple reprocessing cycles. The network was heated to 150 °C for 1 hour and then left for 7 days at ambient temperature before reheating again, until 5 heating cycles had been achieved. The film was analysed *via* FTIR spectroscopy each day and the 696 cm^{-1} absorption monitored. All 5 heat cycles showed similar rates of curing, which is an indication that the material doesn't degrade irreversibly or undergo side reactions from the repeated heating and cooling (**Figure 2.12**). At temperatures exceeding 150 °C the

homopolymerisation of maleimide can occur, which reduces the amount of maleimide available for cross-linking (**Scheme 2.3**). The maximum maleimide absorbance does decrease slightly after each heat which suggests a small amount of this is occurring. Should this cause a significant negative impact on the material, addition of a small radical scavenger such as hydroquinone has been shown to effectively inhibit the homopolymerisation, which is radically initiated. [20]

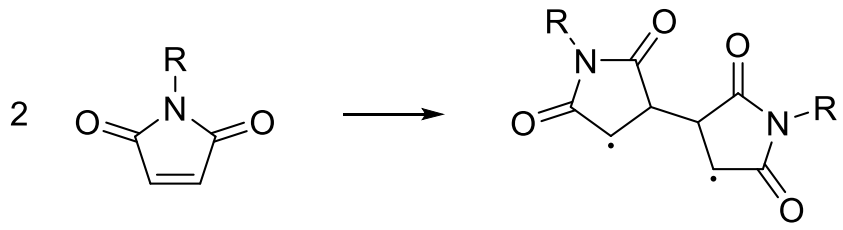

Scheme 2.3 - Maleimide homopolymerisation.

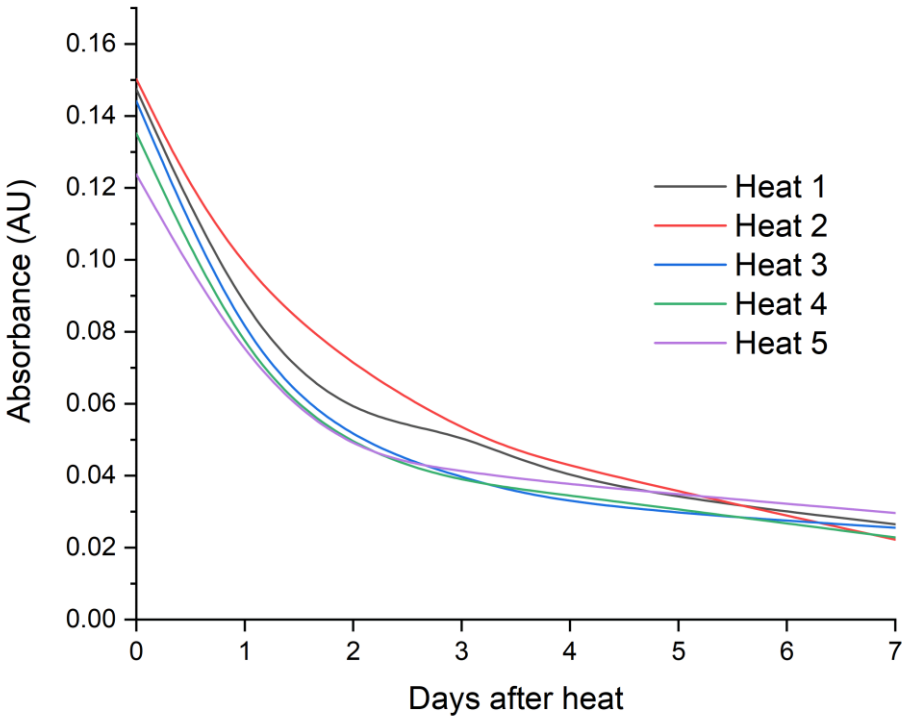

Figure 2.12 - A graph showing the loss in absorbance of the 696 cm^{-1} peak after multiple 150 °C heats.

2.2.5 Gel fraction

The degree of cross-linking can be ascertained by running a 24-hour Soxhlet extraction on the network. Using this method, solvent is continually passed through a sample of the material, washing away any material uninvolved in the network (the sol fraction). A comparison of the sample mass before and after the extraction allows for the gel fraction to be determined (**Table 2.1**).

Table 2.1 - The gel fraction of DA1 in different solvents.

	Boiling point / °C	Gel fraction / %
THF	66	98
Ethyl acetate	77	96
Isopropyl acetate	85	99
Toluene	111	42

The material showed a very high gel fraction, consistently above 95% for the lower boiling solvents, suggesting that practically all the material has been successfully included into the network. However, when using toluene as a solvent, a significantly lower gel fraction is observed. As seen from DSC experiments discussed previously, the value for the T_{rDA} is 115.8 °C at a heating rate of 0.1 °C min^{-1}. The temperature of the boiling toluene in the Soxhlet system will be near this, so it is likely that the network has dissociated and dissolved. In this way, a Soxhlet extraction could be used as a rough guide to the temperature at which the network dissociates; useful information when considering the removal of an adhesive. Swelling degree data would also have been useful, but unfortunately, it was not measured during these experiments. The following equations can be used to give insight into the cross-link density:

$$\text{Solution uptake} = W_{wet} - W_{dry} / W_{dry} \times 100$$

$$\text{Swelling degree} = L_{wet} - L_{dry} / L_{dry} \times 100$$

where W_{wet} and L_{wet} are the weight and length of the wet material after the extraction, while W_{dry} and L_{dry} are the weight and length of the dry material before the extraction, respectively. For cross-linked systems, swelling is a tool to measure the free volume (average) between cross-links and can therefore measure cross-link density. A highly cross-linked polymer will show a less degree of swelling.

2.2.6 Lap shear testing

The infrared experiments proved that the material was able to reform multiple times, but it provides no insight into whether the mechanical properties are maintained. The material, in the form of a 250 µm film, was cut into 25 × 12.5 mm sized pieces, and used to bond two grit-blasted aluminium coupons by assembling the joint and heating for an hour at 125 °C. The joints were cured for 7 days at 23 °C and 50% relative humidity before evaluation. The bond strength was measured by finding the peak stress that the joint can withstand during a lap shear tensile test (**Table 2.2**). The testing showed a high bond strength and concordant results. Although there is adhesive on both parts of the substrate, the failure has occurred mainly at the interface, indicative of adhesive failure (**Figure 2.13**).

Table 2.2 - The bond strength experienced by the sample before failure.

		Bond strength (MPa)
Repeat	1	10.33
	2	10.31
	3	11.20
	4	10.11
Mean		10.49
Standard deviation, σ		0.49

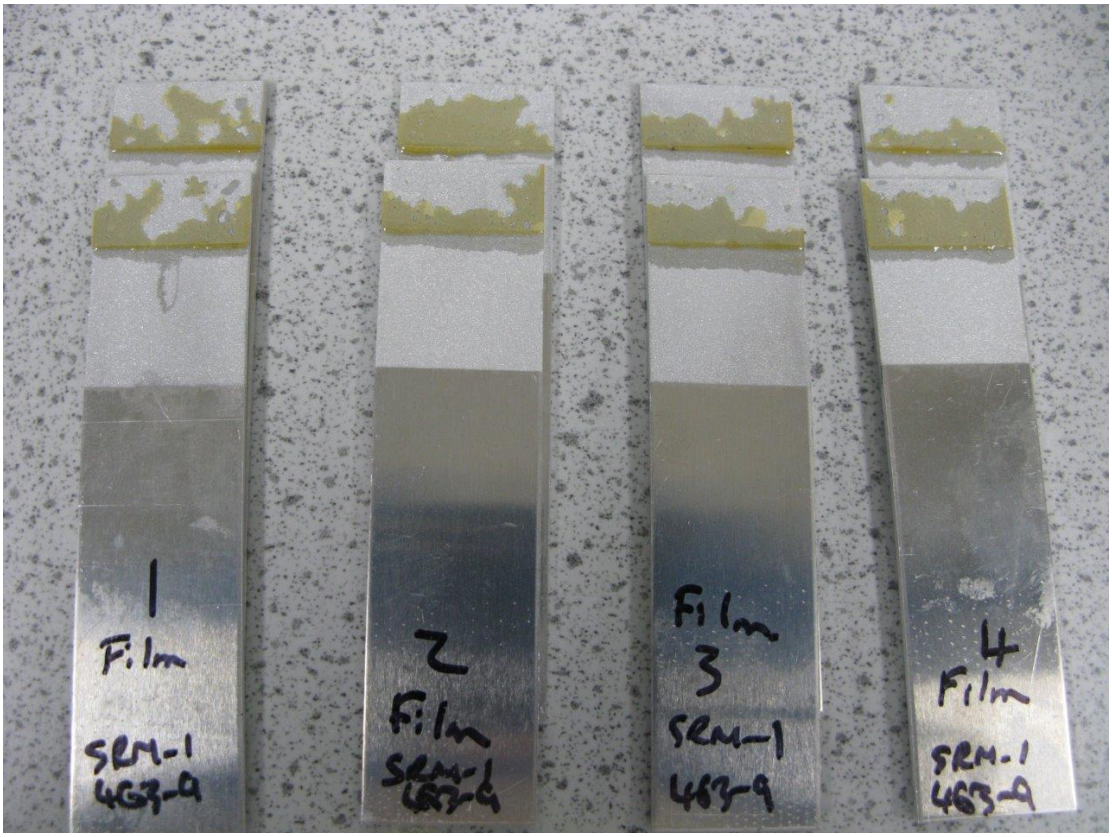

Figure 2.13 - Pairs of aluminium substrates after lap shear testing. The adhesive was applied as a film.

For comparison, a reference moisture-cured adhesive underwent the same testing. This was a one-component PU reactive hot melt adhesive that is widely used for various industrial applications. The irreversible adhesive contains reactive isocyanate functional groups that react with ambient moisture to create irreversible cross-links. Each adhesive was tested on a variety of substrates; acrylonitrile butadiene styrene (ABS), acrylic, poly(vinyl chloride) (PVC), aluminium and wood (**Table 2.3, Figure 2.14**).

Table 2.3 – Comparison of the mechanical properties of the DA network and the reference moisture-cured adhesive on various substrates

Adhesive	Substrate	Bond strength (MPa)	Mean peak strain (%)	Failure mode
Moisture-cured adhesive	ABS	5.44	11.47	Adhesive
	Acrylic	7.52	12.13	Adhesive
	PVC	5.85	11.13	Adhesive
	Aluminium	4.45	9.20	Mixed
	Wood	5.15	-	-
DA network	ABS	5.19	4.83	Adhesive
	Acrylic	2.28	2.11	Mixed
	PVC	11.91	9.83	Mixed
	Aluminium	10.49	10.85	Adhesive
	Wood	4.85	-	-

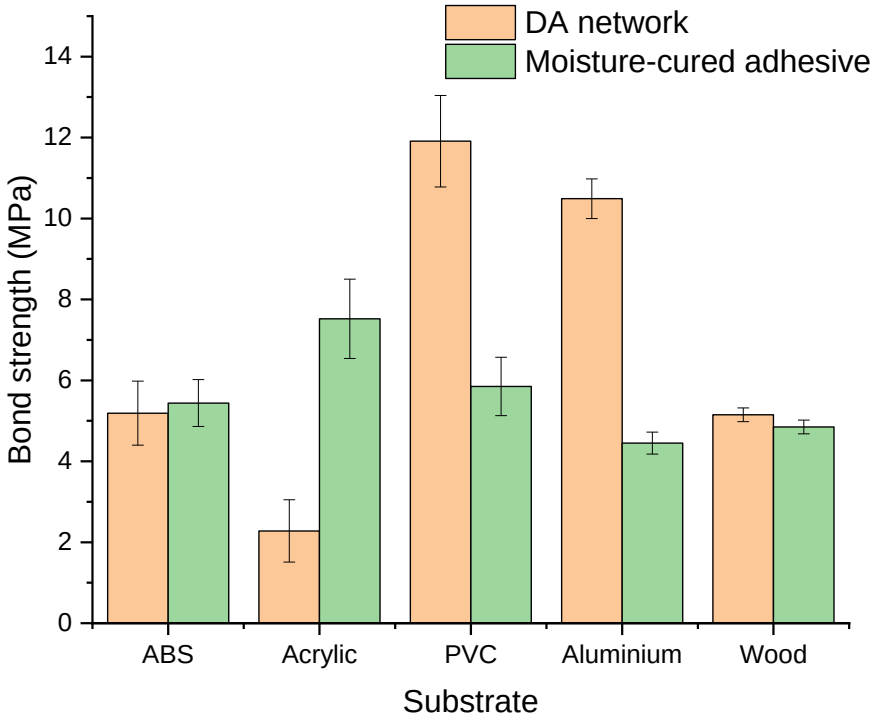

Figure 2.14 – Comparison of the mechanical properties of the DA network and the reference moisture-cured adhesive on various substrates

The DA network provided similar or better performance on the majority of the substrates. The failure mode was mostly adhesive, which means that the integrity of both networks are very strong, and the differences in bond strength arises from the bonding of the adhesive to the substrate.

A significant advantage the DA network has over the reference is that its network is not permanent, and so can be used to rebond the samples again. This was done by realigning the broken joints and clamping, then heating it to 125 °C for an hour to dissociate the network into the lower molecular weight prepolymers and wet the substrate. The joints then underwent the same curing process as previous, before evaluating again. The joints were rebonded four times. The adhesive was able to maintain its high bond strength over all subsequent cycles, proving that the adhesive can be reused without the bond strength deteriorating (**Table 2.4, Figure 2.15**). This would be particularly useful in

situations where components are glued together and need to be separated for a repair or service before being replaced.

Table 2.4 - Average peak stress experienced by the rebonded samples before failure.

Adhesive	Bond strength (MPa)				
	Initial bond	Rebond 1	Rebond 2	Rebond 3	Rebond 4
DA network	10.49	10.46	11.43	11.49	9.85

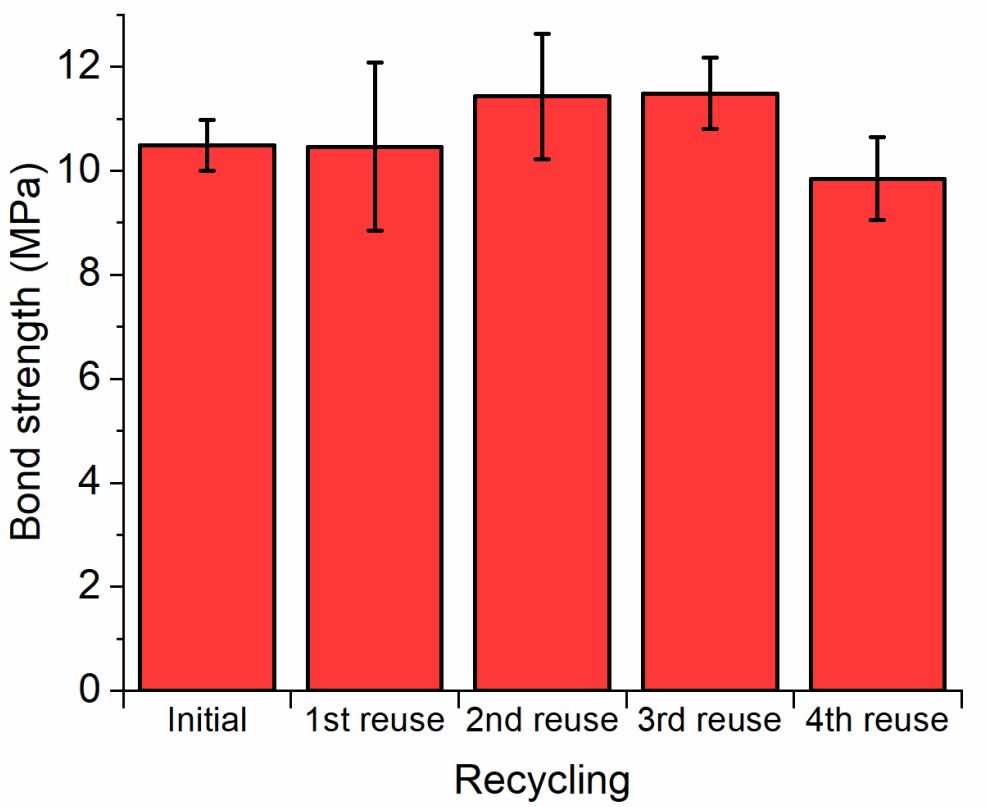

Figure 2.15 - Average bond strength experienced by the rebonded samples before failure.

2.3 Conclusions

A covalent adaptable network cross-linked with maleimide-furan Diels-Alder cycloadducts were synthesised by melt blending a bismaleimide and a trifunctional furan and coating at moderate

temperatures followed by curing in ambient conditions. Diels-Alder cycloaddition was confirmed through characterisation with FTIR spectroscopy, and the presence of Diels-Alder linkages was confirmed by the appearance of a retro-Diels-Alder endotherm in the DSC thermogram. Furthermore, the materials also displayed excellent network reformation properties, returning to near its original cross-link density 7 days after melting, or more rapidly if conditioned at 60 °C. This behaviour was easily reproduced over 5 repeated heating cycles, which is a good indication that the material can be reused.

The stereochemistry of the Diels-Alder product under different conditions was investigated, and it was discovered that ambient temperatures did not provide enough energy to form the thermodynamic *exo* product, instead forming the kinetic *endo* product. The *exo* product can be formed preferentially by conditioning at >50 °C.

Formation of a network was confirmed by running a Soxhlet extraction on the materials. The material did not dissolve indicating successful cross-linking. Once the temperature of the solvent was similar to the rDA of the material, the network dissociated and was able to be dissolved.

The CAN provided versatile adhesion on many substrates, and even outperformed a commercial moisture-curing adhesive on some substrates, such as PVC and aluminium. It was shown that the CANs can be re-used repeatedly producing the same level of performance by heating/cooling cycles of bulk materials without the need for solvents or any additional processing steps to recover the networks.

To conclude, this chapter has demonstrated the bond strength and reusability of networks comprising Diels-Alder bonds, and provided insight to develop these concepts further into different systems.

2.4 Bibliography

1 A. Gandini, *Prog Polym Sci*, 2013, **38**, 1–29.

2 N. Kuramoto, K. Hayashi and K. Nagai, *J Polym Sci A Polym Chem*, 1994, **32**, 2501–2504.

3 X. Chen, M. A. Dam, K. Ono, A. Mal, H. Shen, S. R. Nutt, K. Sheran and F. Wudl, *Science (1979)*, 2002, **295**, 1698–1702.

4 J. H. Aubert, *Journal of Adhesion*, 2003, **79**, 609–616.

5 A. A. Kavitha and N. K. Singha, *ACS Appl Mater Interfaces*, 2009, **1**, 1427–1436.

6 M. Wouters, M. Burghoorn, B. Ingenhut, K. Timmer, C. Rentrop, T. Bots, G. Oosterhuis and H. Fischer, *Prog Org Coat*, 2011, **72**, 152–158.

7 S. Das, S. Samitsu, Y. Nakamura, Y. Yamauchi, D. Payra, K. Kato and M. Naito, *Polym Chem*, 2018, **9**, 5559–5565.

8 D. H. Turkenburg, H. van Bracht, B. Funke, M. Schmider, D. Janke and H. R. Fischer, *J Appl Polym Sci*, 2017, **134**, 1–11.

9 E. Dolci, G. Michaud, F. Simon, B. Boutevin, S. Fouquay and S. Caillol, *Polym Chem*, 2015, **6**, 7851–7861.

10 E. Dolci, V. Froidevaux, G. Michaud, F. Simon, R. Auvergne, S. Fouquay and S. Caillol, *J Appl Polym Sci*, 2017, **134**, 1–11.

11 K. M. A. Kaiser, *J Appl Polym Sci*, 2020, 1–12.

12 A. M. Schenzel, C. Klein, K. Rist, N. Moszner and C. Barner-Kowollik, *Advanced Science*, 2016, **3**, 1500361.

13 J. A. Brydson, *Plastics Materials*, 1999, 810–813.

14 L. M. Sridhar, M. O. Oster, D. E. Herr, J. B. D. Gregg, J. A. Wilson and A. T. Slark, *Green Chemistry*, 2020, **22**, 8669–8679.

15 D. H. Turkenburg, H. van Bracht, B. Funke, M. Schmider, D. Janke and H. R. Fischer, *J Appl Polym Sci*, 2017, **134**, 1–11.

16 S. F. Parker, *Spectrochim Acta A Mol Biomol Spectrosc*, 1995, **51**, 2067–2072.

17 Z. Stirn, A. Rucigaj and M. Krajnc, *Express Polym Lett*, 2016, **10**, 537–547.

18 V. Froidevaux, M. Borne, E. Laborbe, R. Auvergne, A. Gandini and B. Boutevin, *RSC Adv*, 2015, **5**, 37742–37754.

19 R. B. Cassel, *How Tzero™ Technology Improves DSC Performance Part V: Reducing Thermal Lag*, .

20 B. T. McReynolds, K. D. Mojtabai, N. Penners, G. Kim, S. Lindholm, Y. Lee, J. D. McCoy and S. Chowdhury, *Polymers (Basel)*, 2023, **15**, 1106.

3 Diels-Alder cycloadducts as chain extenders in reversible polyurethane adhesives

3.1 Introduction

One of the most common adhesives in industry are one-component moisture-curing adhesives. Classified as a polyurethane (PU) adhesive, the low molecular weight, linear polymer molecules are formed from the step-growth polymerisation reaction between polyisocyantes and a di- or polyfunctional hydroxyl. They contain free reactive isocyanate (NCO) groups that cure in the presence of moisture from the surrounding environment to form permanent urea linkages, eliminating the need for additional curing agents or external heat sources.[1] The electrophilic attack of water on the isocyanate group creates an amine and releases CO_2 (**Scheme 3.1a**). The amine can then react with an isocyanate on another chain, to form a urea linkage and a higher molecular weight linear chain (**Scheme 3.1b**). The material can then cross-link by a reaction between the urea and another isocyanate to form a biuret (**Scheme 3.1c**).[2]

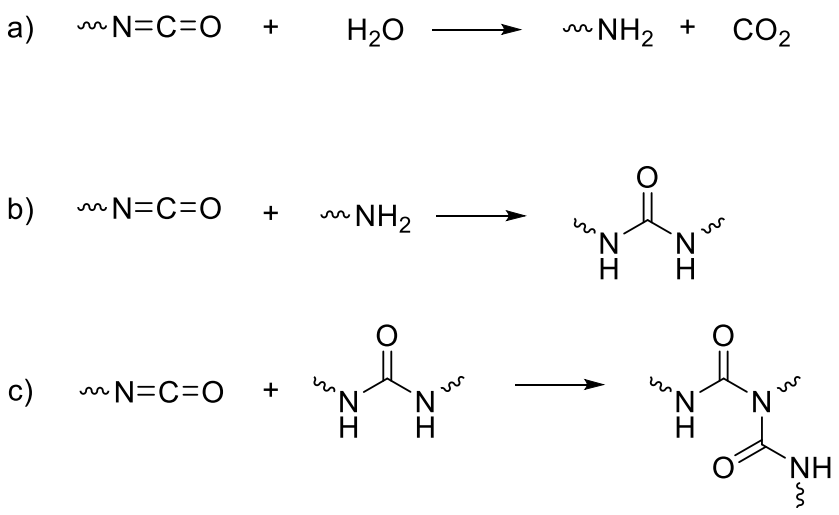

Scheme 3.1 - Reaction mechanism for moisture curing adhesives.

The high reactivity of the isocyanate allows these robust bonds to form rapidly, and they are particularly resistant to heat changes, solvents, and ultraviolet radiation, making them suitable for both indoor and outdoor use. Moisture-curing adhesives are able to bond to a variety of substrates such as metals,[3] plastics,[4] wood,[5] and various porous and non-porous materials,[6] meaning they can be utilised across many industries such as automotive,[7] aerospace,[8] construction,[9] electronics,[7] and medical devices.[10]

All these benefits have made moisture-curing adhesives the preferred choice for many professionals looking to bond dissimilar materials, assemble components or seal joints. Although they provide reliable and durable bonds in demanding environments, it presents difficulty at their end-of-life when components need to be replaced or separated for recycling. In this chapter, this issue is tackled by using the reactive isocyanate groups to incorporate dynamic bonds into the system, creating an adhesive that has the ability to debond on demand (**Scheme 3.2**).

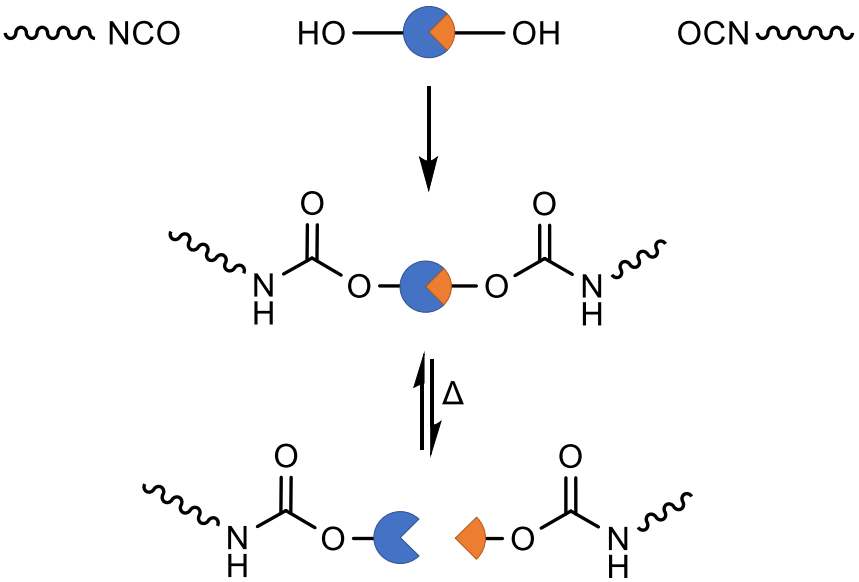

Scheme 3.2 - A moisture-curing adhesive being cross-linked by a dynamic chain extender, which can be separated by heating.

Instead of reacting with atmospheric water and forming permanent cross-links, the NCO can react with a hydroxyl-functionalised chain extender containing a Diels-Alder (DA) adduct. The inherent

dynamic bond makes it possible to switch the adhesive between its cured and uncured state, facilitating its removal from the substrate prior to recycling. This concept allows any moisture-curing adhesive that would typically become a thermoset to become a covalent adaptable network (CAN). To illustrate this idea, two functional chain extenders were synthesised based on the Diels-Alder (DA) adduct of furan and maleimide (**Scheme 3.3**), containing different amounts of OH-functionality to react with the isocyanate groups of the prepolymer. The DA chain extender can uncouple at elevated temperatures to return the polymer chain to its lower molecular weight prepolymers.

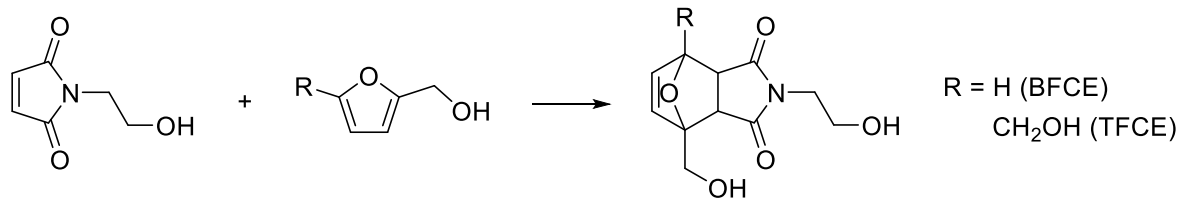

Scheme 3.3 – The functional chain extenders used in this chapter.

Despite maleimides and furans first being used to cross-link polymers over 40 years ago by Stevens *et al*, this will be the first time a hydroxyl-functionalised chain extender bearing a DA adduct within the backbone will be used to synthesise self-healing polymers.[11] The closest related work was performed by Haddleton *et al*, who prepared polymerisation initiators and a dimethacrylic cross-linker containing DA adducts.[12] More commonly, self-healing polymers are prepared by combining multi-maleimides and multi-furans, as demonstrated by Wudl *et al* in 2002.[13] In this form, the fractured polymers were able to recover 83% of their original strength after a 120 °C heat. The polymer can also be made by combining a furan-maleimide A-B monomer.[14] In this work by Gandini, the maleimide functionality was protected by a furan initially, which had to be deprotected *in situ* before the first DA polymerisation. After this, the polymer could be depolymerised by heating to the retro Diels-Alder temperature (T_{rDA}) and a second polymerisation was favoured after cooling to 65 °C.

3.2 Results and discussion

Two different chain extenders were synthesised by the DA addition of the dienophile *N*-(2-hydroxyethyl)maleimide (HEMI) to either furfuryl alcohol or bishydroxymethylfuran (BHMF). HEMI is commercially available but expensive, so was synthesised from maleic anhydride and ethanolamine.[15] The addition of furfuryl alcohol creates the bifunctional chain extender (BFCE) 4,7-Epoxy-1*H*-isoindole-1,3(2*H*)-dione, 3a,4,7,7a-tetrahydro-2-(2-hydroxyethyl)-4-(hydroxymethyl) and the addition of BMHF creates the trifunctional chain extender (TFCE) 4,7-Epoxy-1*H*-isoindole-1,3(2*H*)-dione, 3a,4,7,7a-tetrahydro-2-(2-hydroxyethyl)-4,7-dihydroxymethyl. Chain extending with BFCE will lead to linear polymer chains being made whereas the TFCE will form a network. Furan and maleimide groups are well-studied DA pairs and react quickly at ambient temperatures, making them an appropriate choice to functionalise a commercial grade moisture-curing prepolymer.

3.2.1 Synthesis of *N*-(2-Hydroxyethyl)maleimide (HEMI)

The alkene of maleic anhydride was first protected by the addition of furan through a DA addition reaction to prevent the hydroamination of the anhydride unsaturation in the following step (**Scheme 3.4**).

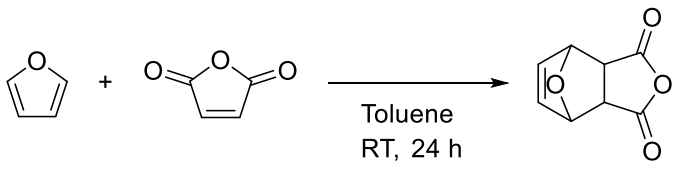

1

Scheme 3.4 – Cycloaddition of furan to maleic anhydride.

The product **1** was a white precipitate that was confirmed *via* ^{1}H nuclear magnetic resonance (NMR) spectroscopy (**Figure 3.1**).

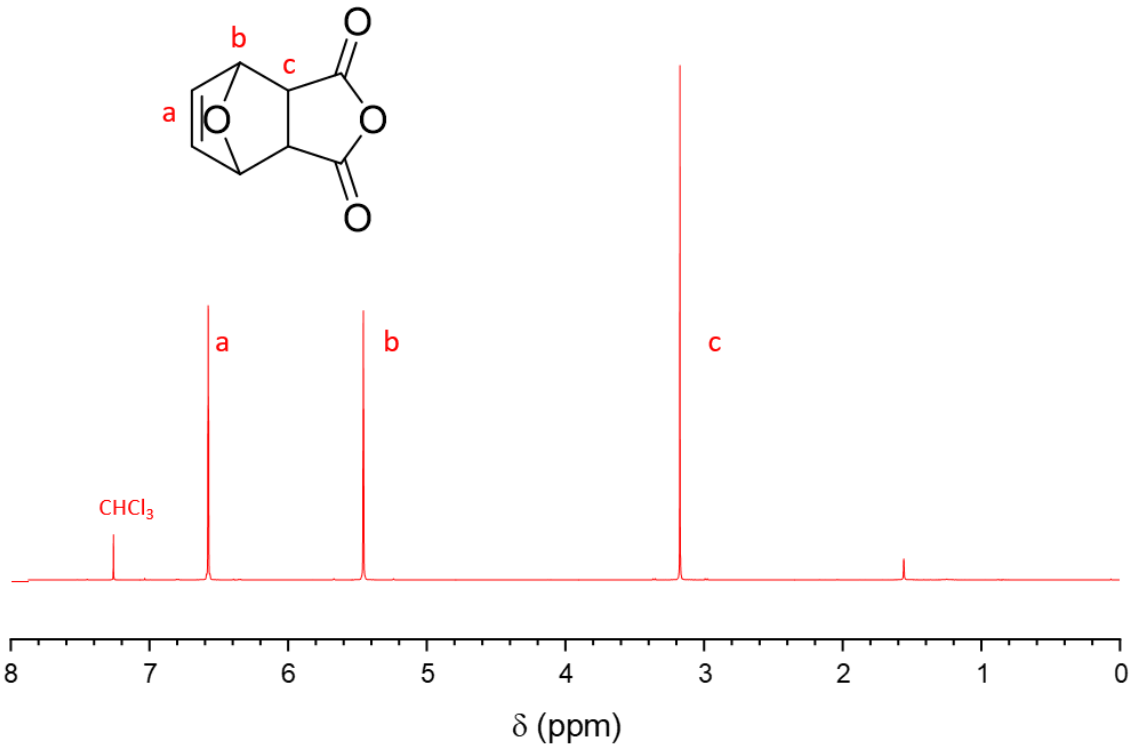

Figure 3.1 - ^{1}H NMR spectrum of the furan and maleic anhydride cycloadduct (400 MHz, $CDCl_3$, 298 K).

The anhydride on **1** is ring-opened by a nucleophilic attack from the ethanolamine (ETA) on the carbonyl carbon, followed by a ring-closure *via* a second nucleophilic attack on the other carbonyl (**Scheme 3.5**). The solution was refluxed for 24 hours before recrystallizing over 48 hours in a fridge. The crystals were filtered and dried and their structure confirmed *via* ^{1}H NMR spectroscopy (**Figure 3.2**).

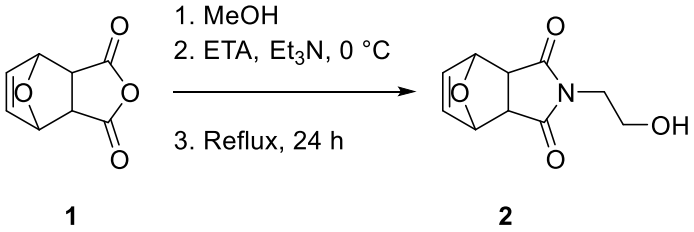

Scheme 3.5 – Addition of ethanolamine to maleic anhydride.

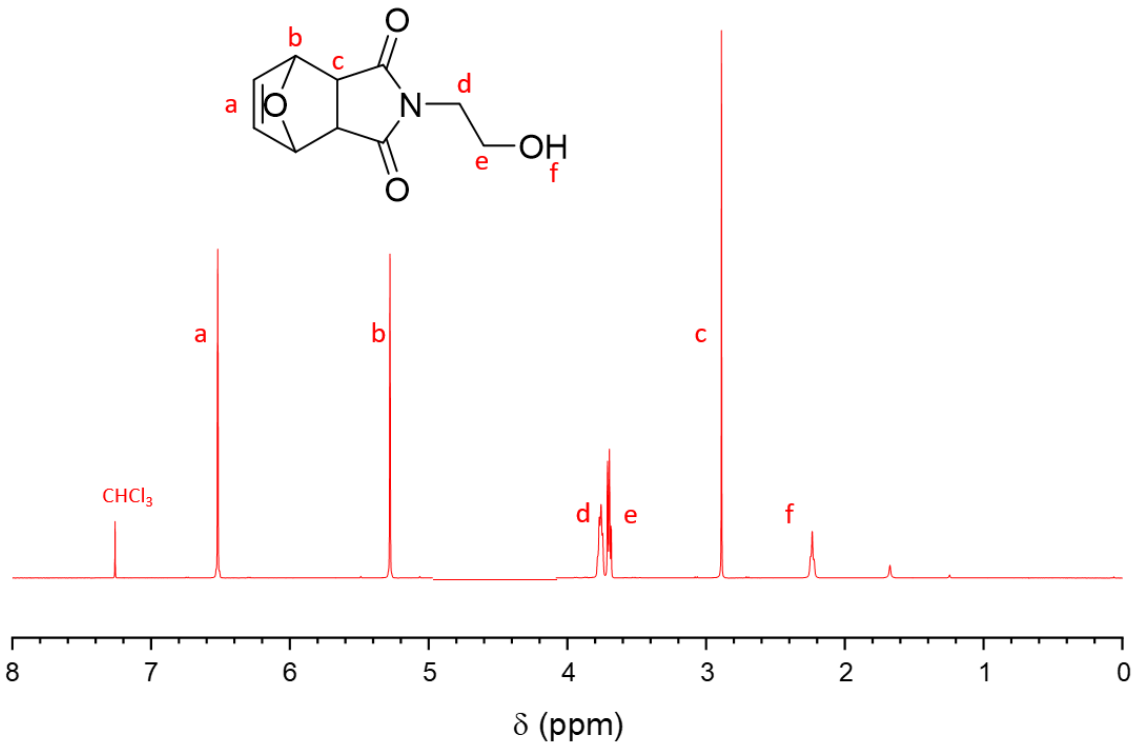

Figure 3.2 - ^{1}H NMR spectrum of the furan and maleic anhydride cycloadduct with the addition of ethanolamine (400 MHz, $CDCl_3$, 298 K).

N-(2-Hydroxyethyl)maleimide (HEMI) was then isolated by the removal of the furan through the retro-Diels-Alder reaction, wherein the crystals from the previous step were refluxed in toluene for 48 hours, at which point all the furan had been removed as a result of its volatility (**Scheme 3.6**). On a larger scale, it would be highly beneficial to recover the furan through distillation, so that it can be recycled to maximise reaction efficiency. When the solution was cooled to room temperature, the HEMI precipitated out as a white solid and characterised *via* ^{1}H NMR spectroscopy (**Figure 3.3**).

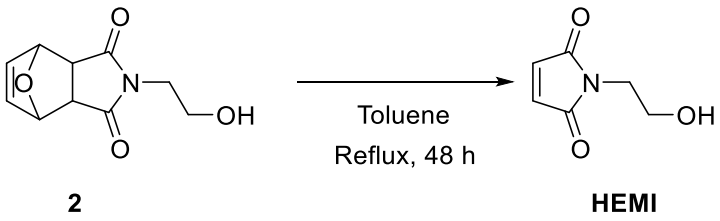

Scheme 3.6 – Removal of furan.

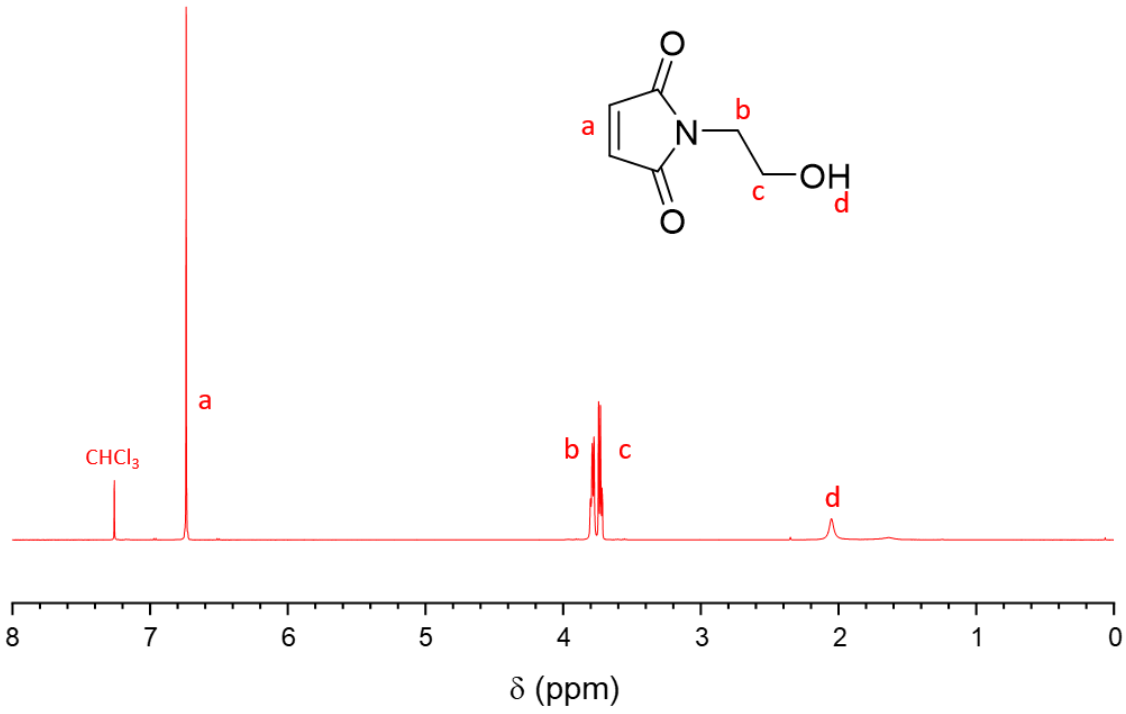

Figure 3.3 - ^{1}H NMR spectrum of HEMI (400 MHz, $CDCl_3$, 298 K).

3.2.2 Synthesis of a bifunctional chain extender (BFCE)

To synthesise BFCE, HEMI and furfuryl alcohol was heated to 80 °C in toluene for 24 hours, during which the product precipitated out as a white solid (**Scheme 3.7**). The product was vacuum filtered, washed with ethyl acetate and dried overnight in a vacuum oven. The final product was fully characterised by ^{1}H and ^{13}C NMR spectroscopy and homonuclear correlation spectroscopy (COSY) in d_6-DMSO (**Figures 3.4, 3.5 and 3.6**).

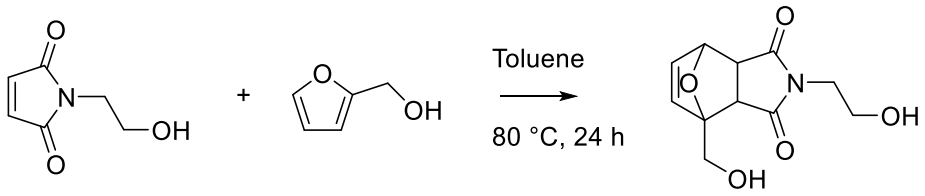

Scheme 3.7 – Addition of furfuryl alcohol to HEMI to form BFCE.

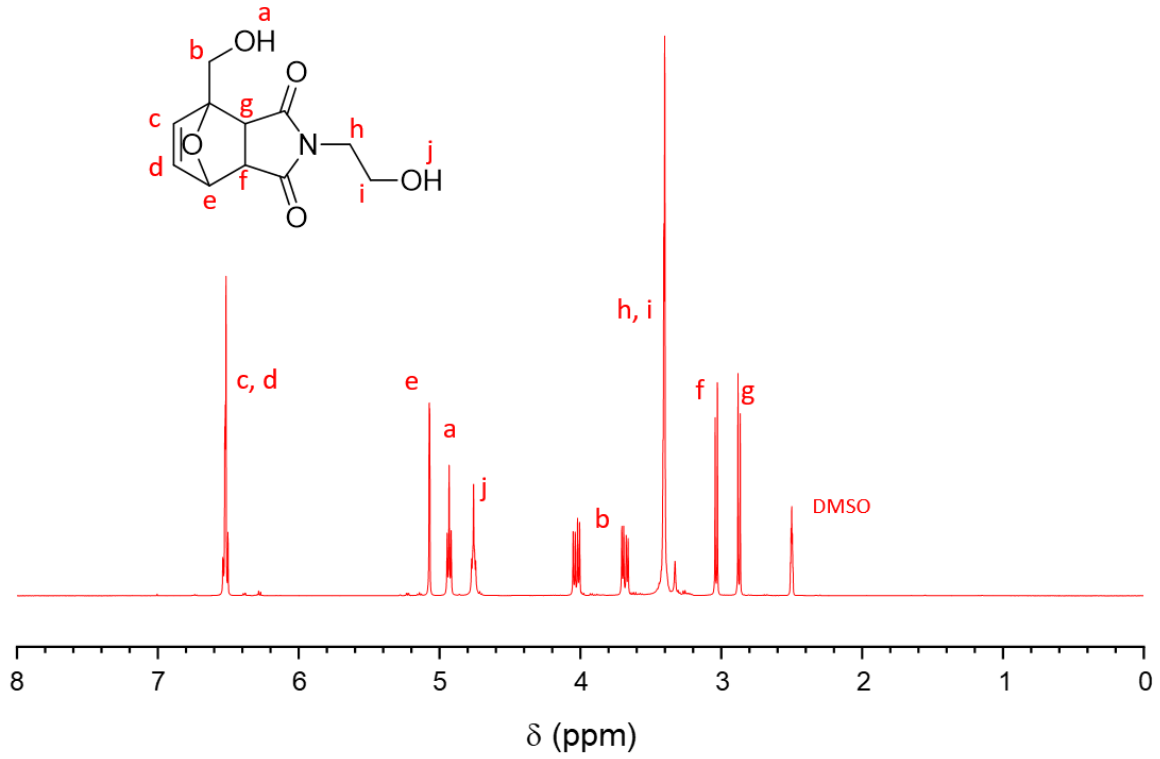

Figure 3.4 - ^{1}H NMR spectrum of BFCE (400 MHz, d_6-DMSO, 298 K).

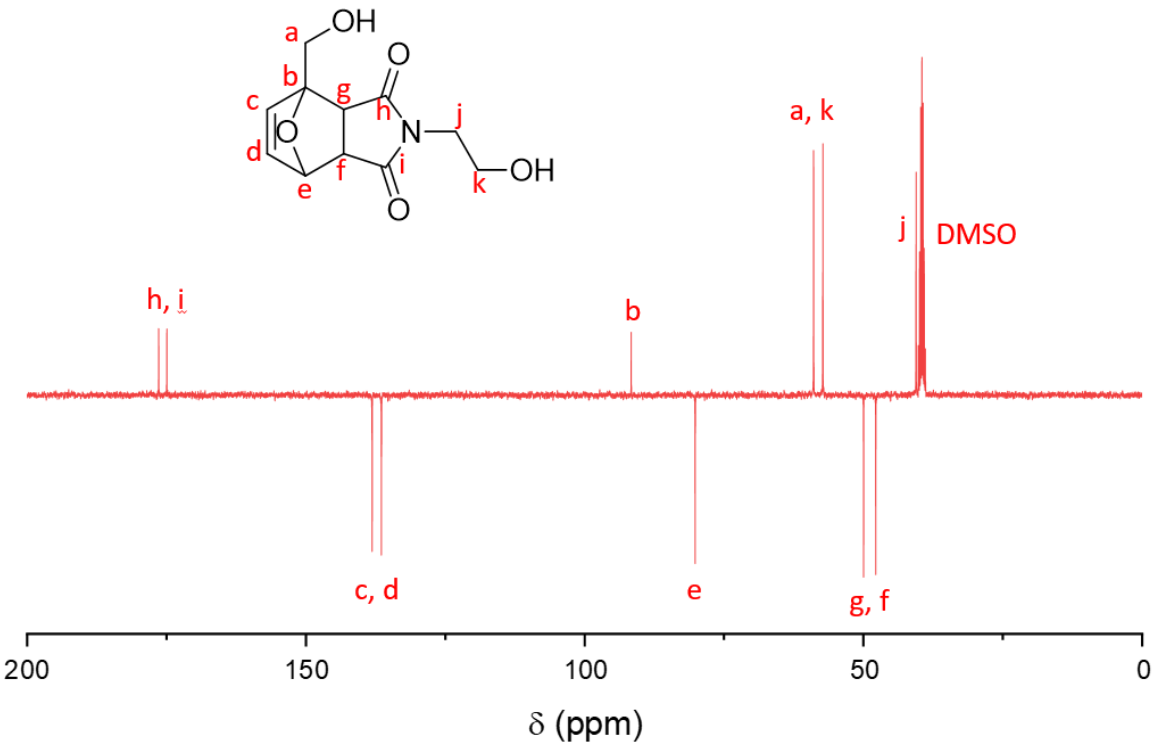

Figure 3.5 – DEPT ^{13}C NMR spectrum of the BFCE (125 MHz, d_6-DMSO, 298 K).

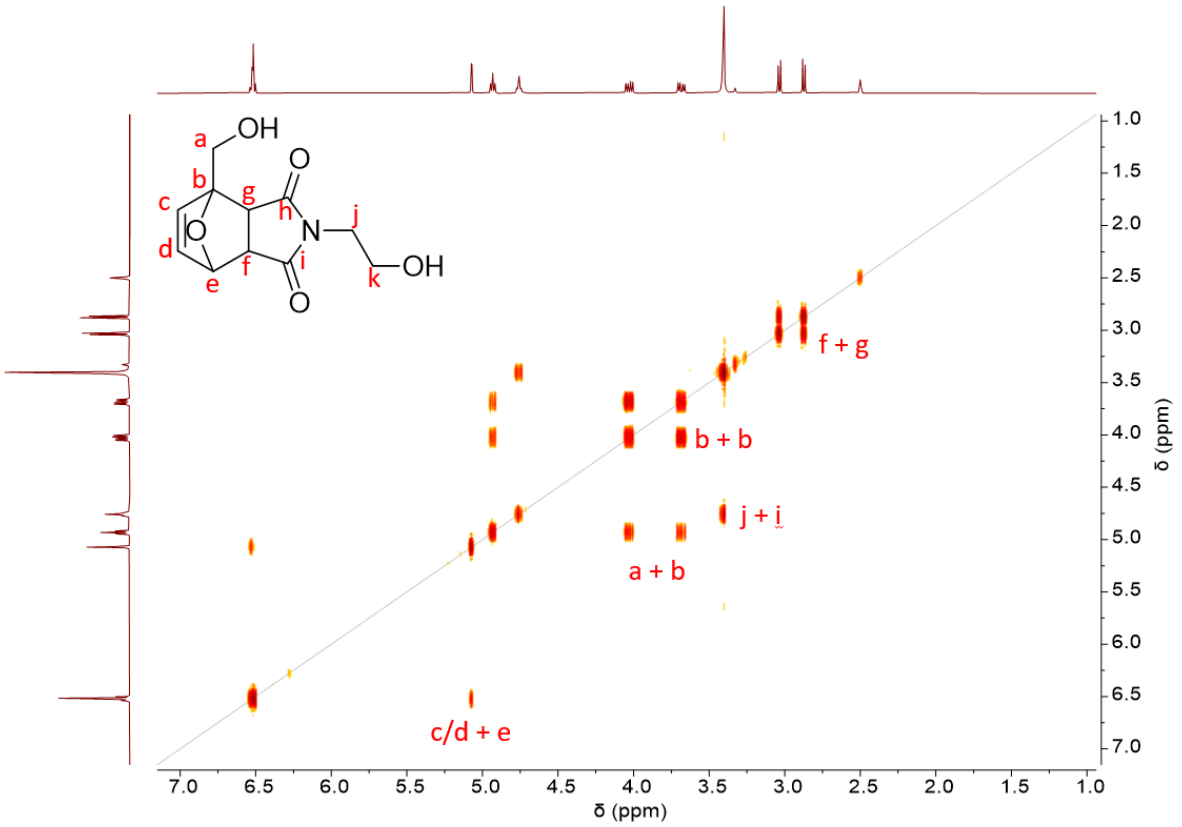

Figure 3.6 - ^{1}H COSY NMR spectrum of the BFCE (400 MHz, d_6-DMSO, 298 K).

BFCE was scanned *via* differential scanning calorimetry (DSC) (**Figure 3.7**). The retro-Diels-Alder (rDA) endotherm from the chain extender uncoupling appears at 113 °C. HEMI and furfuryl alcohol are now observed, and the endotherm from their evaporation is seen. The evaporation of furfuryl alcohol (b.p. = 171 °C) is at 155 °C followed by degradation of the molecule or the homopolymerisation of the maleimide.

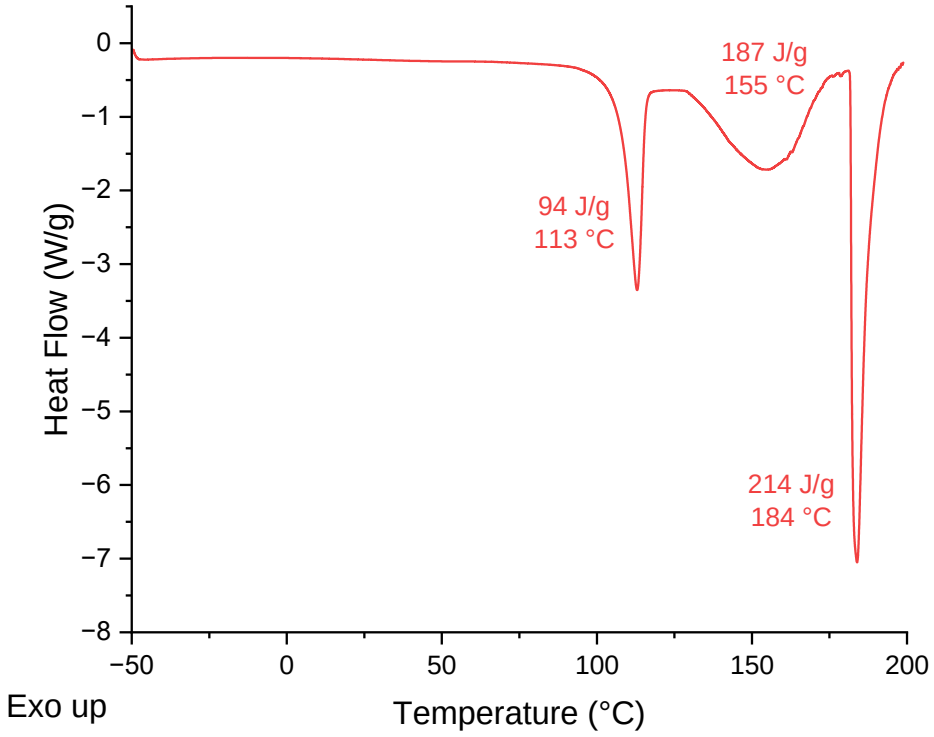

Figure 3.7 – DSC thermogram of BFCE.

3.2.3 Synthesis of a trifunctional chain extender (TFCE)

HEMI and bishydroxymethylfuran (BHMF) were melt blended at 85 °C in an equimolar ratio whilst stirring (**Scheme 3.8**). After 1 hour, they had become homogenous and the mixture was allowed to cool.

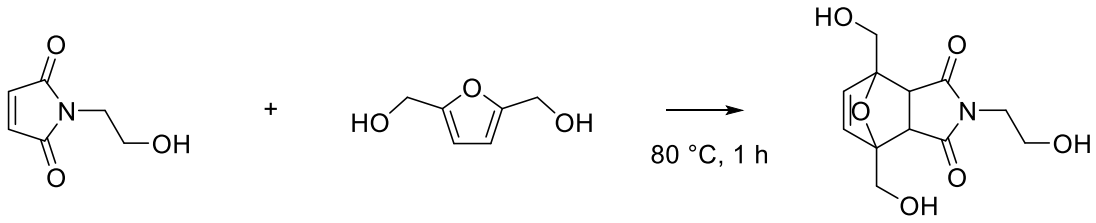

Scheme 3.8 – Addition of furfuryl alcohol to BHMF to form TFCE.

The final solid was characterised *via* ^{1}H NMR and ^{13}C spectroscopy (**Figures 3.8, 3.9**). TFCE contains additional resonances in the NMR spectrum, a result of both *exo* and *endo* isomers being formed.[16] It

is interesting that the bifunctional chain extender behaves differently, however it has been shown that the presence of specific groups on either heterocycle, such as carboxylate, amide and hydroxyl functions, can considerably affect the rates of these DA couplings.[17]

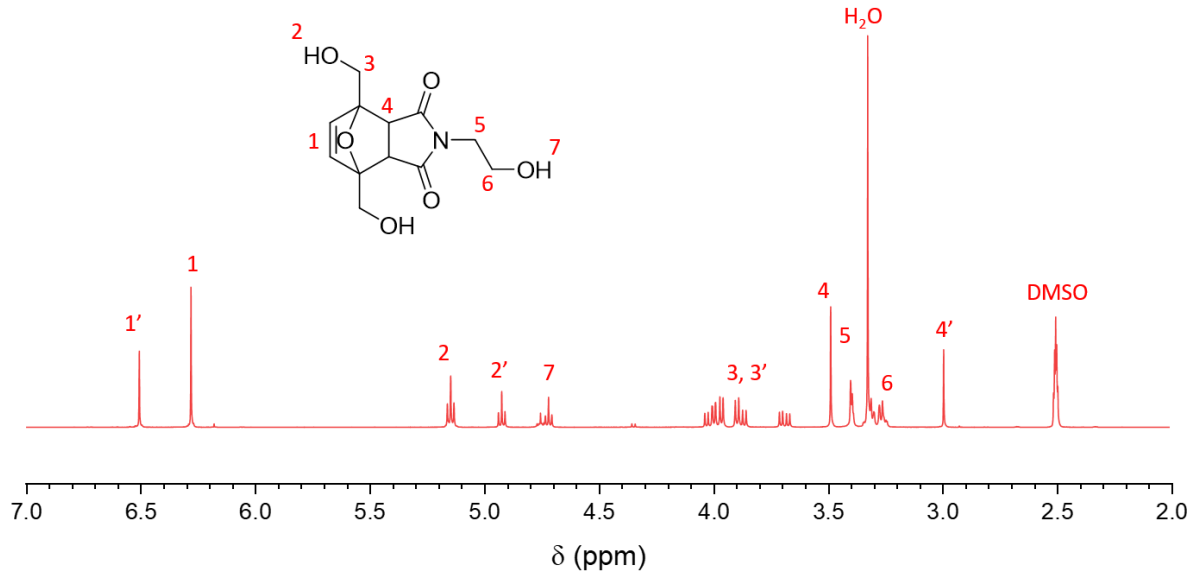

Figure 3.8 - ^{1}H NMR spectrum of TFCE (400 MHz, d_6-DMSO, 298 K). Signals 1-4 and 1'-4' correspond to endo and exo products, respectively.

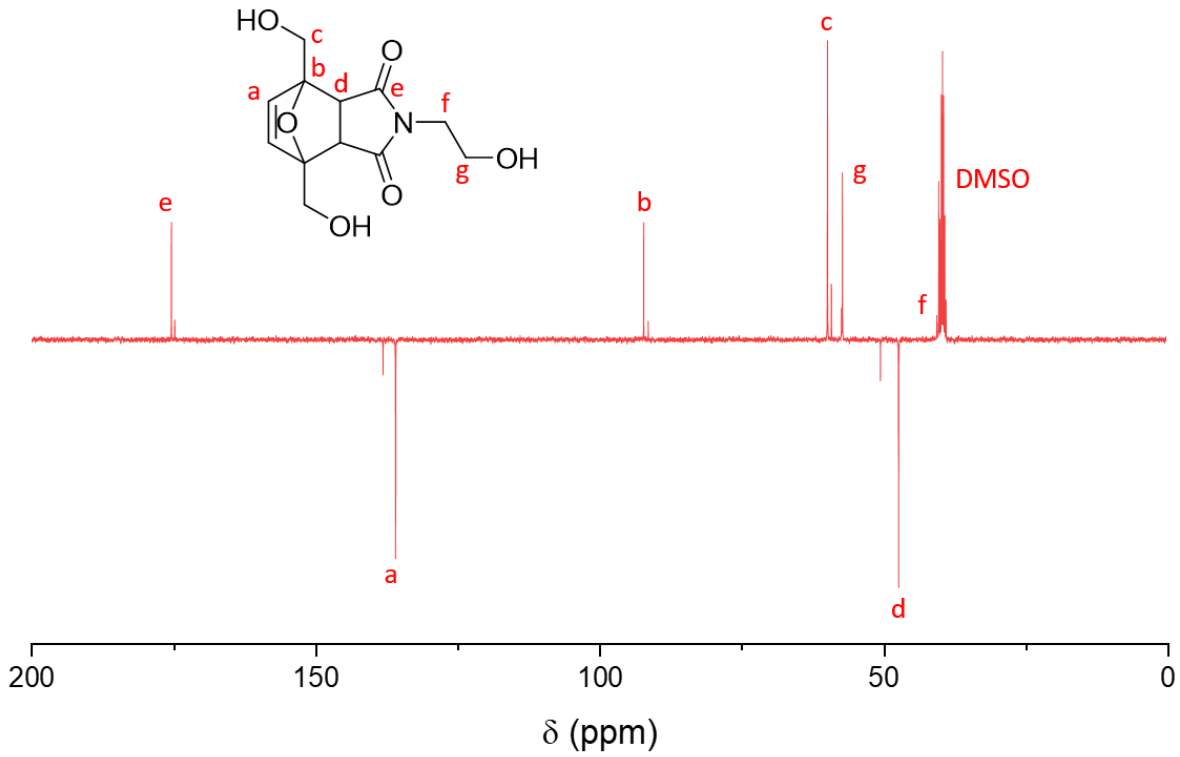

Figure 3.9 – DEPT ^{13}C NMR spectrum of the TFCE (125 MHz, d_6-DMSO, 298 K).

When analysed by DSC, TFCE was observed to be similar to BFCE, with the rDA endotherm at 110 °C (**Figure 3.10**). The next endotherm is either from homopolymerisation of the maleimide or from the molecule degrading as there is no furfuryl alcohol to evaporate and BHMF has a boiling point of 275 °C.

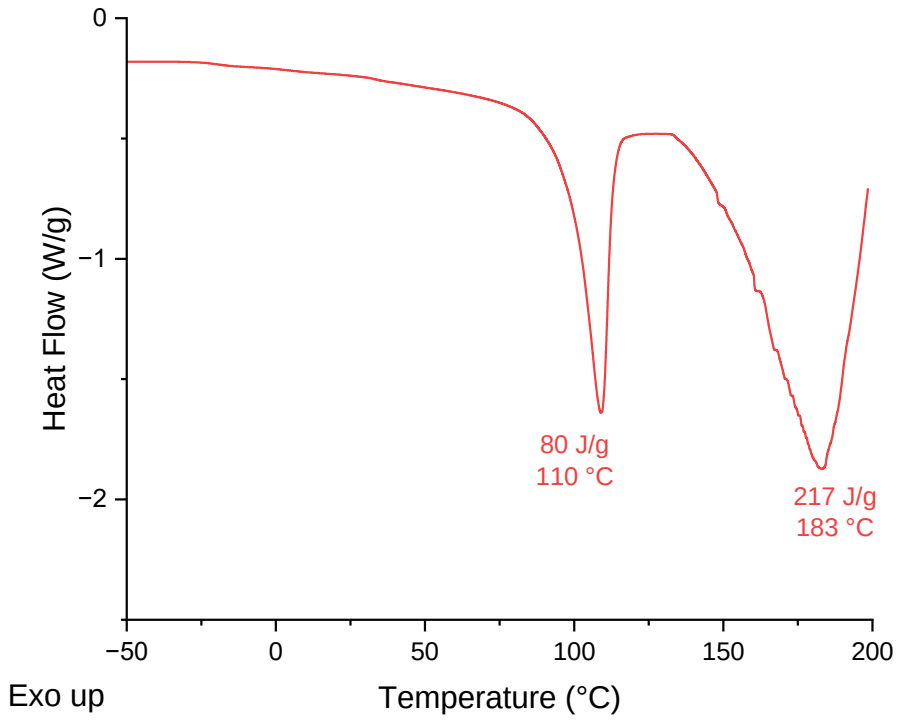

Figure 3.10 – DSC thermogram of TFCE.

3.2.4 Synthesis of moisture-curing polyurethanes

3.2.4.1 Linear DA chains

Priplast™ 1838 is a versatile bio-based polyol with a molecular weight of 2000 g mol^{-1} and is therefore an appropriate starting material for a sustainable adhesive. The polyol can be functionalised through the urethane reaction with 4,4'-diphenylmethane diisocyanate (MDI) with the subsequent addition of the DA chain extender to create the linear chains (**Scheme 3.9**).

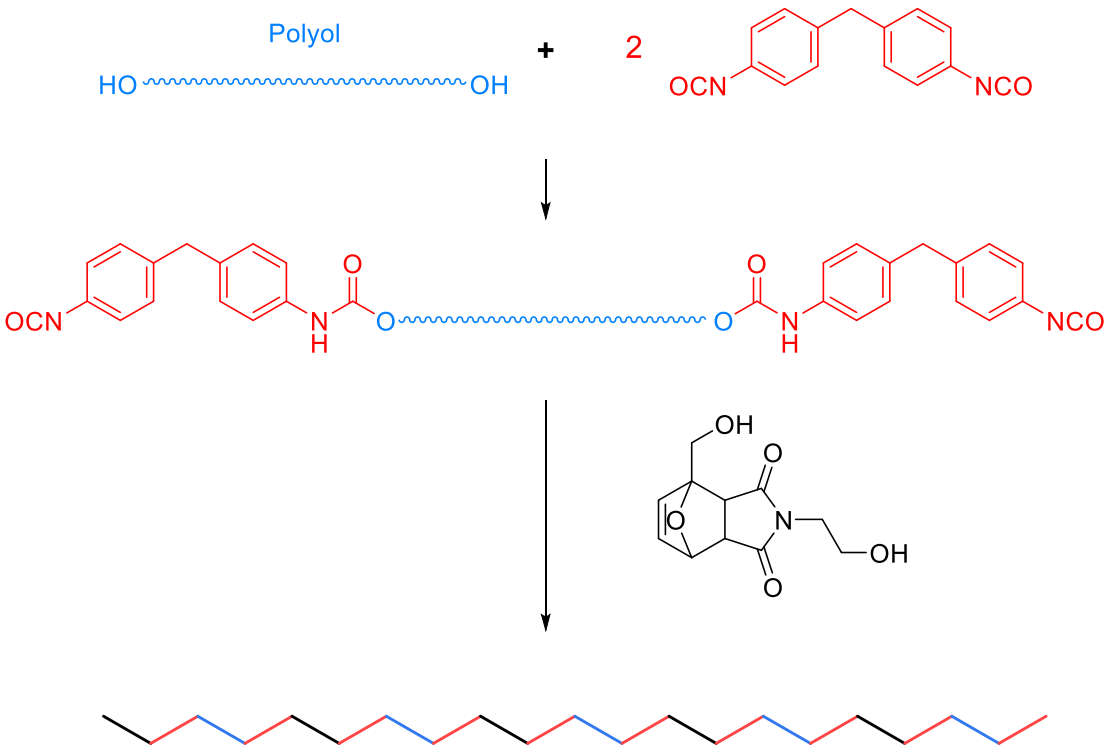

Scheme 3.9 – The steps involved to generate the linear polymer chain with Diels-Alder moieties.

The NCO-terminated prepolymer was synthesised through a step-growth polymerisation. The polyol was heated to 110 °C under vacuum for an hour in oven-dried glassware to remove any residual moisture. 2 equivalents of MDI were then added to the mixture and the vacuum reapplied to yield the isocyanate-terminated prepolymer. 1.3 equivalents (w.r.t. polyol) of the bifunctional chain extender was then added to end-cap the prepolymer. The reaction mixture was monitored periodically *via* Fourier transform infrared (FTIR) spectroscopy and the reaction ended after 3 hours when the NCO resonance at 2200 cm^{-1} stopped decreasing. The NCO resonance did not fully disappear but it was a significant decrease when compared to the NCO-terminated prepolymer (**Figure 3.11**). The final material was able to be spread as a 250 µm film, which cooled and became elastomeric.

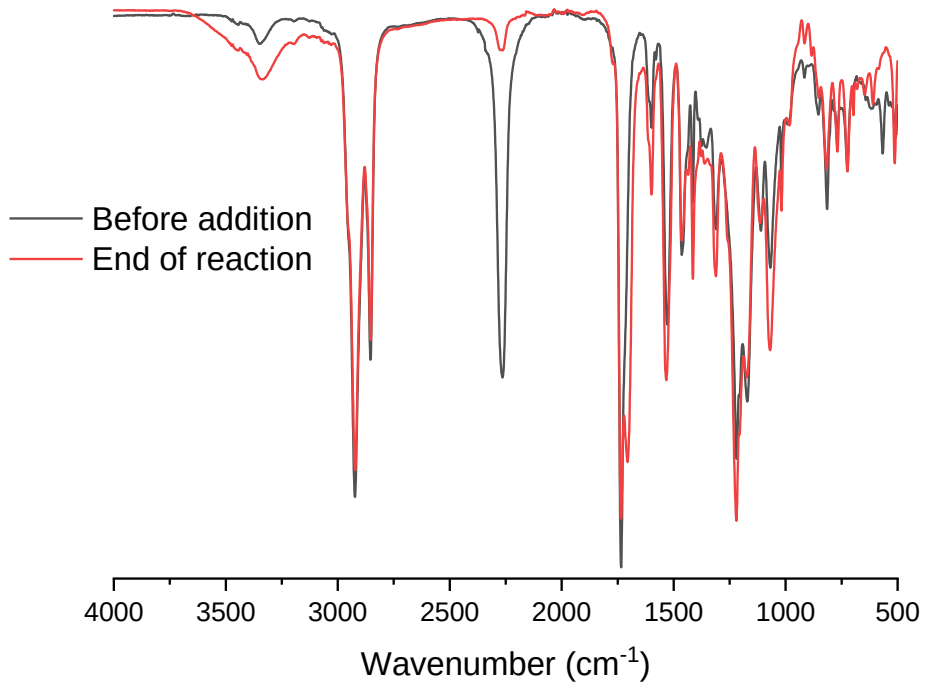

Figure 3.11 – IR spectra showing the difference in size of the 2200 cm^{-1} isocyanate peak before addition of the bifunctional chain extender and at the end of the reaction.

After at least a week to equilibrate, the materials were analysed *via* DSC to look for the presence of the retro-Diels-Alder (rDA) endotherm (**Figure 3.12**). There was a clear rDA endotherm at 141 °C, commonly attributed to the maleimide and furan decoupling. The two endotherms suggests the DA adducts have adopted both the *exo* and *endo* arrangements. The more thermodynamically stable *exo* isomer has the higher rDA temperature.

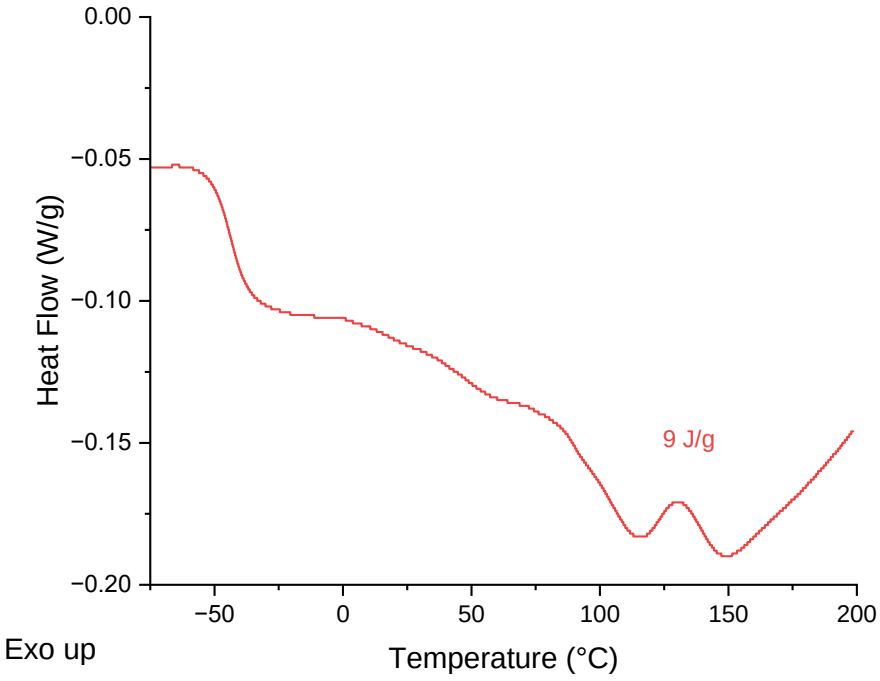

Figure 3.12 – DSC thermogram of the linear chains.

Thermogravimetric analysis (TGA) shows the material to be thermally stable well beyond the T_{rDA}, with 5% of its mass degrading ($T_{deg5\%}$) by 276 °C (**Figure 3.13**).

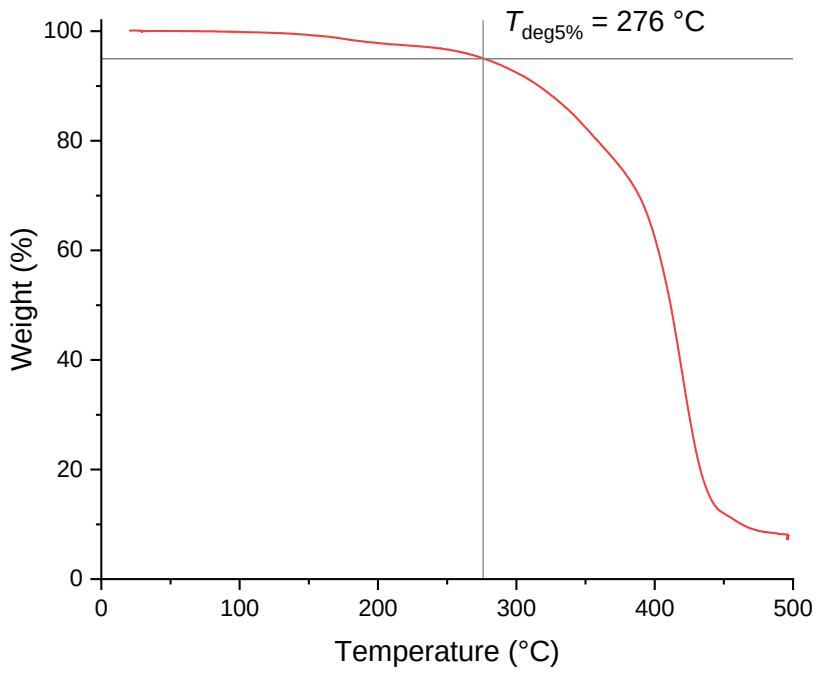

Figure 3.13 - TGA analysis of the linear DA chains.

The ability for the chain to reform after dissociating was proven by FTIR spectroscopy (**Figure 3.14**). The resonance at λ = 696 cm^{-1} arises from the maleimide ring deformation mode.[18] In the polymer before the heat, there is a small resonance at this frequency, which suggests that some of the BFCE has dissociated during the polymerisation. Despite the reaction temperature being below the T_{rDA}, the fact that it is a dynamic equilibrium means that at any elevated temperature, the equilibrium shifts toward dissociation and a higher population of precursors will be observed. After a prolonged heat beyond the T_{rDA} (150 °C for 1 hour), this peak increased significantly, meaning the DA-linked polymer has dissociated into the lower molecular weight prepolymers. Upon cooling, the furan or maleimide chain ends then begin to reassociate with each other and the magnitude of the maleimide peak returned to a level similar to before the heat after 10 days.

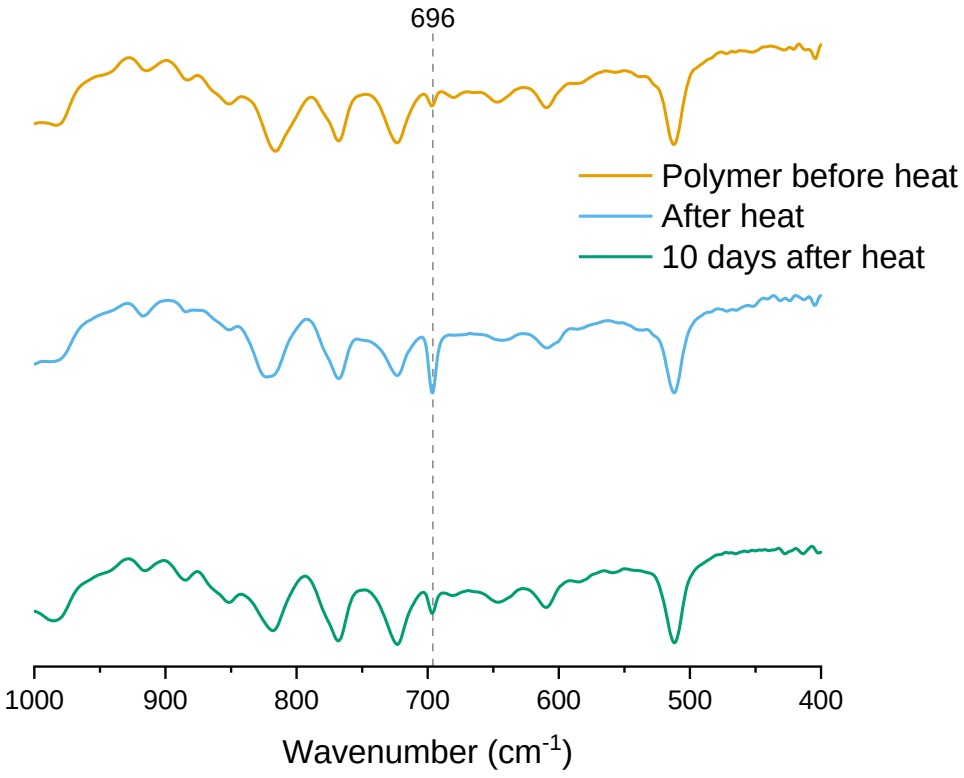

Figure 3.14 – IR spectra showing the emergence of the 696 cm^{-1} maleimide absorbance upon heating, and the following decrease after curing.

Further evidence was acquired by size exclusion chromatography (SEC); the linear polymer is able to be dissolved in chloroform and the rate of association followed by monitoring the increase in molecular weight (**Figure 3.15**). Before heating for 1 h at 150 °C, the polymer had a M_n of 11000 g mol^{-1}, which fell to 7000 g mol^{-1}. The M_n of the Priplast™ is 3000 g mol^{-1} so the polymer is either not fully dissociated from the heat, or has rapidly associated between heating and analysing by SEC. After 1 and 2 days, the M_n had returned to a similar value to before the heat; 13000 and 15000 g mol^{-1} respectively. This is higher than before the heat and the dispersity was lower too. The dispersity was 4.4 before the heat and around 3.3 afterwards.

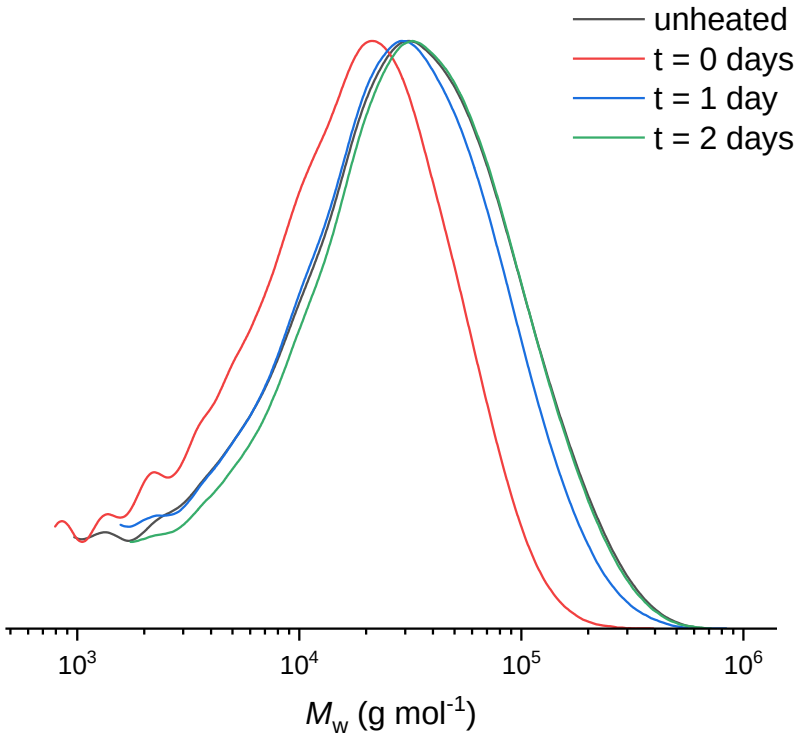

Figure 3.15 – GPC trace of the linear DA chains before and after heating.

3.2.4.2 DA network (bulk)

The use of a trifunctional chain extender instead of the bifunctional chain extender would produce a network rather than linear chains (**Scheme 3.10**).

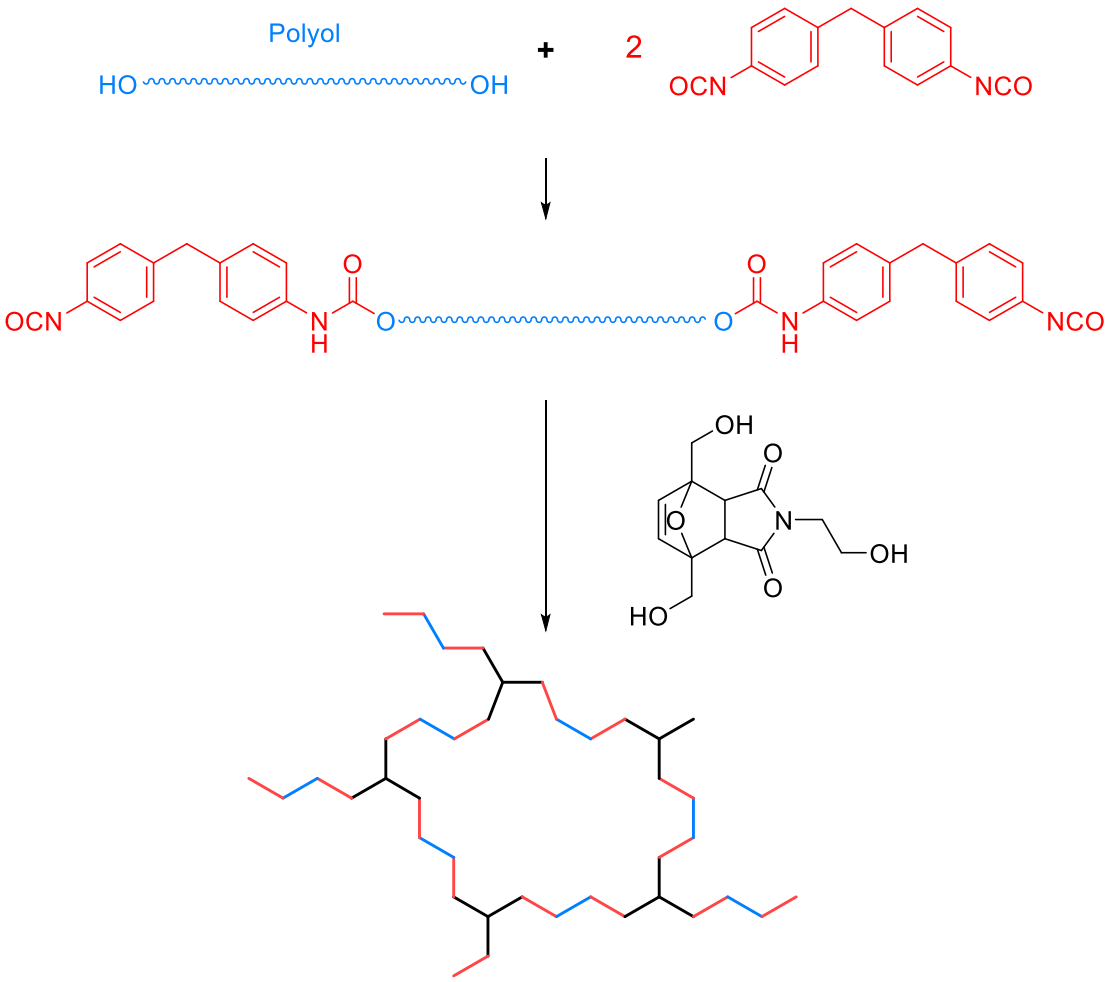

Scheme 3.10 – The steps involved to generate the polymer network with Diels-Alder moieties.

The polyol (44.20 g, 22 mmol) was heated to 110 °C under vacuum for an hour in oven-dried glassware to remove any residual moisture. MDI (11.18 g, 44 mmol) was then added to the mixture and the vacuum reapplied to yield the isocyanate-terminated prepolymer. TFCE (5.21 g, 19 mmol) was then added to cross-link the prepolymer chain ends. The mass of chain extender was calculated to give a 1:1.3 ratio of NCO groups on the prepolymer to OH groups on the chain extender. 3 hours after the addition of the trifunctional chain extender, the mixture had solidified and stopped stirring, so the reaction was ended (**Figure 3.16**). The resultant material was harder and less elastic than its linear analogue. To be removed from the flask, the material had to be heated to 150 °C, but on removal from heat it solidified rapidly making it impossible to spread as a film.

Figure 3.16 – Gelled material from the addition of TFCE to the prepolymer.

This composition would therefore work best as a two-component adhesive. In this form, the prepolymer and chain extender would be packaged separately, to be combined *in situ* at the time of adhesion. If the components are dosed in the correct mixing ratio and evenly, the chemical reaction between the isocyanates of the prepolymer and the hydroxyl groups of the chain extender will occur and generate the solid network in the bondline, mitigating the need to spread the material as a film. The application would be performed using a static mixer, which can inject the components in the desired proportions directly onto the substrate, which will then be bonded to another substrate and left to cure.

Analysis of the network by DSC showed there was a large endotherm in the expected rDA region (**Figure 3.17**). Again, two endotherms were present caused by the *endo* and *exo* isomers of the DA adduct. The incomplete reaction could also mean that there is free TFCE (or dissociated products HEMI and BHMF) present in the material. The melt at 88 °C could be the result of the melting of free HEMI (m.p. = 73 °C). The network was slightly more thermally stable than the linear chains, with a $T_{deg5\%}$ of 304 °C compared to 276 °C.

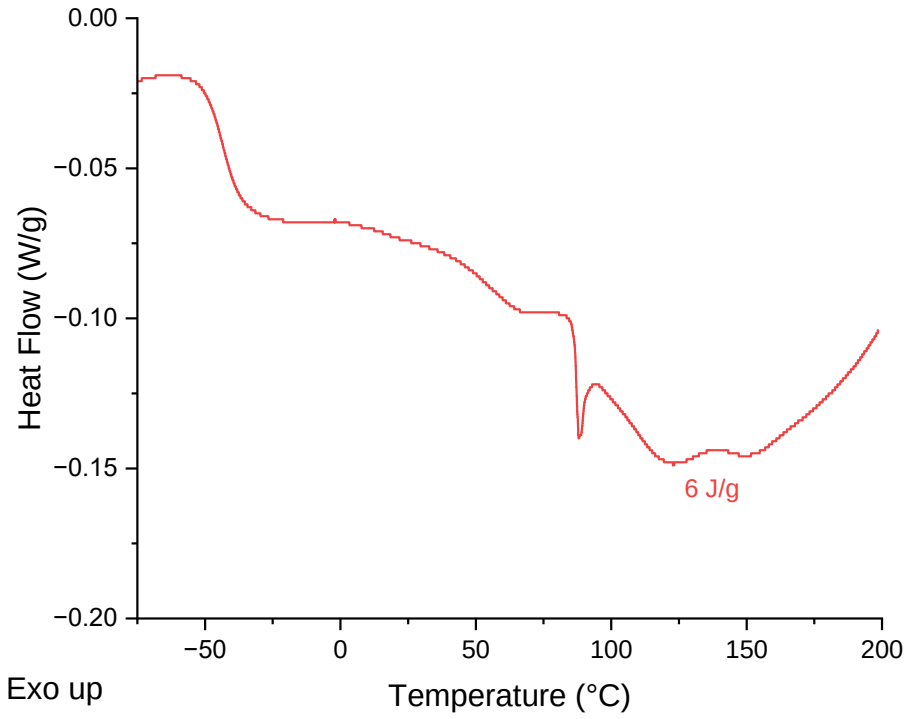

Figure 3.17 – DSC thermogram of the DA network.

The material was compression moulded in order to make a film that could be easily cut for lap shear samples. 5 g of material was chopped into small pieces and spread evenly into a metal compression mould lined with a thin sheet of polytetrafluoroethylene. The metal mould was then placed between two preheated metal plates at 150 °C. 1 MPa of pressure was applied for ten minutes to melt and spread the material into an even film. The mould was then removed from the heat and once cooled to room temperature, the material was removed (**Figure 3.18**).

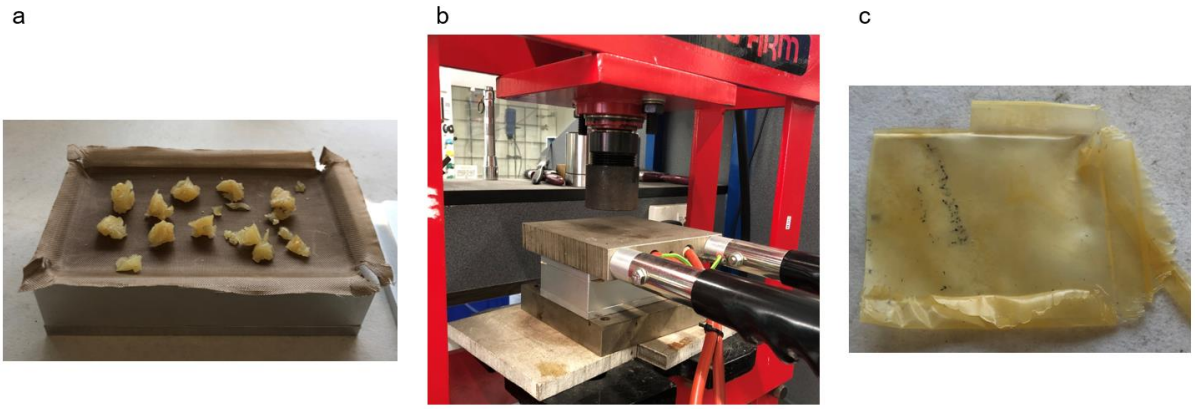

Figure 3.18 – The compression moulding process. a) The material is spaced evenly in the mould and then b) the mould is placed between two heating blocks to produce c) a uniform sheet.

3.2.4.2 DA network (solution)

The cross-linking of the material during the bulk synthesis meant the reaction had to be ended early, potentially incomplete. To mitigate this, the synthesis was performed again in solvent. This allowed the components to mix evenly and react for longer to give a more uniform material.

The polyol was heated to 90 °C under vacuum to remove moisture. After one hour, the atmosphere was switched to nitrogen and anhydrous toluene was added. The temperature was increased to 110 °C and then 2 equivalents of MDI was added. 1.3 equivalents (w.r.t. polyol) of TFCE was added and the reaction was stirred overnight to fully react, which was confirmed *via* FTIR analysis of the NCO bond. The product was cooled to room temperature and then precipitated in chilled diethyl ether. Excess solvent was decanted off and then the product dried. The final material was analysed *via* DSC (**Figure 3.19**). The melt seen previously at 88 °C is no longer present, suggesting there is no free HEMI present in the material. The rDA endotherms were still present, but had a smaller enthalpy change than the material synthesised in bulk. This could be due to solvent still being trapped within the network, which would lower the enthalpy change per gram of material. This does not necessarily mean a lower cross-link density, as it is difficult to distinguish between rDA from networked DA bonds and rDA from free

TFCE. There was no change in thermally stability between the solution and bulk synthesised networks, as determined by TGA.

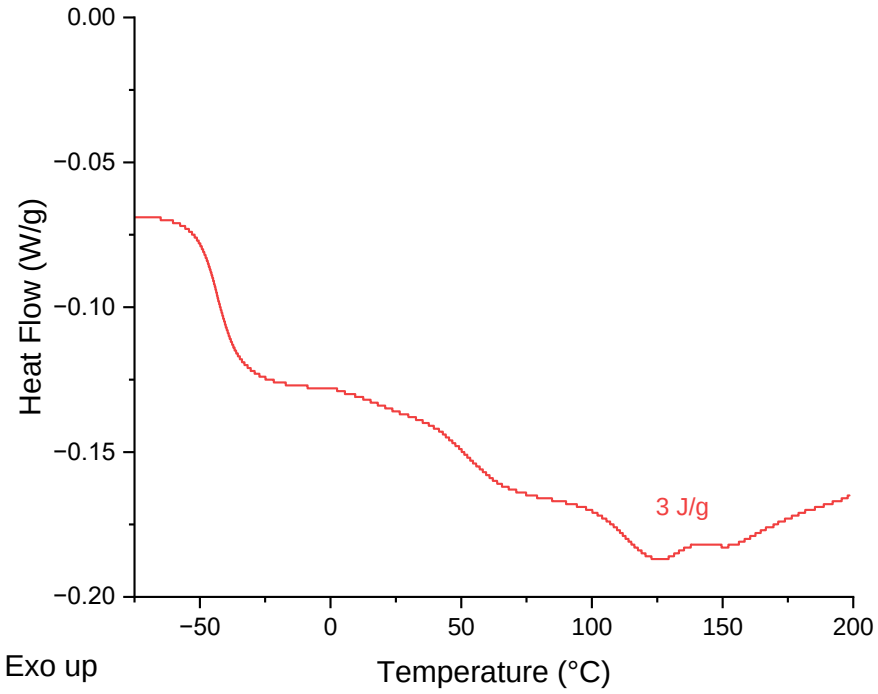

Figure 3.19 – DSC thermogram of the DA network synthesised in solution.

3.2.5 Lap shear testing

The adhesive capability of the materials were analysed through lap shear testing. Wooden lap shear joints were assembled by cutting a 25 × 25 mm film and clamping it between two wood substrates, before heating to 150 °C to bond (**Figure 3.20**).

Figure 3.20 – Step-by-step process of assembling the wood lap shear joints.

The linear DA chains showed excellent adhesive properties, with a break stress of over 4 MPa. It is around this stress that beech wood fails, and this was the case for one of the samples which experienced substrate failure (**Figure 3.21**).

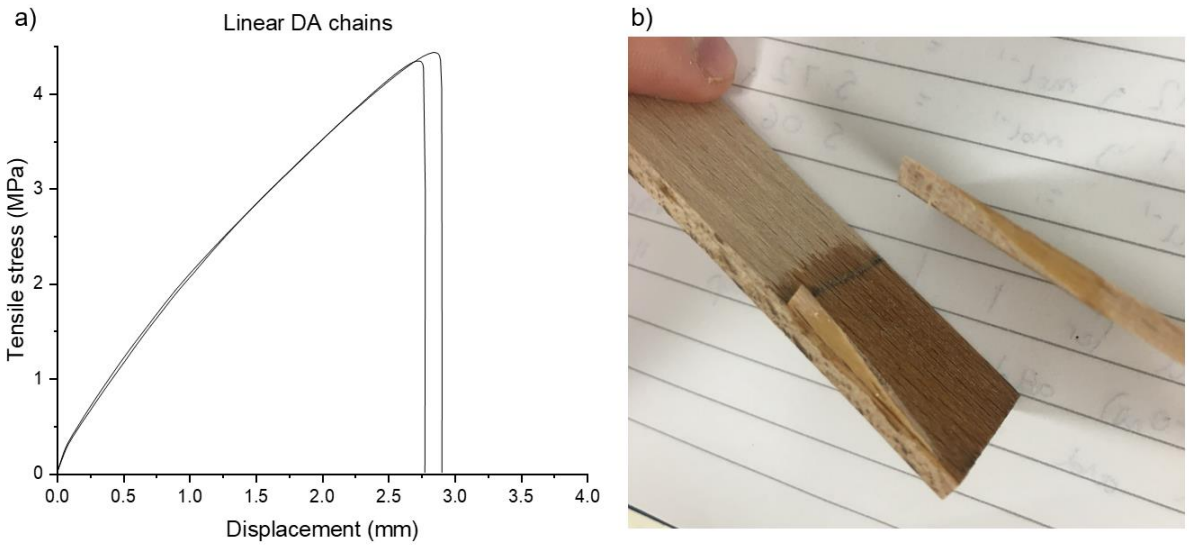

Figure 3.21 - a) Stress vs displacement results from the lap shear tensile testing of P1838 + BFCE on wood and b) substrate failure of the wood.

Both DA networks (bulk and solution synthesised) were tested (**Figure 3.22**). These materials appeared to be slightly weaker than the linear DA chains, however this could have been limited by the strength of the wood as several samples also experienced substrate failure (**Figure 3.23**). The solution-made network performed better than the bulk-made network; the peak stress was higher and it displayed a higher Young's modulus. The more uniform material means that the cross-links are distributed more evenly throughout the network resulting in less chain slippage.

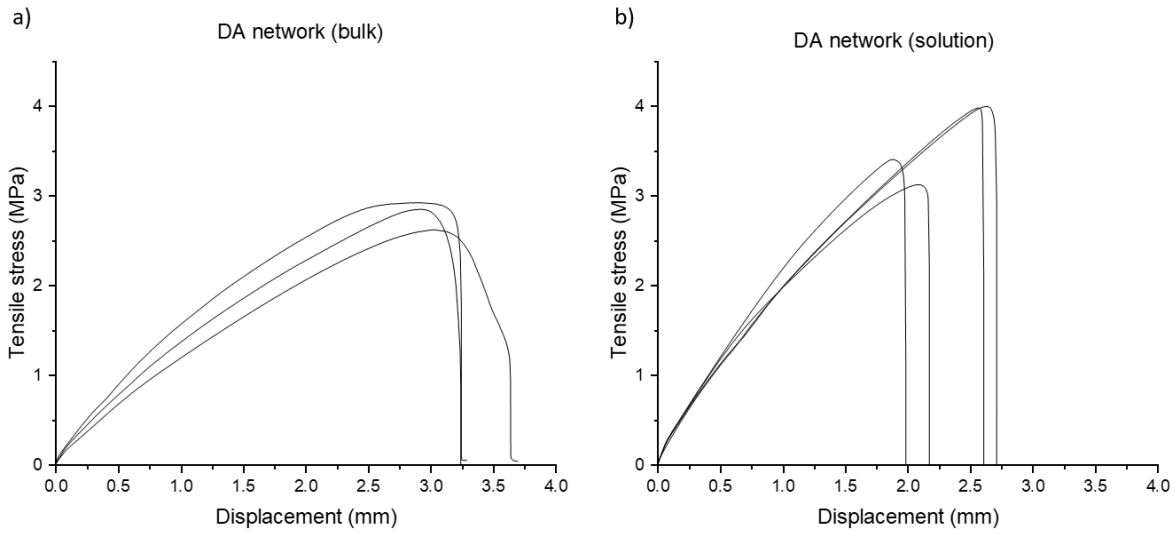

Figure 3.22 - Stress vs displacement results from the lap shear tensile testing of the bulk-made and solution made networks.

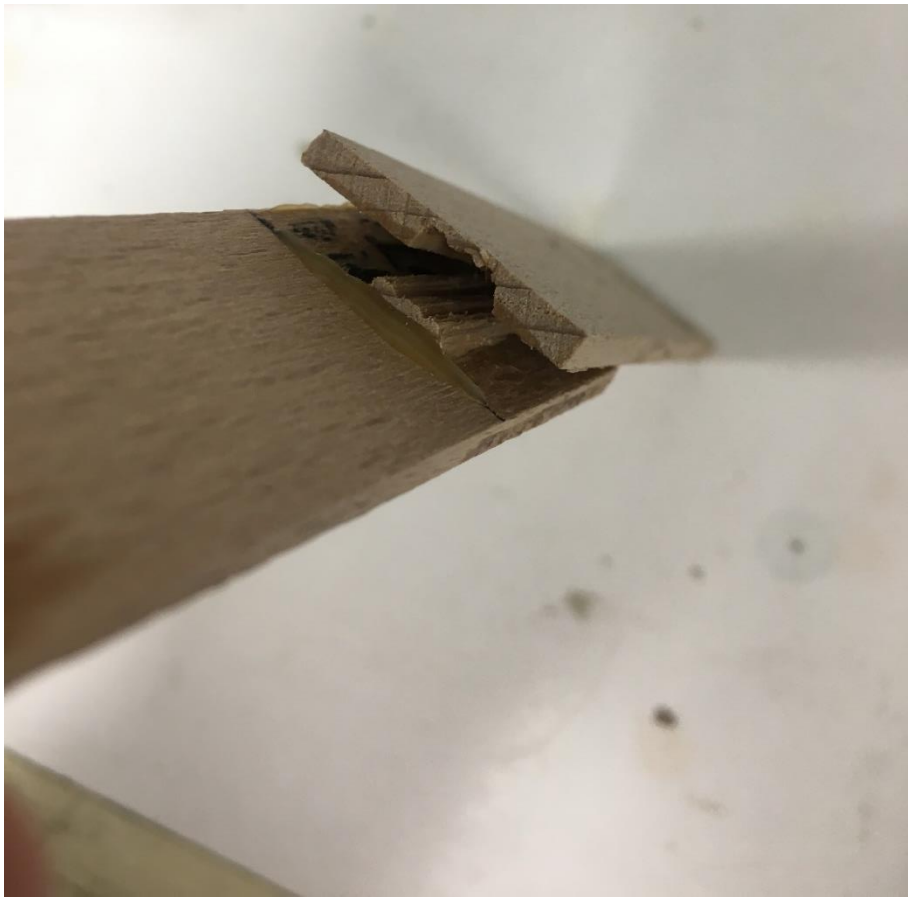

Figure 3.23 - Substrate failure of the wood bonded by the DA network (solution synthesised)

The linear chains had the strongest peak tensile stress and showed substrate failure so the test was repeated on a stronger substrate, aluminium. On this material, the adhesive achieved a break stress as high at 6.5 MPa (**Figure 3.24**).

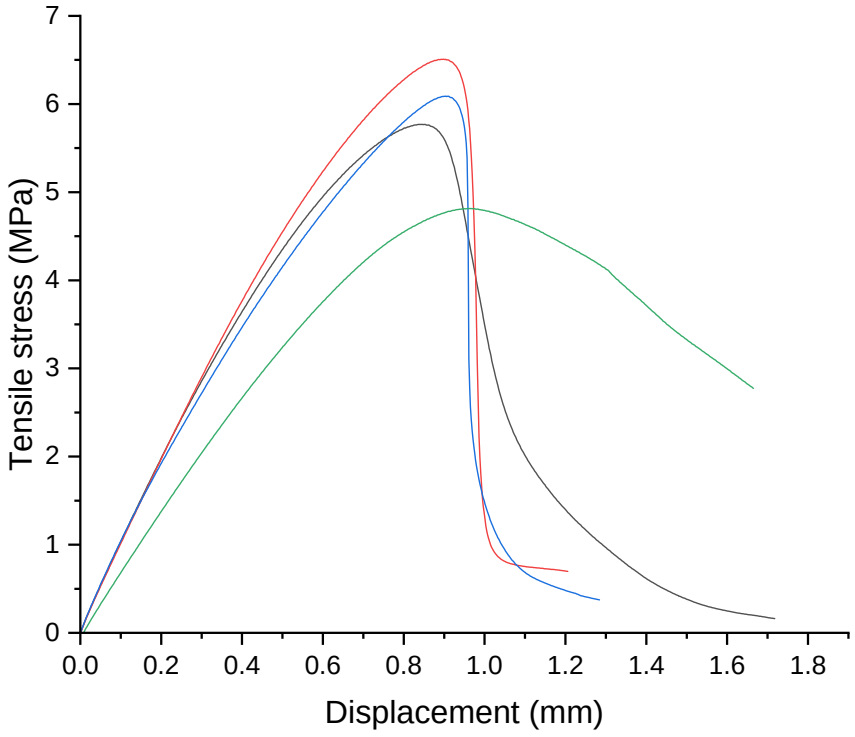

Figure 3.24 - Stress vs displacement results from the lap shear tensile testing of the aluminium bonded by linear chains.

3.2.6 Soxhlet extractions

After curing for 1 week at ambient temperature to allow the network to equilibrate, both polymer networks (bulk and solution synthesised) underwent a Soxhlet extraction in ethyl acetate (b.p. 77.1 °C) to determine the extent of the cross-linking. The bulk-made network had the higher gel fraction of 84% compared to the solution-made network which had 67%. This could be caused by the reaction solvent not being fully removed from the latter material, which could potentially inhibit full network formation.

3.3 Conclusions

A moisture-curing material based on Priplast™ 1838 was synthesised on a 50 g scale using commercially available materials. Chain extender molecules containing a Diels-Alder adduct core and reactive hydroxyl groups were synthesised using maleic anhydride and furan derivatives. These two components were successfully combined to create either a linear polymer or a network, which can dissociate at elevated temperatures back to their monomers and be reshaped. The materials showed excellent adhesion properties too, in some instances caused substrate failure of the wood. The linear polymer was used to bond aluminium coupons, which withstood a strain of 6.5 MPa before breaking. These findings show that it is possible to take a commercial moisture-curing prepolymer, which are typically used to formed permanent bonds, and add a chain extender molecule to generate a debondable adhesive, allowing for easy recycling at its end-of-life.

3.4 Bibliography

1 J. Comyn, *Int J Adhes Adhes*, 1998, **18**, 247–253.

2 J. Comyn, F. Brady, R. A. Dust, M. Graham and A. Haward, *Int J Adhes Adhes*, 1998, **18**, 51–60.

3 S. Camadanli, A. Hisir and S. Dural, *J Appl Polym Sci*, 2022, **139**, 51722.

4 K. Ramani, J. Verho, G. Kumar, N. Blank and S. Rosenberg, *Int J Adhes Adhes*, 2000, **20**, 377–385.

5 G. Clerc, M. Brülisauer, S. Affolter, T. Volkmer, F. Pichelin and P. Niemz, *Int J Adhes Adhes*, 2017, **72**, 130–138.

6 P. Waites, *Pigment & Resin Technology*, 1997, **26**, 300–303.

7 E. Leipold, K. Jörg and H. Fauser, *adhesion ADHESIVES + SEALANTS*, 2022, **19**, 18–21.

8 L. R. Bhagavathi, A. P. Deshpande, G. D. J. Ram and S. K. Panigrahi, *Int J Adhes Adhes*, 2021, **108**, 102871.

9 J. Kozakiewicz, in *Adhesion 13*, Springer Netherlands, Dordrecht, 1989, pp. 114–141.

10 A. Ali, K. Yusoh and S. F. Hasany, *J Nanomater*, 2014, **2014**, 1–9.

11 M. P. Stevens and A. D. Jenkins, *Journal of Polymer Science: Polymer Chemistry Edition*, 1979, **17**, 3675–3685.

12 J. A. Syrett, G. Mantovani, W. R. S. Barton, D. Price and D. M. Haddleton, *Polym Chem*, 2010, **1**, 102–106.

13 X. Chen, M. A. Dam, K. Ono, A. Mal, H. Shen, S. R. Nutt, K. Sheran and F. Wudl, *Science (1979)*, 2002, **295**, 1698–1702.

14 A. Gandini, A. J. D. Silvestre and D. Coelho, *J Polym Sci A Polym Chem*, 2010, **48**, 2053–2056.

15 Merck, N-(2-Hydroxyethyl)maleimide, https://www.sigmaaldrich.com/GB/en/product/aldrich/773263, (accessed 22 August 2023).

16 T. T. Truong, H. T. Nguyen, M. N. Phan and L.-T. T. Nguyen, *J Polym Sci A Polym Chem*, 2018, **56**, 1806–1814.

17 R. J. Pearson, E. Kassianidis and D. Philp, *Tetrahedron Lett*, 2004, **45**, 4777–4780.

18 D. H. Turkenburg, H. van Bracht, B. Funke, M. Schmider, D. Janke and H. R. Fischer, *J Appl Polym Sci*, 2017, **134**, 1–11.

4 Covalent adaptable networks using unsaturated polyesters

4.1 Introduction

Over 60 million metric tons of polyester was produced in 2021.[1] Its strength and flexibility are what makes it so popular and ubiquitous across the construction,[2] transport,[3] and marine[4] industries. Polyesters can also be recycled; the ester bond is susceptible to hydrolysis, meaning the polymer can be depolymerised back into its monomers or other small molecules, such as diols and diacids. For example, poly(ethylene terephthalate) is one of the most recycled plastics, commonly seen in plastic bottles. However, this material is a thermoplastic and for applications requiring higher strength and durability, thermoset materials are better suited. Thermoplastics are simply high molecular weight linear polymeric chains, tangled together and attracted to one another by non-covalent intermolecular forces, which can be easily overcome by heating. Thermosets, on the other hand, are cross-linked by permanent covalent bonds to form a strong network, making them useful for applications requiring high mechanical strength, *e.g.* structural adhesives. However, at this point the polyester chains become very difficult to recycle, as the polyester resin is now permanently bonded into an insoluble network. The creation of a network with reversible bonds would be highly advantageous in order to create a material that benefits from the performance advantages of thermosets, whilst maintaining the recyclability of thermoplastics.

Polyester resins can be categorised as either unsaturated or saturated. Unsaturated polyesters (UPEs) are the most common, exhibiting higher heat resistance, higher tensile and compression strength, and higher resistance to chemical corrosion than their saturated resin counterparts.[5] The unsaturation in the backbone usually comes in the form of a fumarate group, as this confers desirable physical properties on the resin such as high heat distortion temperatures, good tensile strength and chemical resistance. Furthermore, the fumarate *trans* isomer is in a more favourable conformation for cross-

linking, compared to its *cis* isomer, maleate.[6] Despite this, maleic anhydride is used almost exclusively as the unsaturated condensation monomer in most commercial resins, due to its lower cost, higher yield, ease of handling and more facile incorporation into the polyester backbone. Under polycondensation conditions, maleates can isomerise to the more energetically favourable conformer, fumarate, and under the correct conditions, conversions of up to 89% are possible.[7] UPEs are commonly sold as a liquid resin using styrene as a reactive diluent, which solidifies through free radical copolymerisation of the chain unsaturation with the styrene to form a three-dimensional network. The resulting materials possess excellent mechanical properties, but because of the irreversibility of the network, they cannot be reshaped and are very difficult to recycle.

Covalent adaptable networks (CANs) can offer a more sustainable alternative to irreversible networks.[8] These networks can display typical thermoset network properties at service temperatures (the range at which the adhesive is required to operate) that can be reprocessed outside of this range through either network dissociation or restructuring, which are known as dissociative and associative CANs, respectively. Associative CANs, commonly referred to as vitrimers, can restructure their networks at higher temperatures through the addition of loose chains to a linker moiety that initiates an exchange reaction to produce a new linkage and loose chain end (e.g. transesterification, transamination).[9,10] Dissociative CANs undergo chain scission reactions when stimulated (through heat, light or catalyst) to produce non-cross-linked polymer chains that behave more similarly to thermoplastic materials.[11] Once the stimulus is removed, the network covalently reforms. In both processes, the materials can be reprocessed and the net number of cross-links in the networks, as well as the resulting mechanical properties, before and after reprocessing are identical at the service temperature.

Dissociative CANs can be produced through several methods, most commonly utilising Diels-Alder (DA) networks from the reversible cycloaddition of dienes and dienophiles. The most documented DA networks take advantage of furan- and maleimide-functionalised precursors that can be easily

attached to the chain-end of commercially available polymers.[12] Typically, these networks can be reversed at temperatures between 100 and 150 ˚C without risking degradation or side reactions to the remainder of the polymer chain.[13] However, maleimides are expensive, difficult to synthesise are often toxic and non-renewable. Therefore it would be more sustainable to use a dienophile that is renewable and able to be easily incorporated into a polymer chain. Fumaric acid is commonly found in nature, particularly in moss, lichen and fungi and forms part of the Krebs and citric acid cycles. The *cis*-isomer of fumaric acid, maleic acid, has been widely studied for 'green' synthetic routes.[14,15] Both isomers have been used in the production of UPEs through polycondensations with diol comonomers. There is already infrastructure in place to mass produce polyesters, which would make the synthesis of these new, 'green' materials easy and efficient. Similarly, di-esters of both isomers have been demonstrated for use in small molecule DA cycloadditions with cyclopentadiene,[16–18] furan[19] and anthracenes.[20] However, polymers using maleates or fumarates within their backbone have not been documented for post-polymerisation modifications by DA cycloaddition.

This research investigates a more environmentally friendly way of forming networks using the unsaturation of UPEs in CANs utilising Diels-Alder chemistry. The alkene functionality can behave as a dienophile, allowing it to bond to a furan group *via* a cycloaddition. The fact that the Diels-Alder reaction is thermally reversible means that the network can be dissociated by simply applying heat, thus reverting the network back to its constituents. This process is accompanied by a loss in modulus, allowing the user to remove, reshape and reapply the material for whichever application is desired. Currently, there has been little research regarding maleate or fumarate networks formed through Diels-Alder bonds and no direct comparison into the differences observed between the two isomers when cross-linking through this method. In this research, a small variety of furan-functionalised linker molecules were used to cross-link poly(propylene maleate) and poly(propylene fumarate) into adhesive networks (**Figure 4.1**).

Poly(propylene maleate) Poly(propylene fumarate)

Figure 4.1 - The two UPEs used in this research.

4.2 Results and discussion

4.2.1 Synthesis of polyesters

The polyesters in this chapter were provided from external sources; poly(propylene maleate) (PPM) was kindly provided by the Becker Laboratory for Functional Biomaterials at Duke University and poly(propylene fumarate) (PPF) was kindly provided by Scott Bader, a global manufacturer of adhesives, composites and functional polymers. Size exclusion chromatography determined the M_w of PPF 4700 g mol^{-1} to be PPM to be 3100 g mol^{-1}.

PPF was synthesised by the step-growth polymerisation. A mixture of maleic anhydride and propylene glycol with a monobutyltin oxide catalyst was stirred and heated at 220 °C until completion, as determined by volume of water distilled off and acid value calculations. The high temperatures necessary for this process cause the isomerisation of maleate to fumarate, so PPM cannot be synthesised through this method.[21] Instead, PPM was synthesised by the ring-opening copolymerisation (ROCOP) of maleic anhydride and propylene oxide, where the milder conditions allow the stereochemistry of the maleate to be retained.[22] In a moisture-free N_2 environment, maleic anhydride, propylene oxide, a $(BHT)_2(THF)_2$ catalyst and a propargyl alcohol initiator, was made up with toluene to a 4M concentration. The polymerisation was conducted at 80 °C for 24 hours before being quenched in chloroform and precipitated in diethyl ether. The stereochemistry of the polyesters was confirmed *via* ^{1}H nuclear magnetic resonance (NMR) spectroscopy; maleate protons resonate at δ = 6.25 ppm and fumarate protons resonate at δ = 6.85 ppm (**Figures 4.2, 4.3**).

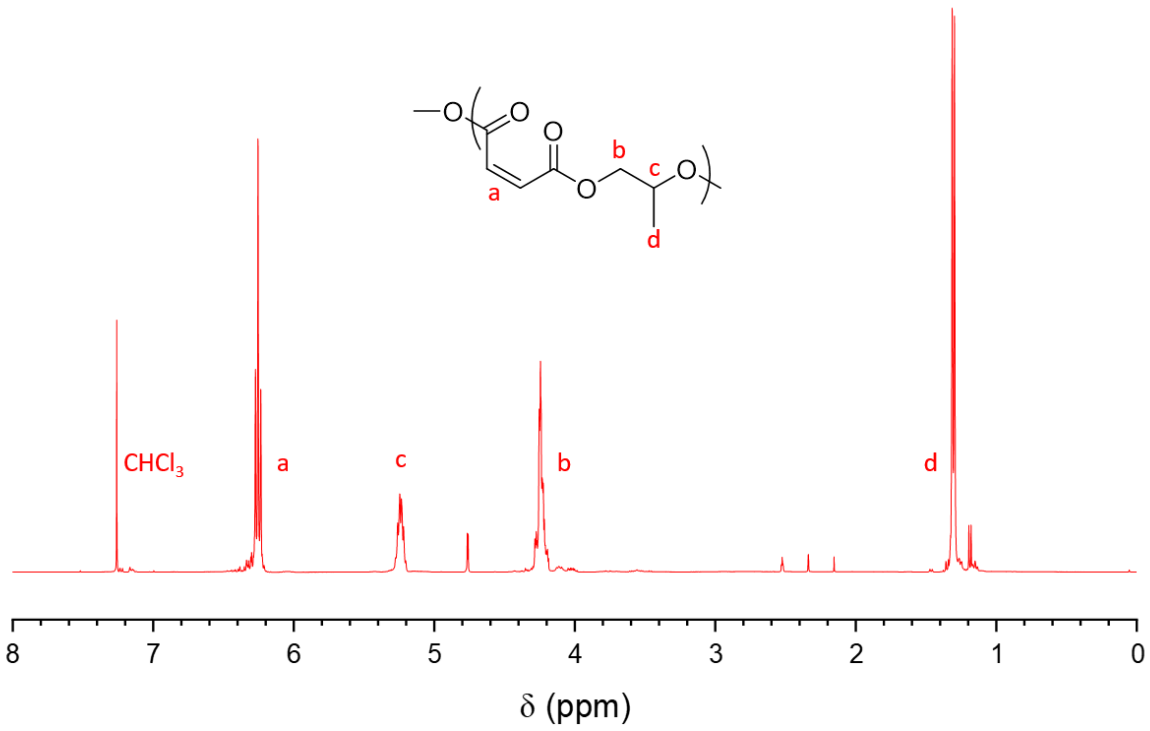

Figure 4.2 - ^{1}H NMR spectrum of poly(propylene maleate) (400 MHz, $CDCl_3$, 298 K)

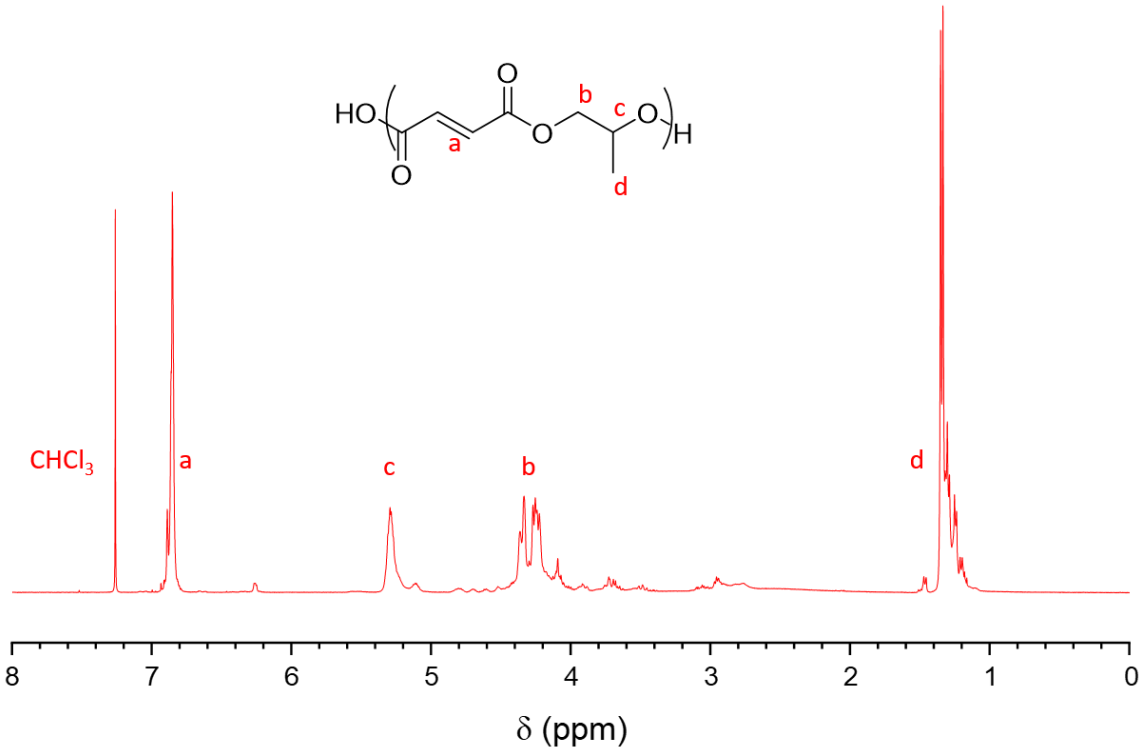

Figure 4.3 - ^{1}H NMR spectrum of poly(propylene fumarate) (400 MHz, $CDCl_3$, 298 K)

4.2.2 Synthesis of furan-functionalised linkers

Furan linkers were produced from the reaction of the commercially available isocyanates 4,4'-methylene diphenyl diisocyanate (MDI), isophorone diisocyanate (IPDI), and hexamethylene diisocyanate trimer (HMDIT) with furfuryl alcohol to form a urethane linkage. This produced the furan-functionalised polyurethane cross-linkers difuran methylene diphenyl carbamate (MDF), difuran isophorone carbamate (IPDF) and trifuran hexamethylene trimer carbamate (HMTF), respectively (**Scheme 4.1**).

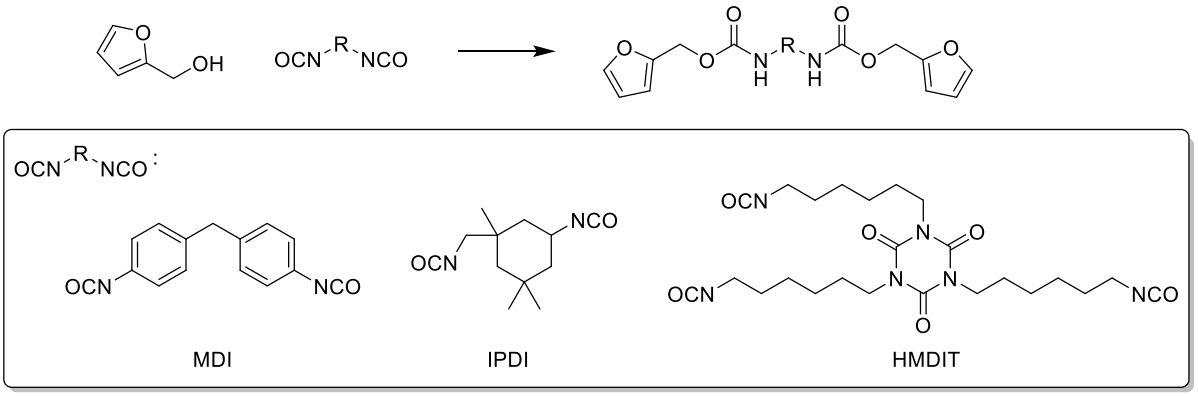

Scheme 4.1 - Synthesis of furan-functionalised linkers from the reaction of furfuryl alcohol with a di- or tri-isocyanate.

Complete addition was confirmed through the determination of the NCO value with a titration, and Fourier transform infrared (FTIR) spectroscopy. The linkers' structures were confirmed *via* ^{1}H and ^{13}C NMR spectroscopy (**Figures 4.4, 4.5, 4.6**).

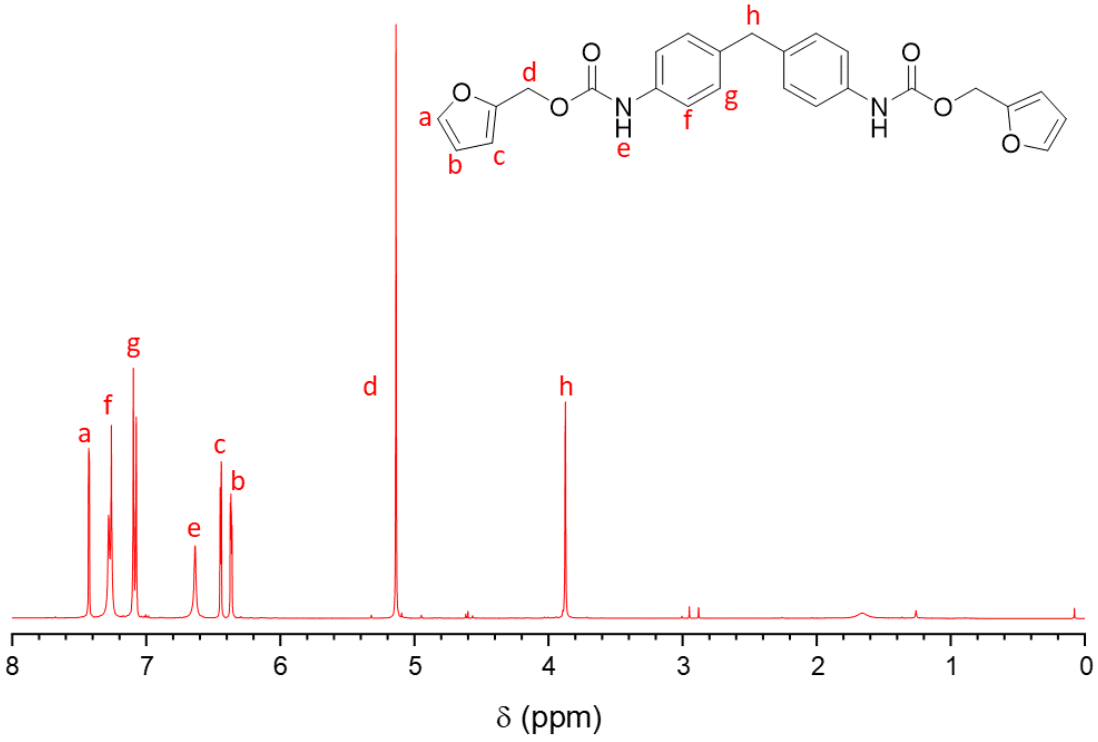

Figure 4.4 - ^{1}H NMR spectrum of MDF (400 MHz, $CDCl_3$, 298 K)

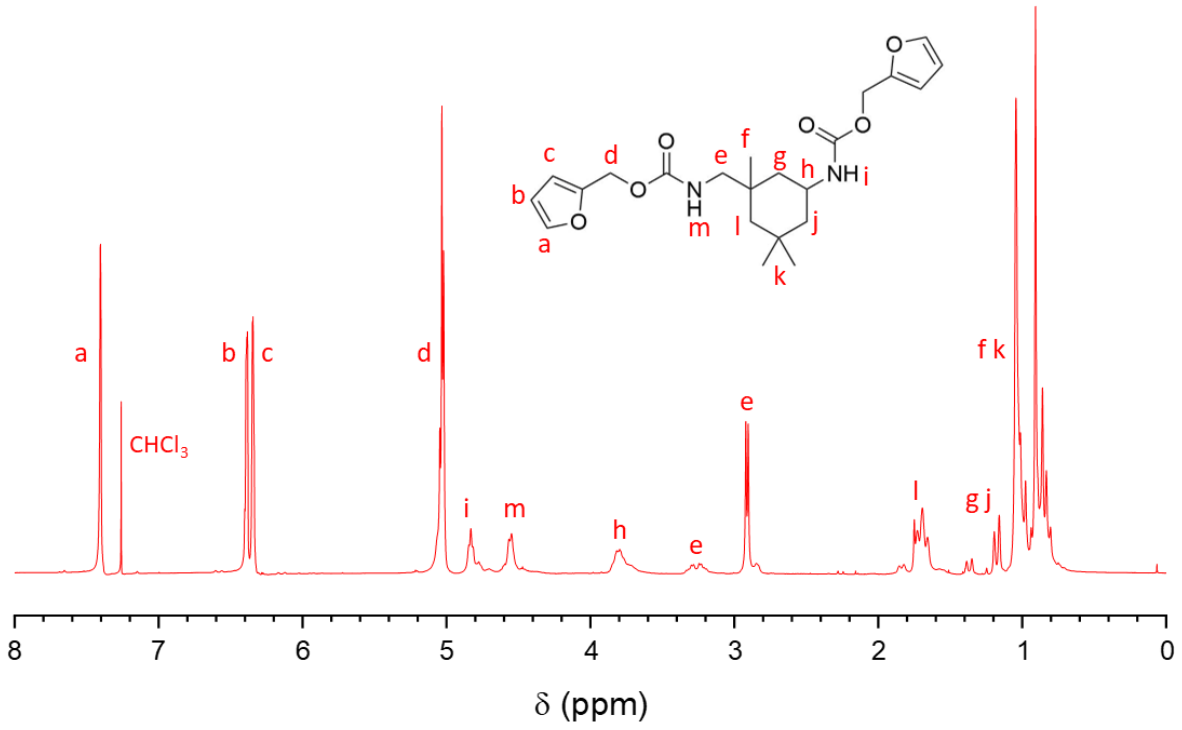

Figure 4.5 - ^{1}H NMR spectrum of IPDF (400 MHz, $CDCl_3$, 298 K)

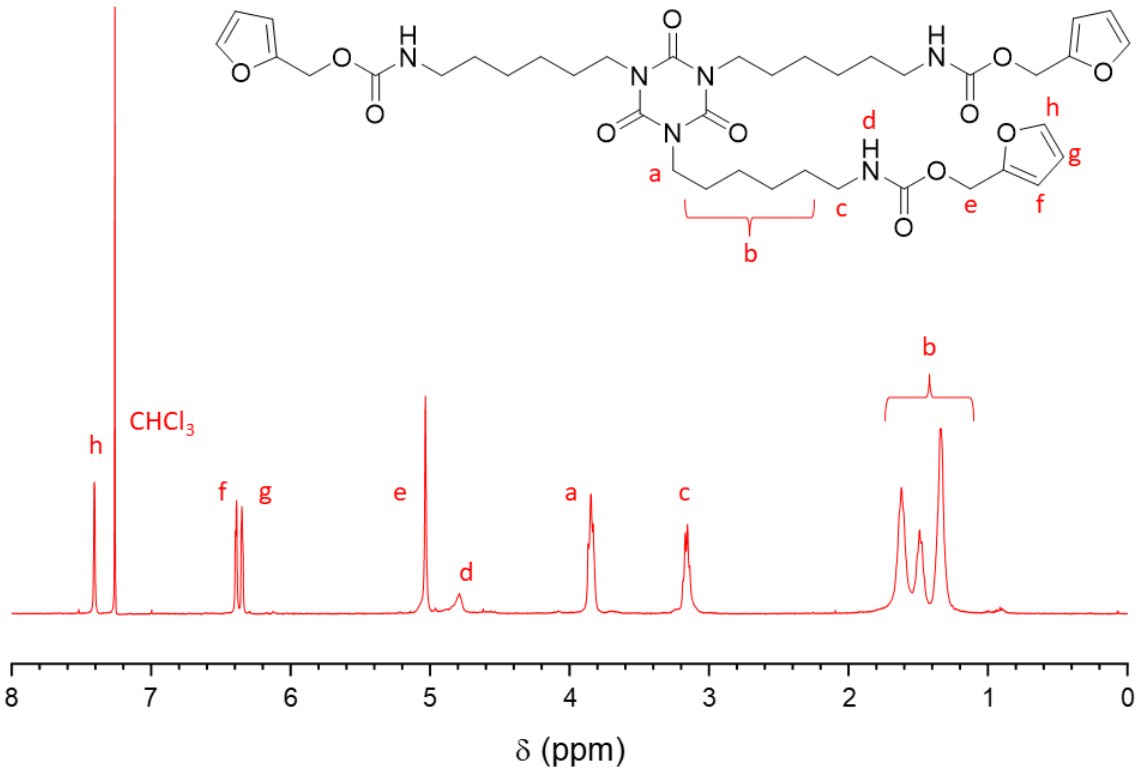

Figure 4.6 - ^{1}H NMR spectrum of HMTF (400 MHz, $CDCl_3$, 298 K)

4.2.3 Synthesis of CANs

Networks were synthesised through the bulk polymerisation of a UPE with a furan-functionalised polyurethane until homogenous, followed by post-curing for at least 7 days at ambient temperature to allow for the furan linkers to covalently bond with the unsaturation and cross-link the polyester chains (**Scheme 4.2**). The masses of polyester and linker used were calculated to give an equimolar ratio of alkene to furan.

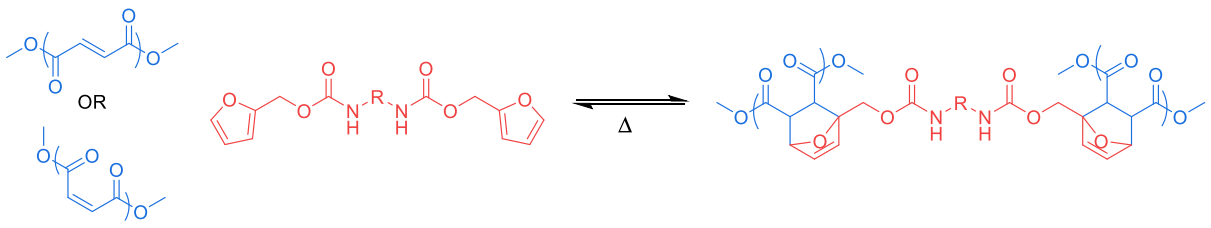

Scheme 4.2 - Network formation through bulk polymerisation with an unsaturated polyester.

4.2.4 Thermal properties of networks

Networks were examined through differential scanning calorimetry (DSC) to quantify the retro-Diels-Alder (rDA) reaction at elevated temperatures. Slow network reformation kinetics only allows the rDA reaction to be observed in the first heating cycle (**Figure 4.7, Table 4.1**). The dissociation is an endothermic process, with a visible peak towards the *endo* region, providing a clear indicator that the network is reverting back to the original furan and UPE components. Furthermore, the crystallinity melts observed in pure MDF and HMTF are not present, as the linkers are dispersed throughout the network. The rDA of all networks was observed between 100 and 130 °C, where the dynamic equilibrium of the Diels-Alder reaction begins to favour dissociation rather than cycloaddition. The temperature of the rDA reaction (T_{rDA}) differed depending on the stereochemistry of the unsaturation, with fumarates dissociating around 100 °C and maleates dissociating around 130 °C, independent of the linker used.

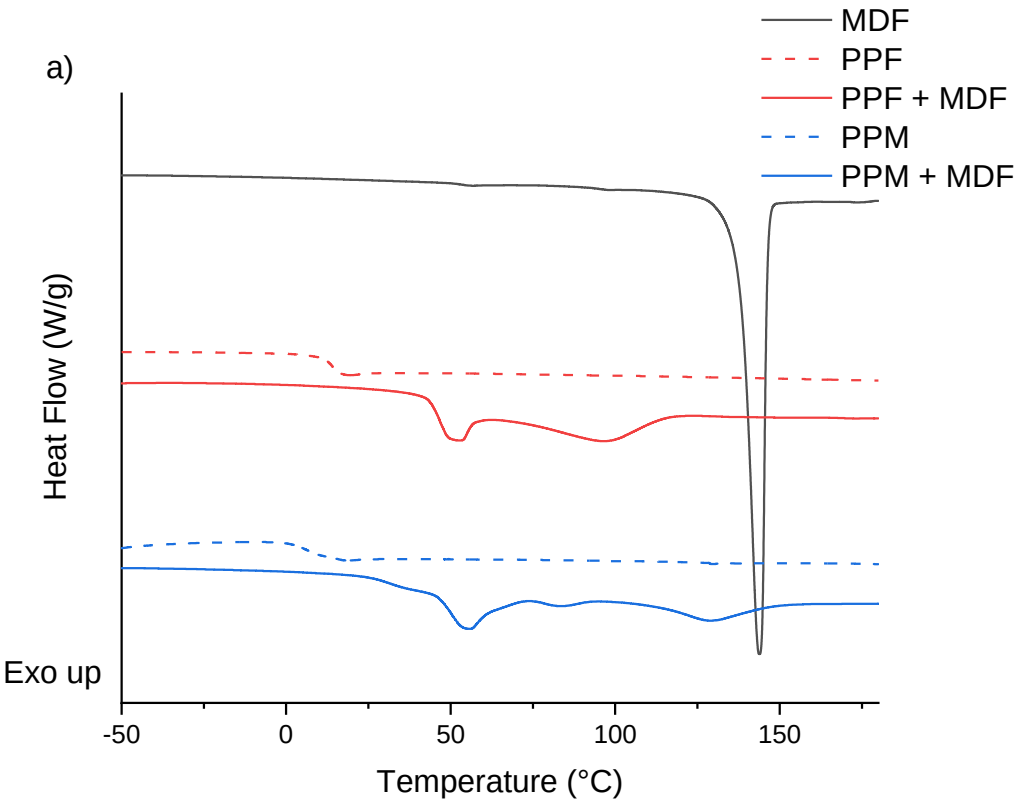
a)
MDF
PPF
PPF + MDF
PPM
PPM + MDF
Heat Flow (W/g)
Exo up
-50
0
50
100
150
Temperature (°C)

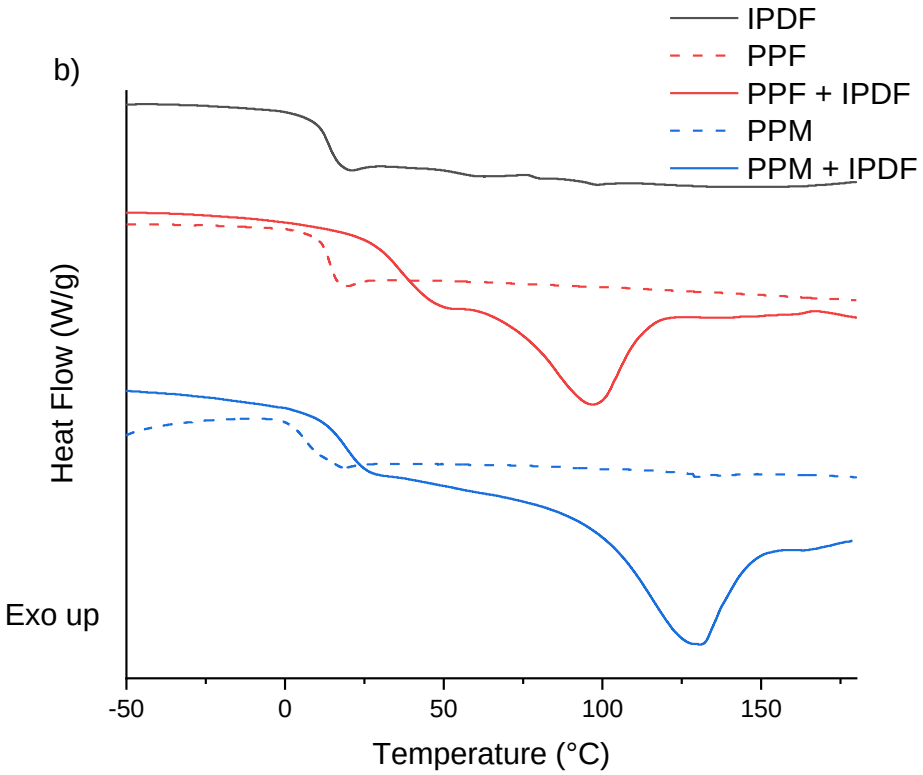
b)
IPDF
PPF
PPF + IPDF
PPM
PPM + IPDF
Heat Flow (W/g)
Exo up
-50
0
50
100
150
Temperature (°C)

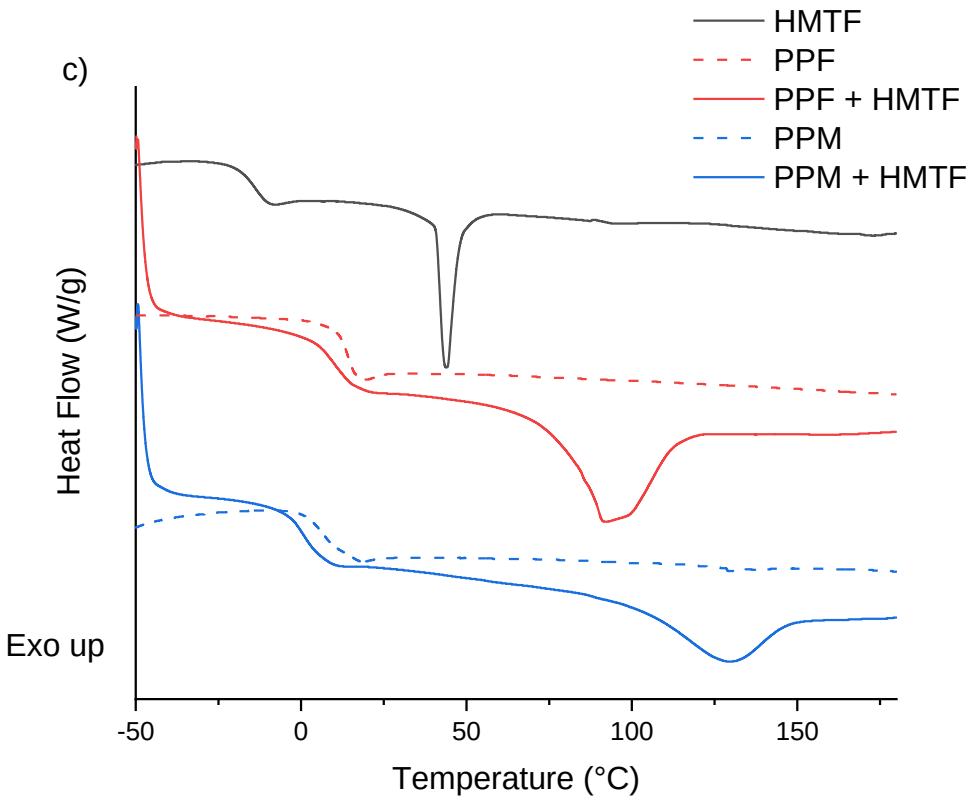

Figure 4.7 - DSC chromatograms of the initial heating cycle from -50 to 180 °C at 10 °C min^{-1} on a) MDF, b) IPDF and c) HMTF and the corresponding associated networks with PPF or PPM. Taken 1 week after synthesis.

Table 4.1 - Properties and thermal properties of synthesised materials.

Material	f_g (mol kg^{-1})[a]	T_g[b] (°C)	T_{rDA}[b] (°C)	η[c] (P)		ΔH_{rDA} (J g^{-1})[b]	
				115 °C	125 °C	1 week	26 weeks
PPF	6.40	14	-	18.8	10.8	-	-
PPF + MDF	2.63	46	96.9	19.9	7.3	16	19
PPF + IPDF	2.74	37	97.0	8.7	3.0	22	24
PPF + HMTF	2.37	11	91.9	8.4	3.3	24	26
PPM	6.40	4	-	3.7	3.6	-	-
PPM + MDF	2.63	50	128.8	20.1	7.6	12	24
PPM + IPDF	2.74	20	128.6	6.4	4.9	20	40
PPM + HMTF	2.37	2	129.0	4.8	2.7	14	46

[a] Concentration of alkene groups in the material. [b] Determined by differential scanning calorimetry. [c] Viscosity determined at 750 RPM.

As observed, a small change in conformation of the backbone has a substantial impact on the T_{rDA} and the resulting thermodynamic stability of the material. This difference can be attributed to the sterics of the unsaturated groups. The stereochemistry of the dienophile is maintained in the cyclohexene product, meaning fumarates will produce enantiomeric *pseudo-trans* cycloadducts whereas maleates will form *pseudo-cis* diastereoisomers with one *endo* and one *exo* ester conformation (**Scheme 4.3**). The T_{rDA} of the fumarate networks are lower as the di-ester dihedral angle increases from 120° to 180° during dissociation, relieving steric strain. In the maleate, the di-ester groups remain eclipsed with no steric strain relief, therefore requiring more energy and higher temperatures to dissociate. This trend is seen throughout literature, for example, in a fulvene and dichloromaleate system, which creates a more sterically hindered adduct comparable to our furan and maleate adduct, has a T_{rDA} as low as 37 °C.[23] The addition of the electron-withdrawing chlorine to the dienophile would normally promote the forward DA reaction.

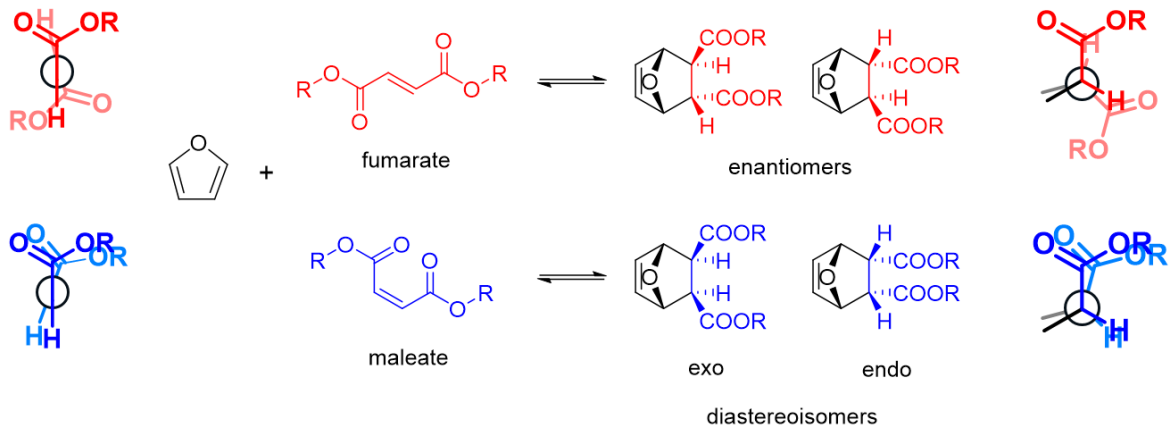

Scheme 4.3 - Different possible stereoisomers that can form from the Diels-Alder cycloaddition of a furan to a fumarate or maleate group.

The melt viscosity of the materials was also measured. Once molten, the stereochemistry of the backbone had little effect and it was the linker that gave rise to varying viscosities. In the molten state, the network dissociates, and the stereochemistry of the backbone becomes less significant compared to the composition of the material. However, it was noted that the maleate networks took noticeably longer to melt when performing the experiments. These are important aspects when considering the wetting of the material onto substrates.

The magnitude of the enthalpy change of the rDA endotherm (ΔH_{rDA}) is a good indication of how much the network has associated, as a larger concentration of Diels-Alder adducts will lead to a higher enthalpy change of dissociation. All networks contain similar degrees of functionality (f_g), or concentration of alkene groups, and should therefore contain comparable cross-link density in the networks if all the functional groups participated in bonding. As there are differences in the ΔH_{rDA} of the materials observed by DSC, it is probable that some networks are more efficient at associating than others. The broad endotherms make accurate integration difficult and thus, only general observations can be made. After 1 week, the network of PPM + IPDF had the largest ΔH_{rDA}, almost 2 times higher than PPM + MDF, suggesting the IPDF linker is much better at reacting with maleate moieties compared to MDF. This is also observed in the fumarate-functionalised backbone, but less

pronounced when analysed by DSC. The materials went through another heat cycle 6 months later and showed little increase in ΔH_{rDA}, suggesting the materials had reached an equilibrium in cross-linking density by 7 days. In contrast, the PPM networks had much larger ΔH_{rDA}s after 6 months. An explanation for this could be the low T_g. This material will have chain movement during the cure, meaning that unreacted Diels-Alder pairs can continue to find each other and bond over time.

The MDF and IPDF networks have a higher T_g, compared to the original polyesters as a result of the chemical cross-links formed preventing the polymer chains from flowing. However, this isn't true for HMTF cross-linker, where the T_g was observed to decrease slightly. The hexamethylene arms increase the overall flexibility of the network and increases the free volume between bonded chains, allowing more chain movement and hence, a lower T_g is observed. The glass transition in the MDF networks are accompanied by an enthalpic relaxation. This is an indication of physical aging from storing below the T_g. MDF is highly crystalline and is likely to associate with itself before being involved in the network. As the material passes through the T_g on the heating cycle, the relaxation of these crystalline regions appear as endothermic transitions. This reduced participation of MDF in the network also accounts for the lower ΔH_{rDA} in comparison to materials with lower T_g and less crystalline linkers.

4.2.5 Solvent resistance

The increased stability in the maleate cycloadduct over the fumarate is also evident in the solvent resistance of the networks. An aliquot of each network was added to ethyl acetate and THF and left for 1 week at ambient temperature, after which each sample had dissolved to varying degrees. The solvent resistance was determined qualitatively by examining how much material remained undissolved and discolouration of the solvent (**Figures 4.8, 4.9**).

Figure 4.8 - Materials left in ethyl acetate for 1 week. From left to right: PPM + HMTF, PPF + HMTF, PPM + IPDF, PPF + IPDF, PPM + MDF, PPF + MDF.

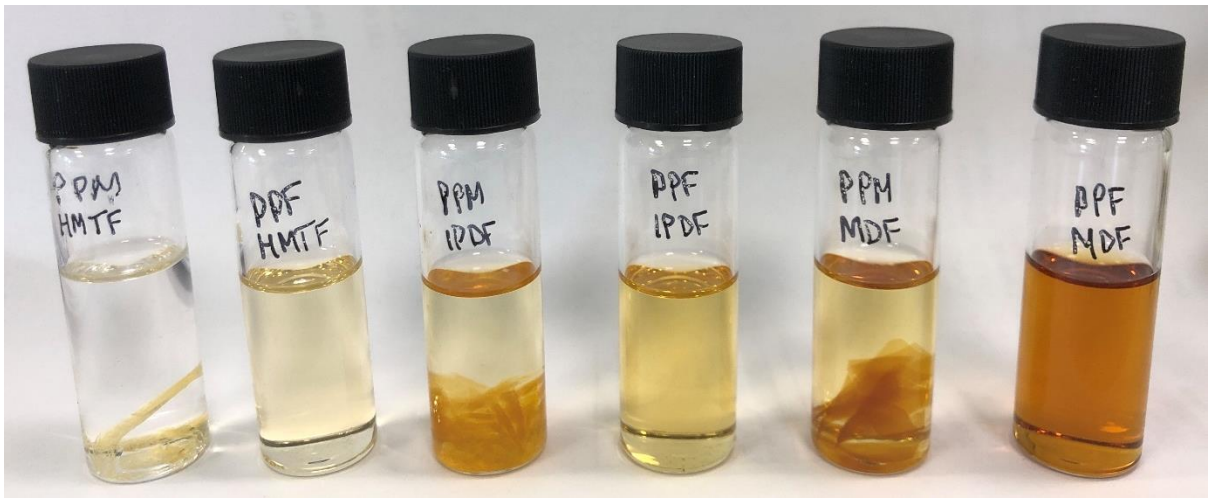

Figure 4.9 - Materials left in THF for 1 week. From left to right: PPM + HMTF, PPF + HMTF, PPM + IPDF, PPF + IPDF, PPM + MDF, PPF + MDF.

Solvent resistance was observed to be best with the use of the trifunctional cross-linker (HMTF) compared to both bifunctional furan cross-linkers (MDF and IPDF). This is likely a consequence of increased cross-linking density and urethane/ester H-bonding hindering dissociation. Networks using an UPE with a maleate backbone provided slightly better solvent resistance compared to networks using a fumarate-based UPE. The solvent was able to slowly dissolve the network as a consequence of the effect of concentration on the dynamic equilibrium. Once a cycloadduct dissociates, the resultant DA pairs are then soluble at a low concentration, making it unlikely they will reform and shifting the dynamic equilibrium drastically in favour of dissociation, which eventually leads the materials to full

dissociation and dissolution. None of the materials showed any gel fraction after a 24-hour Soxhlet extraction in ethyl acetate (b.p. 77 °C) due to the aforementioned solvent effect and increased temperature of the solution leading to more rapid dissociation.

Another explanation for the network collapse is that the UPEs and the linkers hadn't fully associated, as it was shown above that the network continued to associate for at least 26 weeks. With this in mind, the materials underwent another Soxhlet extraction under identical conditions after a 26 week cure. The materials showed varying amounts of solubility, with PPM + HMTF having a gel fraction of 99%. PPM + IPDF had 76% and PPM + MDF had 55%. The PPF-based materials fully dissolved, as their lower T_{rDA} allowed the warm solvent to affect the equilibrium and dissociate the network.

4.2.6 Isomerisation

During the retro-Diels-Alder reaction, there is potential for a maleate adducts to isomerise into a fumarate addend. This can be seen by performing a heat ramp on a sample of a PPM network multiple times. The network went through an initial heat (Heat 1), which dissociates the network, before being left at ambient temperature for 24 hours to reassociate, then another heat (Heat 2) and so on (**Figure 4.10a**).

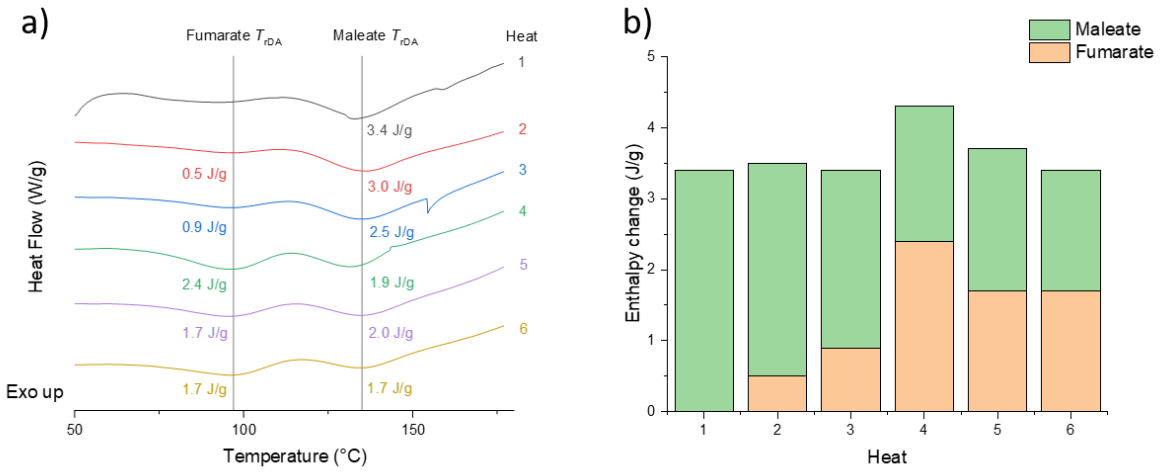

Figure 4.10 - a) Repeated heating ramps on a single sample of PPM + IPDF. b) The maleate and fumarate content of the unsaturation in the polyester backbone in each heat run.

On the first heat run, all the adducts have formed from PPM, so the rDA endotherm appears completely in the maleate T_{rDA} (130 °C) range. The high temperature during the heat run causes the maleate to isomerise to fumarate and so when the network reassociates, some fumarate adducts are formed. This is evident by the emergence of an endotherm in the fumarate T_{rDA} (100 °C) range in the following heat ramp. Subsequent heats show that the fumarate enthalpy change increases while the maleate enthalpy change decreases, as the network becomes more fumarate in character. This suggests that during each cycloreversion, some maleate isomerises to fumarate, gradually changing the proportion of the unsaturation in the backbone to be more fumarate (**Figure 4.10b**). This was confirmed *via* ^{1}H NMR spectroscopy with the appearance of the fumarate alkene proton resonances at δ = 6.85 ppm (maleate proton resonances occur at δ = 6.25 ppm) which integrated to 5% of the maleate signal after a single heat. Heating PPM under the same circumstances did not show any isomerization to the fumarate, indicating that the cycloreversion facilitates the isomerisation and it is not the maleate thermally isomerising into fumarate. This process is irreversible; once in the thermodynamically favoured fumarate conformation, it will not isomerise back into the maleate.

4.2.7 Self-healing

In order to avoid isomerisation complications and solely quantify the rate of network reformation, an alternative DSC experiment was conducted where the material was dissociated by heating to a lower temperature of 150 °C for 10 minutes before post-curing in ambient conditions. Different samples were taken from this material daily to undergo a heating cycle to 180 °C at 10 °C min^{-1} by DSC and the enthalpy change of the T_{rDA} reaction was recorded (**Figure 4.11**). The network showed an enthalpy change (ΔH_{rDA}) of 2.5 J g^{-1} at the T_{rDA}, which remained constant for the first 4 days and increased to above 5 J.g^{-1} after 7 days. This is quite a slow rate of formation, but it is comparable to maleimide and furan networks, which can also take a week to equilibrate.[24] Maleimide and furan addition is often considered "click chemistry", so materials reacting at a similar rate whilst being maleimide free is noteworthy.[12,25]

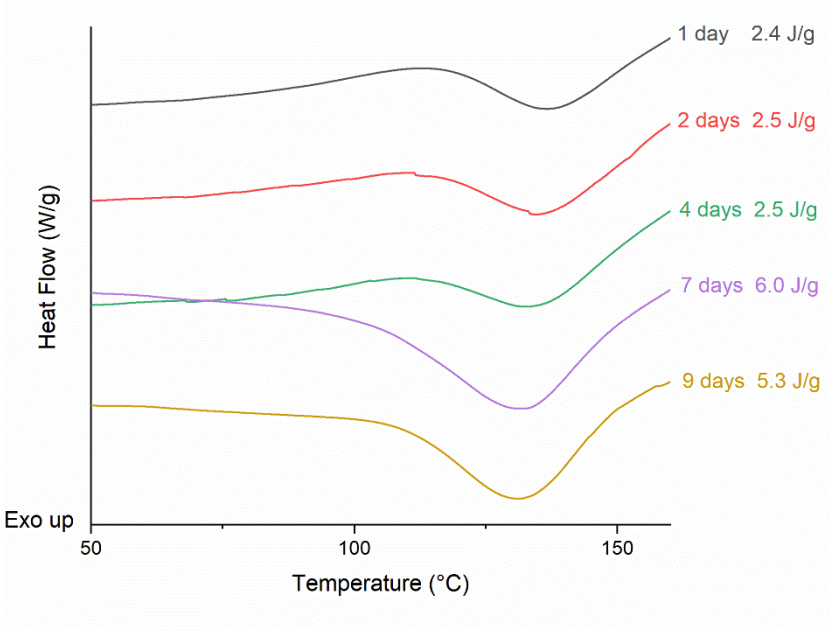

Figure 4.11 - The increase in the enthalpy change of rDA endotherms of PPM + IPDF as a result of changing cure time.

Fortunately, the rate of network reformation can be increased significantly by gentle heating. Fresh samples of all materials were prepared and half of each network was cured overnight at room temperature and the other half was cured at overnight 65 °C. Analysis by DSC of the networks showed

that the elevated temperature had minimal effect on the ΔH_{rDA} of the PPF-based networks, whereas the PPM-based networks showed significant increases (**Figure 4.12**). It is possible that the higher temperature also affects the rate of the reverse DA reaction in the fumarate networks, negating the increase in rate of the forward DA cycloaddition. The heating rate of the DSC (10 °C min^{-1}) means there will be some thermal lag in the transitions, and the true T_{rDA} will be lower than shown on the DSC trace. The maleate networks benefited remarkably from the increased curing temperature, reaching a ΔH_{rDA} of >20 J g^{-1}. At ambient temperatures, you would expect the materials to take a week to reach the same degree of curing.

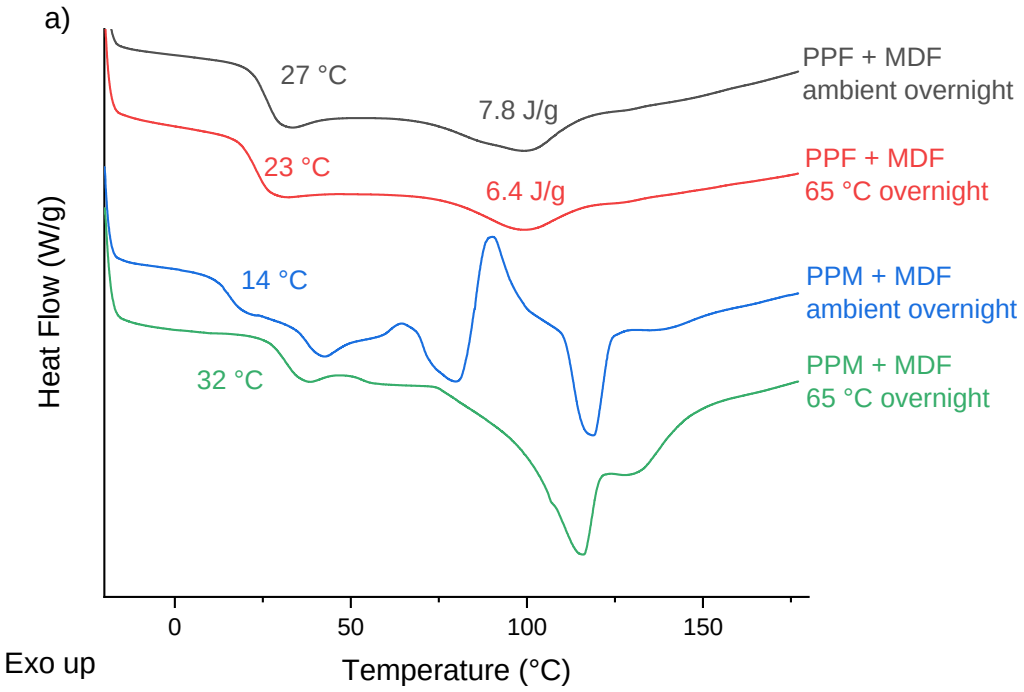
a)
27 °C
7.8 J/g
PPF + MDF
ambient overnight
23 °C
6.4 J/g
PPF + MDF
65 °C overnight
14 °C
PPM + MDF
ambient overnight
32 °C
PPM + MDF
65 °C overnight
Heat Flow (W/g)
0
50
100
150
Exo up
Temperature (°C)

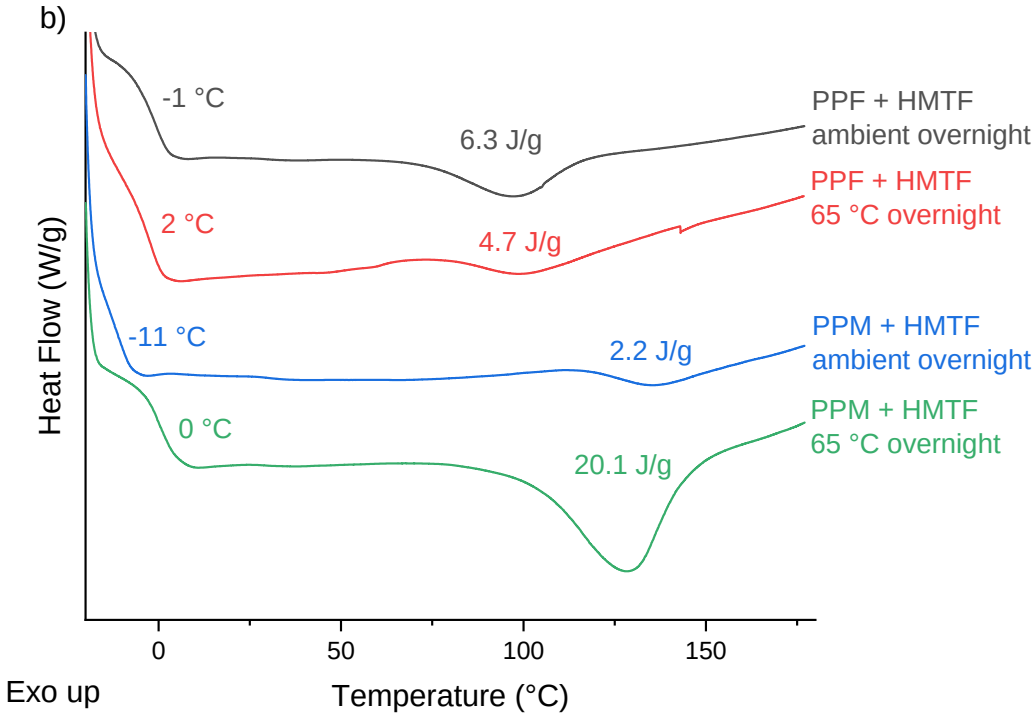
b)
-1 °C
6.3 J/g
PPF + HMTF
ambient overnight
2 °C
4.7 J/g
PPF + HMTF
65 °C overnight
-11 °C
2.2 J/g
PPM + HMTF
ambient overnight
0 °C
20.1 J/g
PPM + HMTF
65 °C overnight
Heat Flow (W/g)
0
50
100
150
Exo up
Temperature (°C)

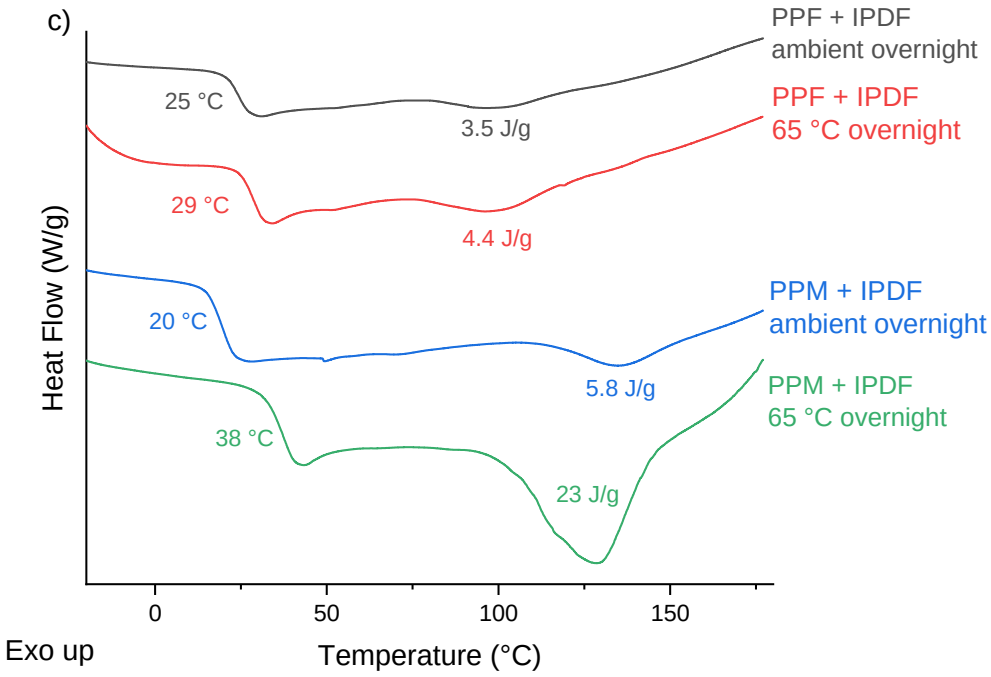

Figure 4.12 – The effect of curing at elevated temperatures on the ΔH_{rDA} and T_g of a) MDF, b) IPDF and c) HMTF networks.

4.2.8 Lap shear strength

The networked materials were used to bond two aluminium substrates together in a single lap-shear joint with a bond overlap of 25 × 16.5 mm^2 and a bondline thickness of 0.1mm. The samples underwent tensile testing at a displacement speed of 1.27 $mm.min^{-1}$ to determine the peak stress and extension of the joint at peak (**Table 4.2**). PPF + HMTF showed a remarkably higher shear strength than the other materials, with an average peak stress of 9.95 MPa (**Figure 4.13**). This is comparable to other recent results for DA-based adhesives in literature, with Wu and co-workers demonstrating ≈6 MPa peak stress with a hot-melt adhesive based on a furan-terminated polyurethane prepolymer linked with a bismaleimide.[26]

Table 4.2 – Mechanical properties of the synthesised networks.

Material	Peak stress (MPa)		Extension at peak (mm)		T_g (°C)
	Mean	Standard deviation	Mean	Standard deviation	
PPF + MDF	0.72	0.08	0.03	0.00	27
PPF + IPDF	0.72	0.22	0.04	0.01	36
PPF + HMTF	9.95	0.47	0.93	0.08	11
PPM + MDF	0.79	0.13	0.04	0.01	25
PPM + IDPF	1.66	1.11	0.10	0.09	20
PPM + HMTF	0.38	0.09	1.29	0.26	2

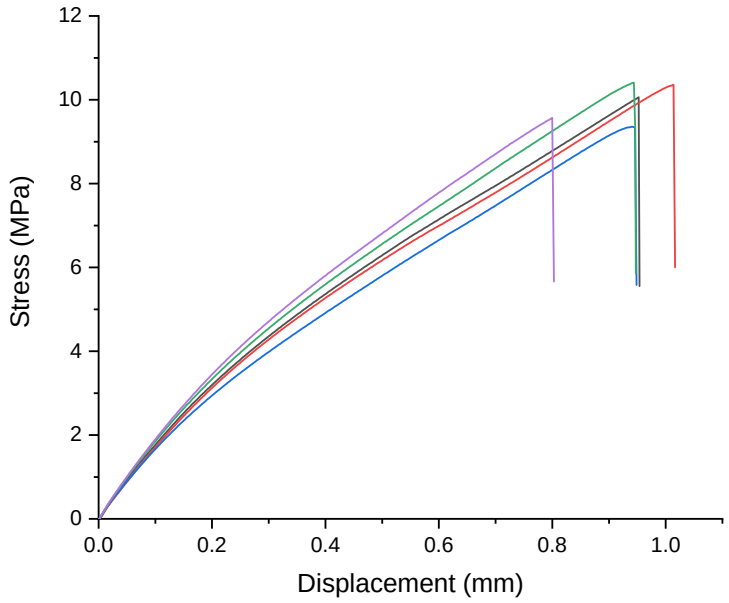

Figure 4.13 – Stress vs displacement results from the lap shear tensile testing of PPF + HMTF.

The IPDF- and MDF-linked networks displayed poor tensile strength, as the high cross-link density produced materials too brittle to withstand any strain. To improve the tensile strength, a lower molar

ratio of linker furans to UPE alkenes could be used to lower the cross-linking density. In previous compositions, the number of furan groups was equal to the degree of unsaturation of the polyester. A new composition was produced using half the amount of cross-linking agent, halving the potential number of cross-links possible. Unfortunately, the resulting material was still very brittle with a T_g of 30 °C and consequently showed no lap shear strength.

Another approach to lowering the cross-link density is to increase the distance between unsaturated groups in the polyester chain. This was achieved by synthesising a new series of polyesters, replacing some of the fumarate groups with succinate groups. The succinate group is a saturated analogue of the fumarate group, allowing the dienophile to be separated with minimal effect on the overall chain composition (**Figure 4.14**). Increasing the distance between unsaturation reduces the concentration of Diels-Alder bonds, lowering cross-link density and the resultant T_g. Additionally, succinate groups are more flexible than fumarate groups, where the π bond of the fumarate is locked in conformation, the σ bond of the succinate group can rotate, introducing more degrees of flexibility to chain and the overall flexibility of the material.

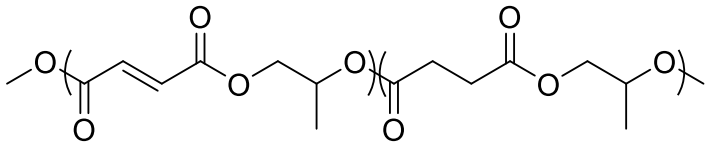

Figure 4.14 – Using a succinate group to spread out the fumarate groups in the polyester chain.

Poly(propylene fumarate-*co*-propylene succinate) (PPFPS) with a 75:25, 50:50 and 25:75 fumarate to succinate molar ratio was synthesised through step-growth polymerisation in bulk from maleic anhydride, propylene glycol and succinic acid. The PPFPS polymers were bulk polymerised in melt with all three linkers in an equimolar ratio of unsaturation to furan functionality to produce new UPE CANs with lower cross-linking density and greater flexibility. As expected, the resulting DSC traces taken a week after synthesis showed a clear decrease in T_g as the amount of fumarate decreased. Furthermore,

the ΔH_{rDA} decreases as the concentration of fumarate decreases, providing more evidence for the reduction of cross-link density (**Figure 14.15**). This also means the thermodynamic stability will be reduced, which should be considered depending on the application of the material. The endothermic relaxation of the MDF networks also disappears, which is a combined effect of the lower T_g and reduced quantity of MDF in the material.

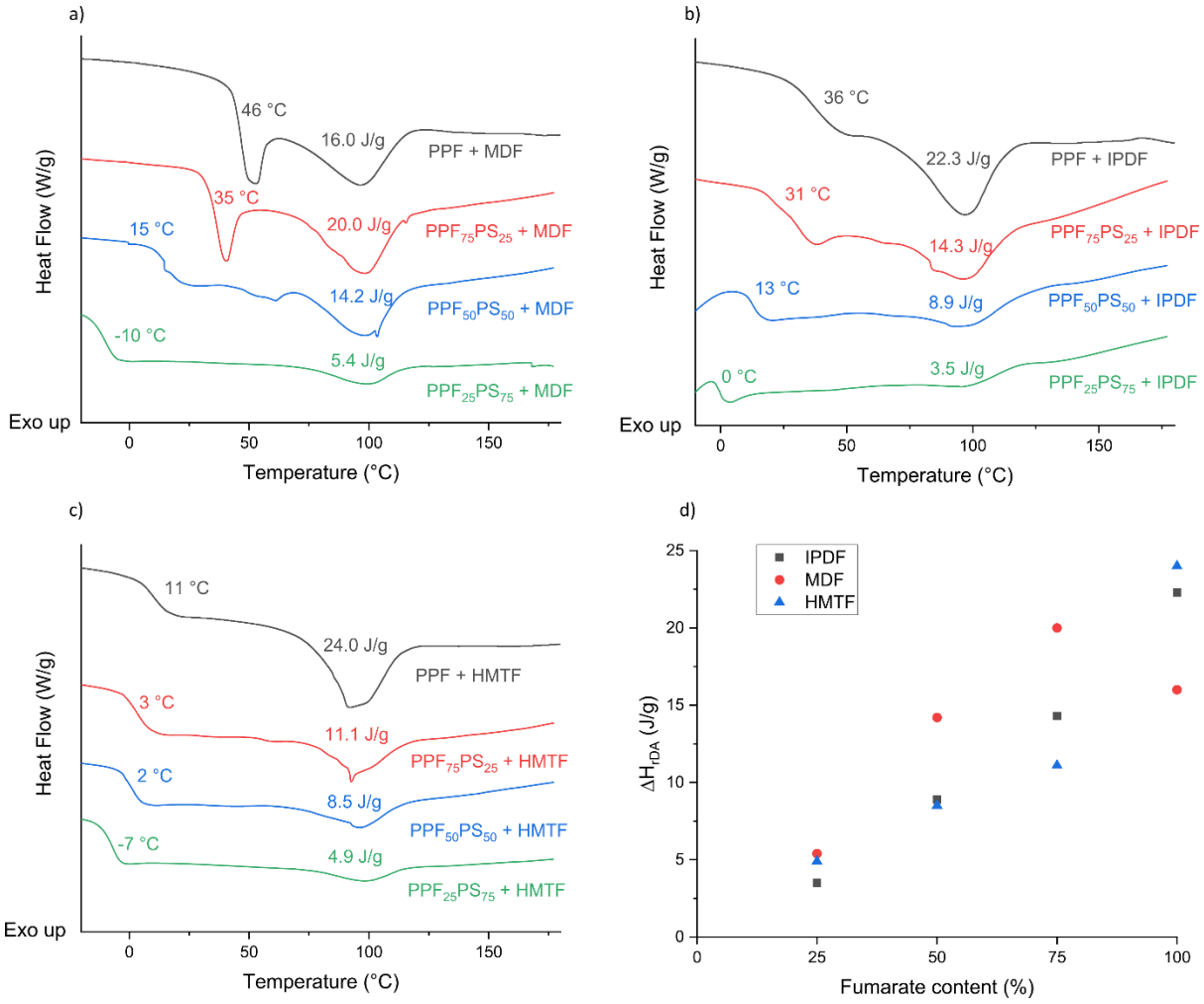

Figure 4.15 – DSC traces of polyester networks with varying proportions of fumarate and succinate groups in the backbone with linkers a) MDF, b) IPDF and c) HMTF. d) Positive correlation between increasing fumarate content in the UPE backbone and the rDA enthalpy.

The materials with a 50/50 succinate to fumarate ratio had their T_gs lowered sufficiently enough to longer be brittle, and were selected to undergo lap shear testing to ascertain whether the added

flexibility to the polymer improves its tensile strength (**Table 4.3**). In the case of the MDF- and IPDF-linked networks, introducing 50% succinate into the composition increased the tensile strength by a whole order of magnitude (0.72 MPa to 8.70 MPa and 0.72 MPa to 7.78 MPa, respectively). PPF + HMTF already performed well, but adding further flexibility resulted in a lower Young's modulus and deformation under tensile stress.

Table 4.3 – Mechanical properties of the synthesised PPFPS networks.

Material	Peak stress (MPa)	Extension at peak (mm)	T_g (°C)
PPF + MDF	0.72	0.03	27
$PPF_{50}S_{50}$ + MDF	8.70	0.71	15
PPF + IPDF	0.72	0.04	36
$PPF_{50}S_{50}$ + IPDF	7.78	1.18	13
PPF + HMTF	9.95	0.93	11
$PPF_{75}S_{25}$ + HMTF	6.39	0.66	3
$PPF_{50}S_{50}$ + HMTF	1.48	0.82	2

This highlights how the performance of UPE CANs can be significantly tuned to a specific application through a simple change in the composition of the polyester. The wide array of acids and glycols available to use means the number of possible compositions is effectively limitless.

4.3 Conclusions

The synthesis of dissociative CANs produced from UPEs and multi-functional furans was achieved under industrially relevant conditions. These materials are maleimide-free, making them a greener and safer alternative to most other debondable adhesives being researched today. Instead, the dienophile comes from the unsaturation in polyesters, which can be purchased or synthesised on a large scale and are safe to handle. The networks can be easily dissociated with heat and reformed

multiple times, as shown by the reappearance of a retro-Diels-Alder endotherm in each heating run. Both fumarate- and maleate-based UPEs were shown to form dissociative CANs with a T_{rDA} of around 90 and 130 ˚C, respectively. Repeated heating and cooling cycles did exhibit isomerisation of maleates into fumarates but did not affect the ability of the network to reform, and the reformation can be accelerated by applying mild heat. The reprocessability provides a pathway for unsaturated polyesters to be involved in a circular economy, whereas typically, end-of-life materials are sent to landfill. The materials have the potential to be used as adhesives; the shear strength of PPF + HMTF is comparable to other recently reported results in literature. The strength of other networks can be improved significantly through a small change in the formulation to incorporate higher flexibility and lower cross-linking density. The plethora of different UPEs and furan-functionalised cross-linkers available means that the final properties of the materials can be fine-tuned to meet a variety of different applications.

4.4 Bibliography

1 Statista, https://www.statista.com/statistics/912301/polyester-fiber-production-worldwide/, (accessed 10 March 2023).

2 M. H. Irfan, in *Chemistry and Technology of Thermosetting Polymers in Construction Applications*, Springer Netherlands, Dordrecht, 1998, pp. 230–239.

3 Y. Gao, P. Romero, H. Zhang, M. Huang and F. Lai, *Constr Build Mater*, 2019, **228**, 116709.

4 A. Buketov, M. Brailo, S. Yakushchenko and A. Sapronova, *Advances in Materials Science and Engineering*, 2018, **2018**, 1–6.

5 Tricel Composites, https://www.tricelcomposites.co.uk/blog-polyester-resin/, (accessed 10 March 2023).

6 L. G. Curtis, D. L. Edwards, R. M. Simons, P. J. Trent and P. T. Von Bramer, *Industrial and Engineering Chemistry Product Research and Development*, 1964, **3**, 218–221.

7 I. Vancsó-Szmercsányi, K. Maros-Gréger and E. Makay-Bödi, *Journal of Polymer Science*, 1961, **53**, 241–248.

8 C. J. Kloxin, T. F. Scott, B. J. Adzima and C. N. Bowman, *Macromolecules*, 2010, **43**, 2643.

9 W. Denissen, J. M. Winne and F. E. Du Prez, *Chem Sci*, 2016, 7, 30–38.

10 W. Denissen, G. Rivero, R. Nicolaÿ, L. Leibler, J. M. Winne and F. E. Du Prez, *Adv Funct Mater*, 2015, **25**, 2451–2457.

11 A. Jourdain, R. Asbai, O. Anaya, M. M. Chehimi, E. Drockenmuller and D. Montarnal, *Macromolecules*, 2020, **53**, 1884–1900.

12 M. A. Tasdelen, *Polym Chem*, 2011, 2, 2133–2145.

13 A. Gandini, *Prog Polym Sci*, 2013, **38**, 1–29.

14 R. Wojcieszak, F. Santarelli, S. Paul, F. Dumeignil, F. Cavani and R. V Gonçalves, *Sustainable Chemical Processes*, 2015, **3**, 2–9.

15 X. Li, B. Ho, D. S. W. Lim and Y. Zhang, *Green Chemistry*, 2017, **19**, 914–918.

16 S. Bains, R. M. Pagni and G. W. Kabalka, *Tetrahedron Lett*, 1991, **32**, 5663–5666.

17 M. G. Silvestri and C. E. Dills, *J Chem Educ*, 1989, 66, 690–691.

18 N. Windmon and V. Dragojlovic, *Green Chem Lett Rev*, 2008, **1**, 155–163.

19 T. A. Eggelte, H. de Koning and H. O. Huisman, *Tetrahedron*, 1973, **29**, 2491–2493.

20 V. N. Huynh, M. Leitner, A. Bhattacharyya, L. Uhlstein, P. Kreitmeier, P. Sakrausky, J. Rehbein and O. Reiser, *Commun Chem*, 2020, **3**, 158.

21 A. Fradet and P. Arlaud, in *Comprehensive Polymer Science*, Pergamon Press, Oxford, 1st edn., 1989, vol. 5, pp. 331–334.

22 S. Paul, Y. Zhu, C. Romain, R. Brooks, P. K. Saini and C. K. Williams, *Chemical Communications*, 2015, **51**, 6459–6479.

23 Z. Wei, J. H. Yang, X. J. Du, F. Xu, M. Zrinyi, Y. Osada, F. Li and Y. M. Chen, *Macromol Rapid Commun*, 2013, **34**, 1464–1470.

24 L. M. Sridhar, M. O. Oster, D. E. Herr, J. B. D. Gregg, J. A. Wilson and A. T. Slark, *Green Chemistry*, 2020, **22**, 8669–8679.

25 N. K. Devaraj and M. G. Finn, *Chem Rev*, 2021, **121**, 6697–6698.

26 M. Wu, Y. Liu, P. Du, X. Wang and B. Yang, *Int J Adhes Adhes*, 2020, **100**, 102597.

5 Synthesis and characterisation of unsaturated polyesters via step-growth polymerisation and ring-opening copolymerisation

5.1 Introduction

The stereochemistry around the double bond in an unsaturated polyester (UPE) results in two different isomers, maleates and fumarates (**Figure 5.1**). Polyesters containing maleate moieties in the backbone have advantages over fumarate-functionalised polymers when involved in covalent adaptable networks, such as better thermal stability and solvent resistance (Chapter 4). Therefore, it would be beneficial to generate networks from UPEs with maleate backbones.

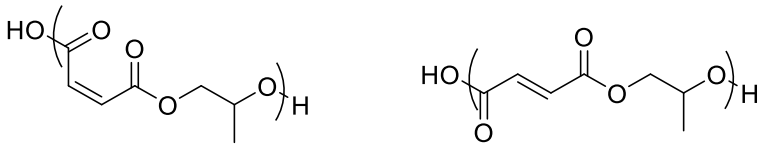

Poly(propylene maleate) Poly(propylene fumarate)

Figure 5.1 - Two isomeric unsaturated polyesters.

However, the vast majority of UPEs on the market are fumarates because the *trans* alkene conformation exhibits higher reactivity towards styrene during the cross-linking stage, allowing for a faster cure.[1] Despite the final polyester containing fumarate groups, maleic anhydride is the most widely used unsaturated condensation monomer for polyester resin production, as it is cheaper than fumaric acid. During the high temperature polyesterification, the maleates are partly or wholly converted into fumarates.[2] Preventing this isomerisation could open up a synthetic route to a polyester that has a high maleate content.

The isomerisation of maleates to fumarates is caused by a number of factors; mainly high temperatures, glycol choice and catalyst. High temperatures cause isomerisation by enabling the *cis* alkene to overcome the energy barrier of rotation from the p orbital overlap and isomerise to the *trans* isomer (**Scheme 5.1**). The maleic anhydride opens *via* glycol attack at around 80 °C to give the maleate half-ester and this can isomerise at temperatures exceeding 180 °C.

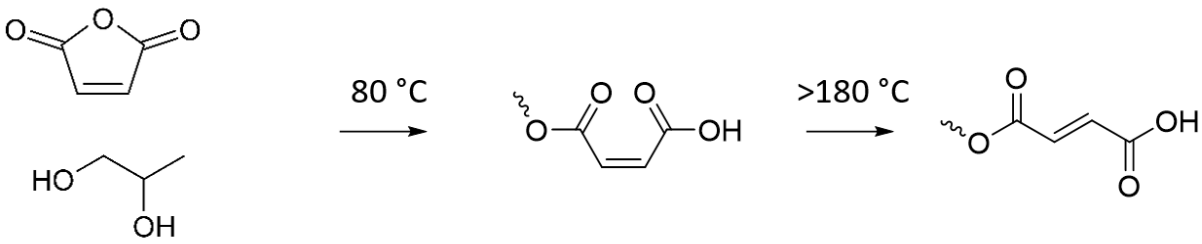

Scheme 5.1 – Maleic anhydride opening from the glycol attack, following by subsequent isomerisation at high temperatures.

The glycol used to attack the maleic anhydride also has an effect on the degree of isomerisation.[3] Short-chain glycols (2-3 carbons) enable the nucleophilic hydroxyl group to attack the maleate double bond and form a cyclic intermediate (**Scheme 5.2**). The electron rearrangement causes the shift of the double bond and the σ-bond that remains is free to rotate to the lower energy *trans* conformer. The reverse electron rearrangement and ring-opening locks the ester in the fumarate conformer.[4] Therefore, to minimise isomerisation, low temperatures and long-chain or rigid diols should be used.

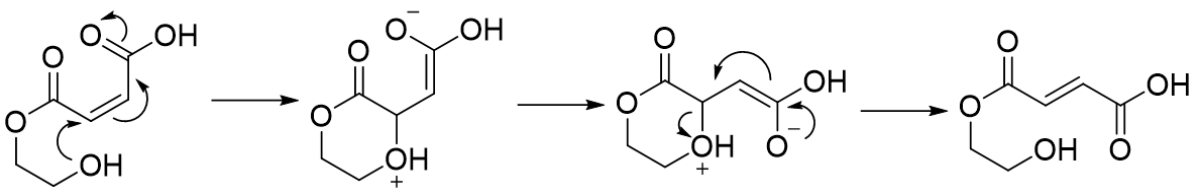

Scheme 5.2 – Formation of a cyclic intermediate and subsequent rotation to fumarate conformation.

Unfortunately, practically all industrial UPE production follows this pathway, so a readily available supply of maleate-containing polyester would be difficult to source. There have been multiple investigations into factors causing isomerisation, but these have been written with the goal of maximising isomerisation to form the classically more desirable fumarate. Thus far, there has been no research that attempts to achieve minimal isomerisation. In 1961, Vancsó-Szmercsányi *et al* carried out a thorough investigation into the isomerisation with various glycols throughout the esterification.[3] Maleic anhydride and a variety of glycols were polymerised in the melt without a catalyst for 12-14 hours at 175 °C. Aliquots were taken throughout the reaction and the fumarate content plotted against molecular weight. All compositions experience a fast increase in fumarate content before reaching a constant value, normally around 10 degrees of polymerisation. Aligning with the mechanisms above, the longest chain diol, diethylene glycol, had the least isomerisation with 31.3% fumarate. The research established that the glycol structure exercises a considerable influence on the isomerisation, with longer chain lengths causing the least isomerisation. This chapter aims to improve on this work by using milder conditions, a catalyst and another glycol, in order to minimise the isomerisation to fumarate.

Another method of synthesising UPEs is ring-opening copolymerisation (ROCOP). ROCOP between maleic anhydride and propylene oxide can be performed at lower temperatures than step-growth polymerisation and does not form cyclic intermediates, retaining the maleate stereochemistry. Rings containing strongly polarised bonds such as esters, carbonates, amides, urethanes and phosphates are particularly susceptible to ROCOP.[5] However, heterocyclic monomers with less electrophilic groups such as ethers, amines and thioethers can also be polymerised if they have large degree of ring-strain.[6] The polymerisation can be initiated by anionic initiators such as alcoholates,[7] carboxylates,[8] thiolates,[9] alkoxides,[10] and tertiary amines.[11]

Herein, the dominant factors that cause maleate isomerisation and the best way to limit it will be investigated. A comparison between the two methods of synthesising the unsaturated polyesters, namely step-growth polycondensation and ROCOP will be discussed.

5.2 Results and discussion

Step growth polymerisation

Polyesters were synthesised on a large-scale (1 kg) using step-growth polymerisation. The proportion of anhydrides and diols were calculated to give a 10% OH excess and to a total mass of around 1 kg. A degree of polymerisation of 15 was targeted, with the amount of water liberated and final acid value for this point was calculated. A 2 L reactor was charged with the anhydride, diol and monobutyltin oxide catalyst. The reactor was fitted with a heated glycol column followed by a water-cooled condenser (**Figure 5.2**). The heated glycol column was set at 105 °C to allow for the removal of water without losing any volatile reagents. The mixture was heated gently under N_2 with stirring and then held isothermally at the first signs of condensation. When the temperature at the still head dropped, the reaction temperature was increased to a maximum of 180 °C. The volume of distillate was monitored, and when it reached the calculated amount, acid values were taken as a more accurate indicator of reaction progression. Once the acid value was within specification, <30 mg KOH/g, the reaction was stopped.

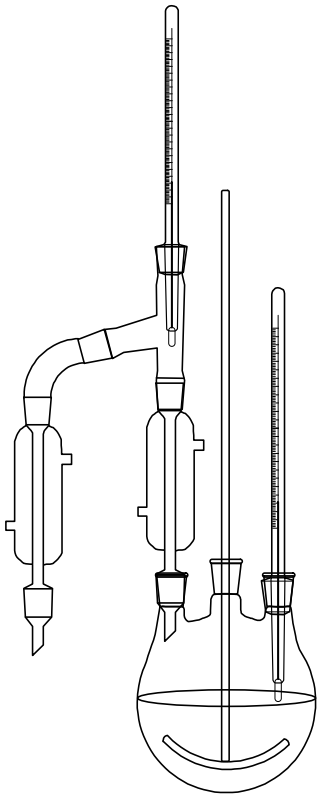

Figure 5.2 – Example polycondensation setup.

Three different diols were chosen to investigate their effect on the isomerisation (**Figure 5.3**). 1,2-propylene glycol (PG) and diethylene glycol (DEG) have both been used in previous literature, so the results could be compared and provide a reference. Cyclohexanedimethanol (CHDM) has not been investigated previously and was selected based on its rigid structure, which would prevent the formation of the cyclic intermediate and the isomerisation.

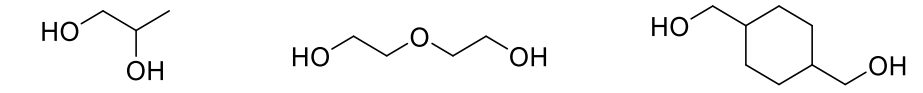

Propylene glycol Diethylene glycol Cyclohexanedimethanol

Figure 5.3 – Diols used in the step growth polycondensation with maleic anhydride.

The first attempt at synthesising a high-maleate content polyester involved the condensation reaction between maleic anhydride and 1,2-propylene glycol (PG). PG is a very common starting material for the production of polymers; in 2016, the production of PG was estimated at about 1400 million pounds

per year and was predicted to increase annually by 4%.[12] The single largest use for PG is the manufacture of unsaturated polyester resins, with approximately 45% of PG produced going toward this one application. It is polymerised with isophthalic acid and maleic anhydride and ultimately cured to yield a hard, cross-linked, thermoset composite that can then be used in automotive plastics, fibre-reinforced glass boats and construction.[2] Despite the ability of propylene glycol to form an intramolecular cyclic intermediate, it was hoped that keeping the polymerisation temperature at ≤180 °C is enough to minimise isomerisation. At such a low temperature, the rate of polymerisation is very slow and after 16 hours the acid value hadn't reached the desired end point. However, water had stopped condensing so the reaction was ended. The polyester was analysed with ^{1}H NMR spectroscopy, and by integrating the fumarate and maleate signals (δ = 6.84 and 6.27 ppm, respectively) relative to each other, it was determined that the maleate content of the final polyester was 13% (**Figure 5.4**).

Lowering the temperature was not sufficient to prevent isomerisation, so the second synthesis used DEG as the diol. This longer chain diol has six bonds between the hydroxyl groups, so therefore is less likely to form the cyclic intermediate. DEG is another commonly used glycol as it imparts flexibility on the polyester resin but the introduction of ether linkages between the end groups reduces the water-resistance of the resin due to the hydrophilicity induced by the polarity of the ether oxygens.[13] The reaction temperature was kept below 180 °C and the polymerisation reached the desired monomer conversion within 12 hours. DEG has two primary hydroxyl groups, which are more susceptible to esterification than the secondary hydroxyl group present on the PG. The longer chain diol was successful in reducing the isomerisation; achieving a final maleate content of 62%. Although it is a longer diol, it may still be possible for some cyclic intermediates to form and cause the formation of some fumarate. Dipropylene glycol (DPG) has two more carbons in the chain than DEG and synthesis using this diol achieved an even higher maleate content of 82%.

Finally, 1,4-cyclohexanedimethanol (CHDM) was used as the diol. This rigidity afforded to the molecule by the cyclohexane ring means that the formation of the cyclic intermediate is not possible. This resulted in the best retention of maleate, with 86% maleate in the final polyester. Furthermore, the reactive primary alcohol groups allow for a faster and milder reaction so the polymerisation had reached completion in just 5 hours at 160 °C, which also reduces the likelihood of alkene rotation.

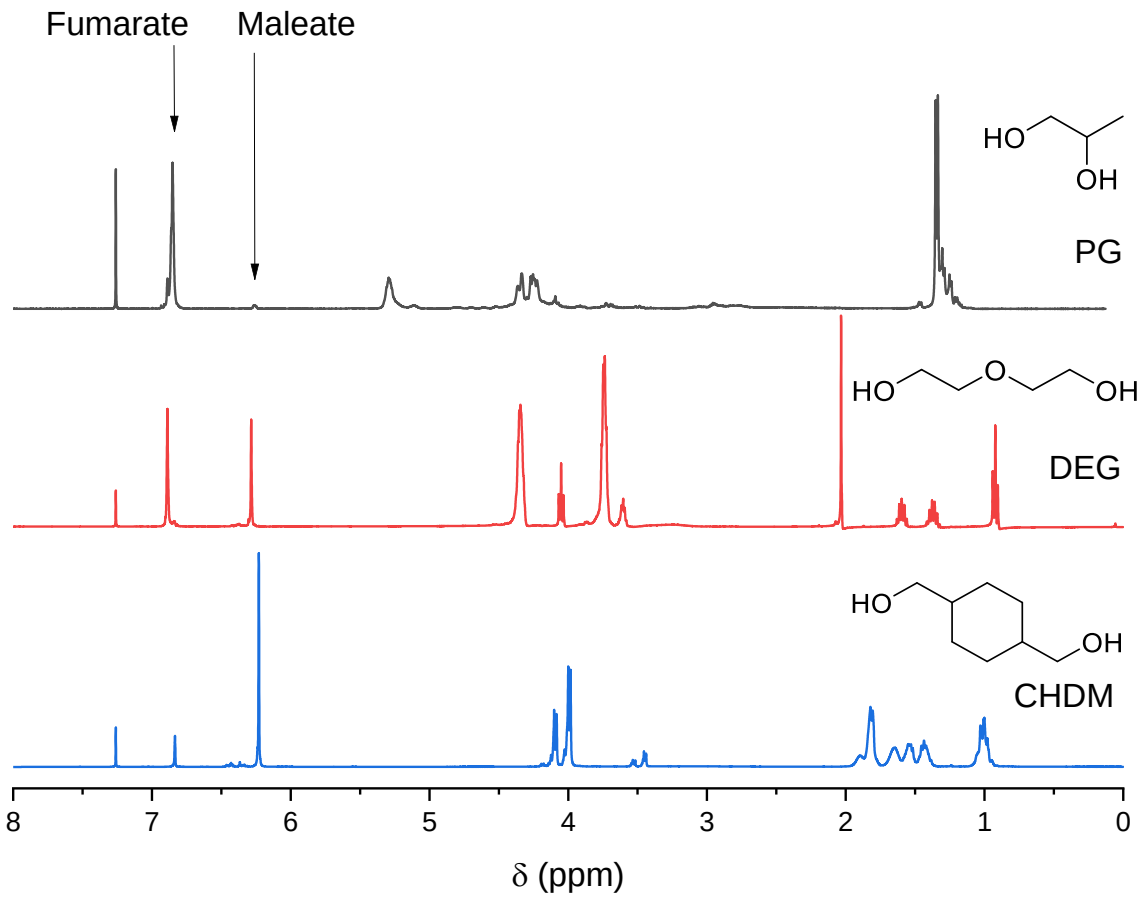

Figure 5.4 - ^{1}H NMR spectra of the polyester synthesised *via* step-growth polymerisation, named according to which diol was copolymerised with maleic anhydride. Top: propylene glycol. Middle: Diethylene glycol. Bottom: Cyclohexanedimethanol. (400 MHz, $CDCl_3$, 298 K).

Glycol choice plays a significant role in reducing the isomerisation, and cyclohexanedimethanol was the best choice of the three, reacting the fastest and having the least isomerisation (**Table 5.1**). To determine how much effect temperature has on the isomerisation, CHDM was used again in another

polymerisation at a higher temperature of 200 °C. The reaction was complete in less than 2 hours and retained a high amount of maleate at 78%. For some applications, it may be beneficial to sacrifice maleate content for a faster reaction time.

Table 5.1 - Table showing final maleate content of the UPEs synthesised from different glycols and their reaction conditions.

Glycol	Max temperature (°C)	Reaction time (mins)	Final acid value (mg KOH/g)	Final maleate content (%)
Propylene glycol	170	960	23	13
Diethylene glycol	170	720	13	62
Cyclohexanedimethanol	160	300	25	86
Cyclohexanedimethanol	200	110	15	78

The polymers synthesised *via* step growth were closer to a random copolymer than an alternating copolymer as shown by matrix-assisted laser desorption/ionisation-time of flight (MALDI-TOF) mass spectrometry. Mass spectrometry is a useful tool for identifying the chain sequence of the polymer backbone because the difference between the mass-to-charge ratios (*m/z*) of the fragment peaks indicates the sequence of monomers along the backbone. A propylene glycol fragment would have *m/z* = 58.1 and a maleic anhydride fragment would have *m/z* = 98.1. There are a number of peaks that are separated by the same *m/z*, indicating sequential addition of the same monomer (**Figure 5.5**). This would cause the alkene functionality of some chains to be lower if they contained less maleate units, ultimately affecting its ability to form a network.

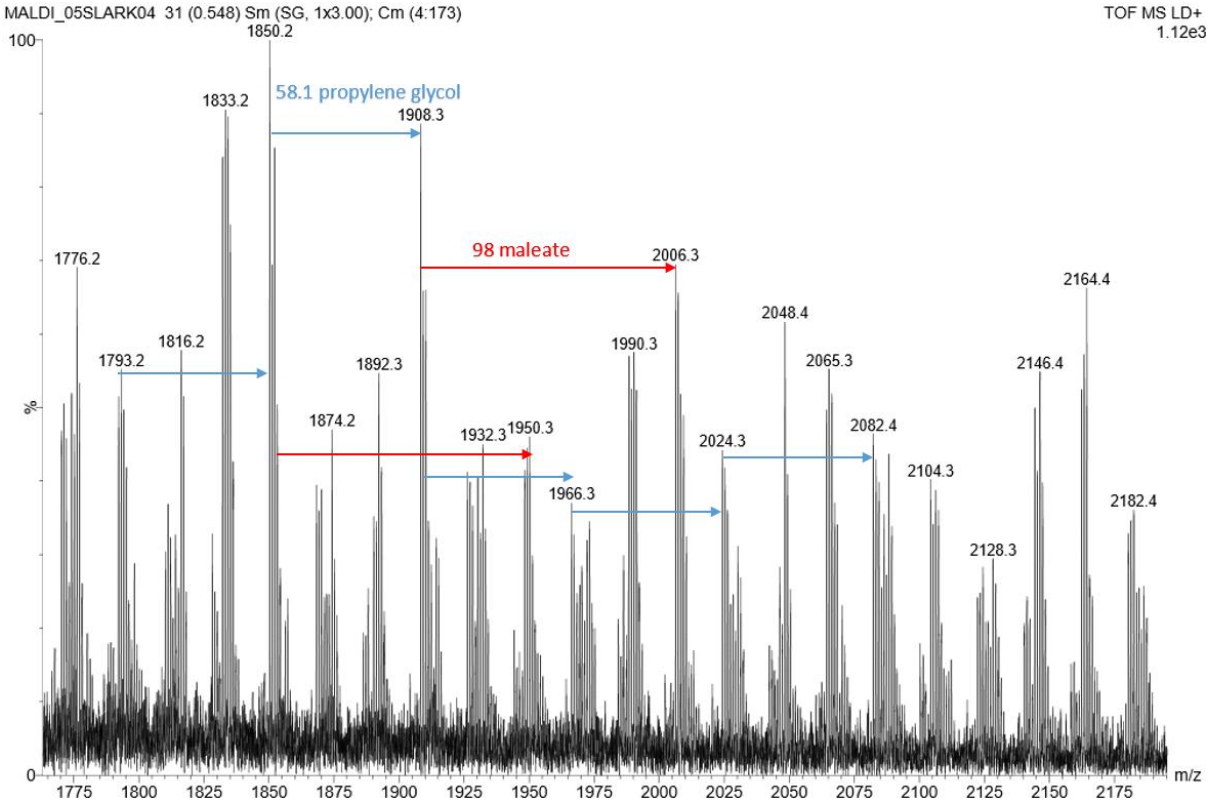

Figure 5.5 - MALDI-TOF mass spectrum of poly(propylene fumarate) synthesised *via* step growth with maleic anhydride and propylene glycol.

Ring-opening copolymerisation

A range of unsaturated polyesters were synthesised *via* the ROCOP of propylene oxide and anhydrides. The anhydrides used were maleic anhydride, itaconic anhydride and citraconic anhydride, to yield poly(propylene maleate) (PPM), poly(propylene itaconate) (PPI) and poly(propylene citraconate) (PPC), respectively (**Scheme 5.3**).

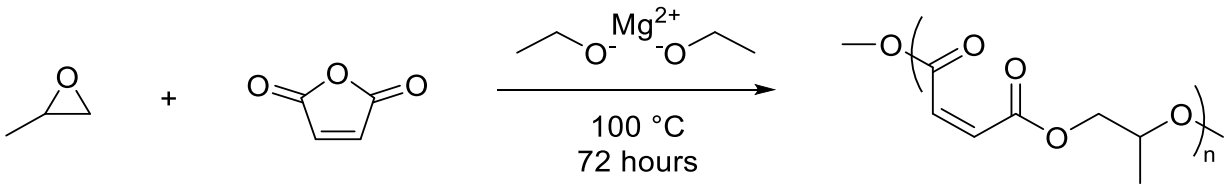

Scheme 5.3 – Ring-opening copolymerisation of propylene oxide and maleic anhydride to make poly(propylene maleate).

Under air-free and moisture-free conditions, propylene oxide, maleic anhydride, magnesium ethoxide and anhydrous toluene was added to a Schlenk flask and stirred for 72 hours at 100 °C. By this point, the polymer has become immiscible and crashed out of the solution. A sample of the bottom product layer was used to calculate conversion *via* ^{1}H NMR spectroscopy. When ring-opened, the maleic anhydride proton resonance shifts from δ = 7.02 ppm to δ = 6.25 ppm. The signals from the maleate and maleic anhydride resonances were integrated and normalised to give a conversion of 86% (**Figure 5.6**). The absence of a fumarate resonance at δ = 6.84 ppm indicates that no isomerisation has occurred.

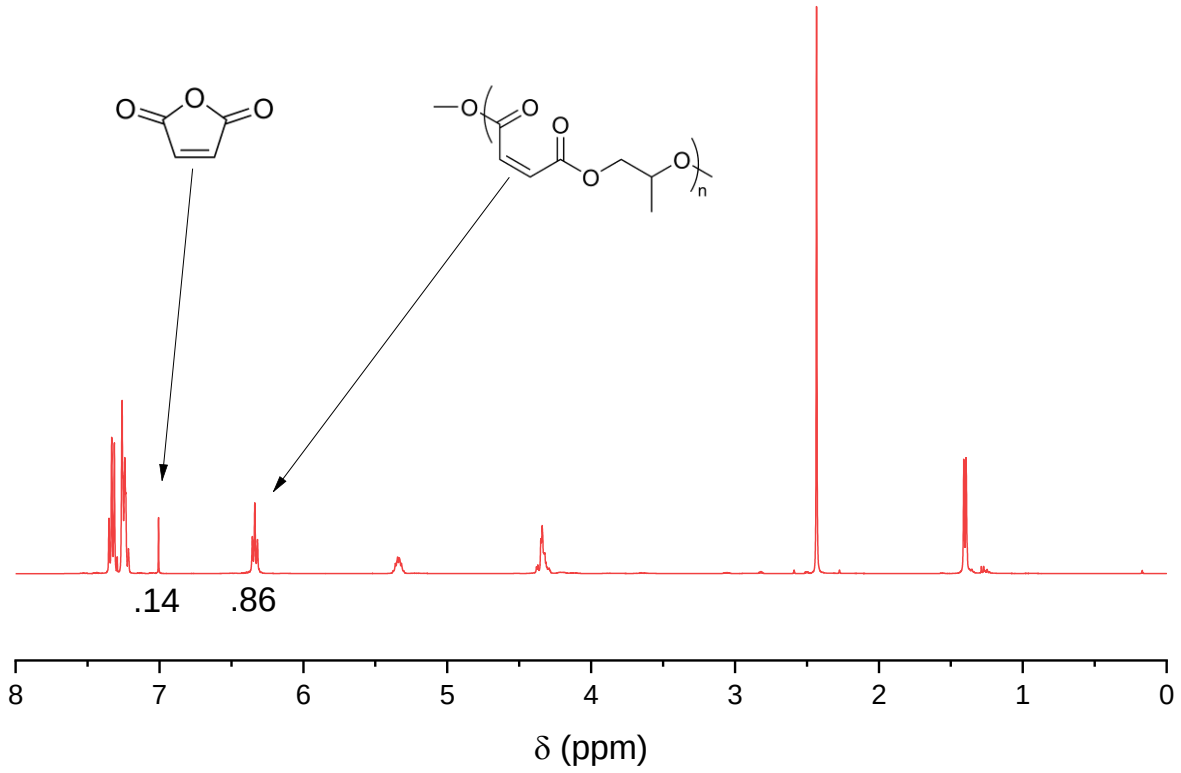

Figure 5.6 – ^{1}H NMR spectrum of the crude PPM to calculate conversion. (400 MHz, CDCl3, 298 K).

The top solvent layer was decanted off and the product was washed by dissolving in chloroform and precipitating in diethyl ether. The solvent was decanted off again and the final products dried

overnight in a vacuum oven. MALDI-TOF mass spectroscopy confirmed the backbone to be an alternating copolymer (**Figure 5.7**). The *m/z* difference between the peaks alternate between maleate (*m/z* = 58.1) and propylene oxide (*m/z* = 98.1) units.

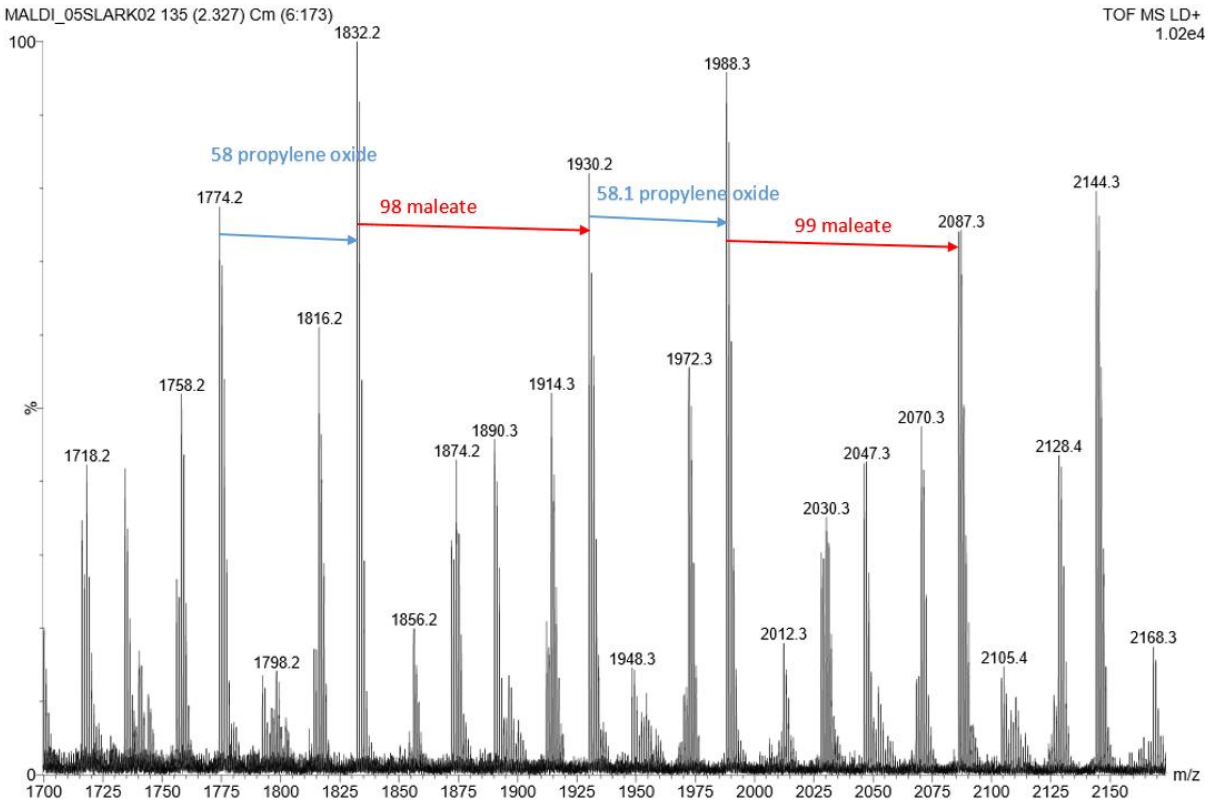

Figure 5.7 - MALDI-TOF mass spectrum of poly(propylene maleate) initiated from magnesium ethoxide.

The other unsaturated polyesters were synthesised using the same method, replacing maleic anhydride with citraconic anhydride or itaconic anhydride to alter the type of unsaturation in the polyester (**Figure 5.8**). Another diol, 1,2-epoxybutane was also introduced to provide more variation in the backbone. In total, PPM, PPC, PPI, poly(butylene maleate) (PBM) and poly(butylene citraconate) (PBC) were synthesised.

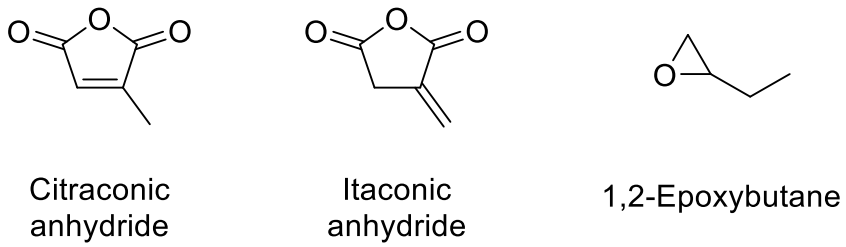

Figure 5.8 – Other anhydrides and epoxies used in ROCOP.

Polymerisations using maleic anhydride were able to be performed with good control over chain length. A degree of polymerisation (DP) of 40 was targeted using the equation $DP = \frac{[monomer]}{[initiator]}$ and size-exclusion chromatography (SEC) confirmed this and indicated low dispersities ($Đ_M$) of <1.3 (**Figure 5.9, Table 5.2**).

Changing the anhydride resulted in less successful polymerisations; the final products did not have a smooth consistency and they had higher and inconsistent $Đ_M$s. PPC and PBC has $Đ_M$s of 2.1 and 1.8, and PPI had a very large $Đ_M$ of 4.2. This could be caused by the polymers being less soluble, and crashing out of solution early. Future tests could involve performing the ROCOP in other solvents.

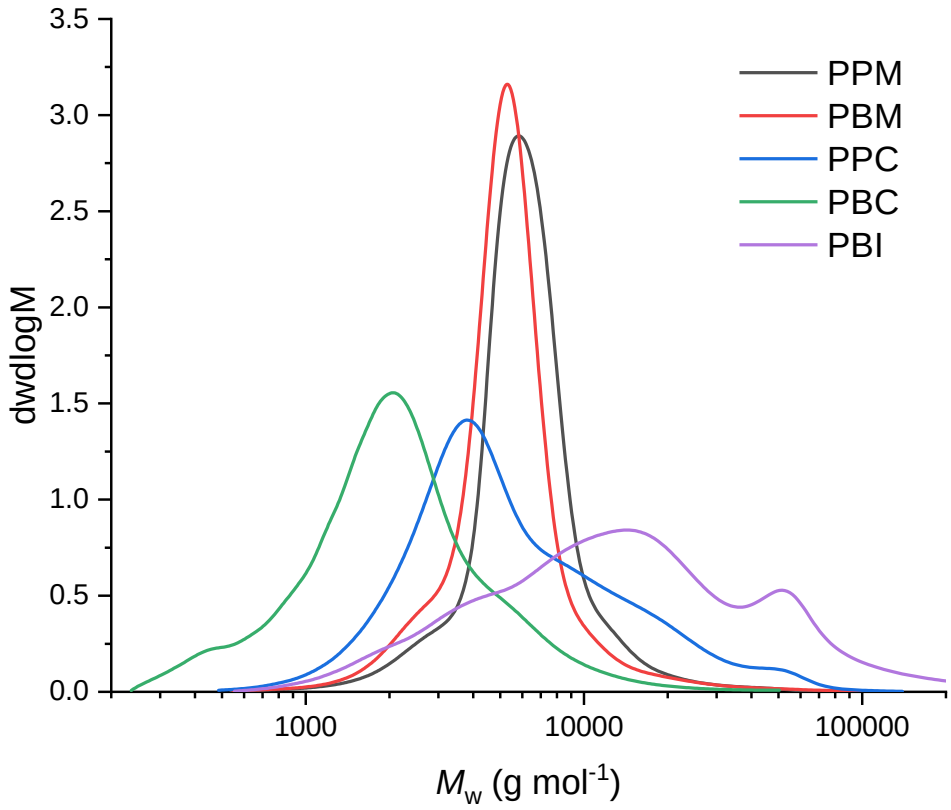

Figure 5.9 – SEC chromatograms of unsaturated polyesters synthesised *via* ROCOP.

Table 5.2 – SEC analysis of unsaturated polyesters synthesised *via* ROCOP.

	M_n (g mol^{-1})	M_w (g mol^{-1})	Dispersity $Đ_M$
PPM	5400	6780	1.26
PBM	4600	6040	1.30
PPC	4000	8530	2.14
PBC	1500	2840	1.84
PBI	7300	30860	4.20

5.3 Conclusions

Two different methods of synthesising unsaturated polyesters with the aim of maximising maleate content were investigated. ROCOP resulted in the highest maleate content, with no detectable isomerisation to fumarate by ^{1}H NMR spectroscopy. However, the stringent reaction conditions and

low yield make it an unlikely method to be viable to produce unsaturated polyesters on an industrial scale. For applications where strict control over the backbone sequence is required, ROCOP would be preferred as this method was more successful in linking monomers alternately.

For large-scale polymerisation, step-growth is already adopted as the method of choice for the production of unsaturated polyesters in industry, and the changes made in this chapter were proven to minimise the isomerisation of the maleate groups. Lowering the temperature reduced the isomerisation slightly but the increased reaction time makes this alteration unattractive. Changing the glycol to a rigid, primary diol reduced the isomerisation much more significantly and shortened the required reaction time and temperature. The best performing diol was cyclohexanedimethanol, which reached the desired completion within 2 hours at 200 °C and had a maleate content of 78%. An even better maleate content of 86% can be achieved by reducing the reaction temperature to 160 °C at the cost of a longer reaction time. At the time of writing, there are no other publications that have achieved a better retention of maleate content than this.

There is scope to improve these results further. For example, the *cis-trans* isomerisation is acid catalysed so that the acidity of the diacid is an important consideration.[14] Also, factors such as changing the catalyst or performing the reaction under reduced pressure are yet to be investigated.

5.4 Bibliography

1 L. G. Curtis, D. L. Edwards, R. M. Simons, P. J. Trent and P. T. Von Bramer, *Industrial and Engineering Chemistry Product Research and Development*, 1964, **3**, 218–221.

2 A. Fradet and M. Tessier, in *Synthetic Methods in Step-Growth Polymers*, John Wiley & Sons, Inc., Hoboken, NJ, USA, 2003, pp. 17–134.

3 I. Vancsó-Szmercsányi, K. Maros-Gréger and E. Makay-Bödi, *Journal of Polymer Science*, 1961, **53**, 241–248.

4 Darren Coniff, Anglia Polytechnic University, 1997.

5 O. Nuyken and S. Pask, *Polymers (Basel)*, 2013, **5**, 361–403.

6 O. Nuyken and S. D. Pask, *Polymers (Basel)*, 2012, **5**, 361–403.

7 O. Rexin and R. Mülhaupt, *J Polym Sci A Polym Chem*, 2002, **40**, 864–873.

8 O. Coulembier, P. Degée, J. L. Hedrick and P. Dubois, *Prog Polym Sci*, 2006, **31**, 723–747.

9 L. C. Kagumba and J. Penelle, *Macromolecules*, 2005, **38**, 4588–4594.

10 A.-L. Brocas, C. Mantzaridis, D. Tunc and S. Carlotti, *Prog Polym Sci*, 2013, **38**, 845–873.

11 Y. Du, X. Xue, Q. Jiang, W. Huang, H. Yang, L. Jiang, B. Jiang and S. Komarneni, *Polym Chem*.

12 J. A. Okolie, *iScience*, 2022, **25**, 104903.

13 A. Fradet and P. Arlaud, in *Comprehensive Polymer Science*, Pergamon Press, Oxford, 1st edn., 1989, vol. 5, pp. 331–334.

14 F. R. Jones, in *Brydson's Plastics Materials*, Elsevier, 2017, pp. 743–772.

6 One-step covalent adaptable networks from unsaturated polyesters

6.1 Introduction

Unsaturated polyesters (UPEs) are commonplace in the polymer industry, with their strength and flexibility making them ideal materials in the construction,[1] transport,[2] and marine sectors.[3] To achieve their high mechanical strength and chemical resistance, they are cross-linked at their unsaturated bonds by a reactive monomer such styrene, to generate a three-dimensional network. However, this process is irreversible, creating a thermoset which is difficult to recycle.

An alternative use for this reactive site on the UPE would be to add a substituent that can participate in Diels-Alder (DA) reactions for reversible cross-linking. The furan group is the most common diene used in the DA reaction because it adds readily to dienophiles, such as maleimides.[4–9] Furans also have the ability to undergo a DA cycloaddition to unsaturated esters, such as maleates and fumarates (Chapter 4), meaning a UPE partially functionalised with a furan would have the ability to cross-link both intra- and inter-molecularly. This would grant the UPE the potential to form thermally-reversible cross-links between chains and join an increasingly popular group of copolymer systems, known as covalent adaptable networks (CANs) (**Scheme 6.1**).

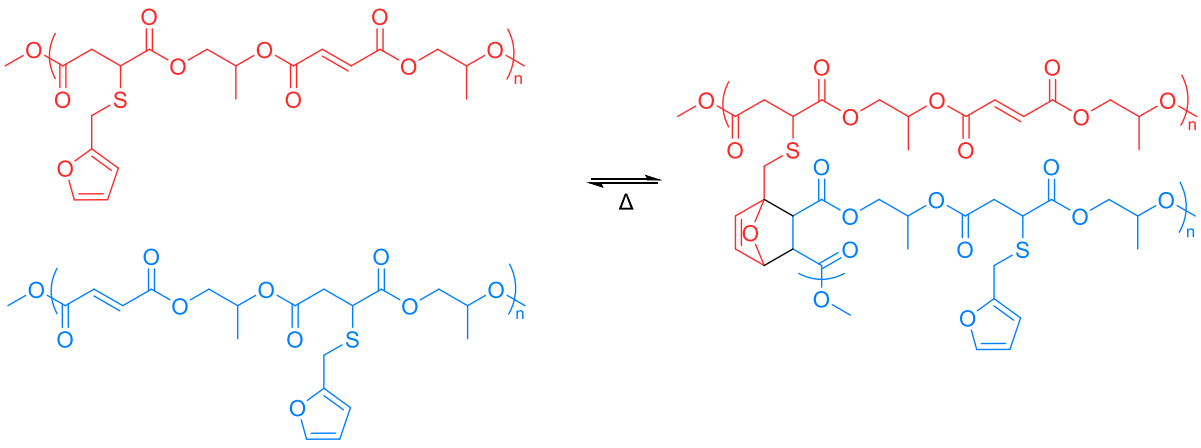

Scheme 6.1 – Formation of a cross-link between two partially functionalised UPEs.

Furfuryl mercaptan can be added onto the double bond *via* the thiol-ene addition (**Scheme 6.2**), which proceeds by a radical or anionic addition polymerisation, and achieves quantitative yields, stereoselectivity, and rapid reaction rates; fulfilling many of the criteria to consider it a "click" reaction.[10,11]

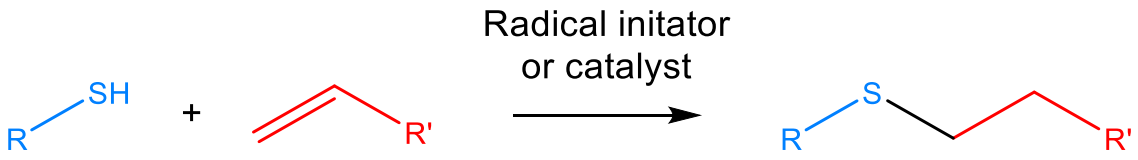

Scheme 6.2 – General thiol-ene addition with the use of either a radical initiator or a catalyst.

Reactions of thiols with carbon-carbon double bonds have been demonstrated as early as 1905.[12] Traditionally, the thiol-ene addition is radically mediated with electron-rich alkenes, to form cross-linked polymers with narrow glass transition temperatures (T_g) and low polymerisation shrinkage stress.[13] However, the reaction between a thiol and an electron-deficient alkene can also happen readily with the use of a catalyst, and is often termed a thiol-Michael addition.

Catalyst-mediated thiol-Michael addition is preferred as the reaction conditions are milder than free radical thiol-ene addition and enable high chemoselectivity, reducing the likelihood of unwanted side reactions.[14] There is no need for radical initiators or terminators, so product purification is simple and functional groups that could be sensitive to radical conditions may also be used. Other advantages include high stereocontrol, regioselectivity and kinetic control.

In this chapter, the thiol-Michael addition was used to add furfuryl mercaptan to the unsaturation on poly(propylene fumarate) (PPF). The ability of this material to form dynamic bonds and generate CANs was then investigated.

6.2 Results and discussion

6.2.1 Thiol-ene addition

The following methodology was derived from an article researching the most efficient catalyst for thiol-Michael addition reactions of a range of thiols onto a poly(butylene maleate) scaffold.[15] The researchers achieved full addition in 1 minute at room temperature in the presence of 1,5,7-triazabicyclo[4.4.0]dec-5-ene (TBD). Although maleate networks have been shown to have better thermal resistance, this synthesis aims to emulate this with fumarate UPE as they are more readily available on a large scale and the ^{1}H nuclear magnetic resonances of the fumarate and furan protons are distinct and provide easy references for calculating addition.

A series of UPEs with varying amounts of furan functionalisation were synthesised by dissolving poly(propylene fumarate) (PPF) and furfuryl mercaptan in chloroform, and then adding TBD (**Scheme 6.3**). The solution was stirred for 10 minutes at room temperature and pressure before being quenched in cold methanol. The precipitate was centrifuged and dried overnight in a vacuum oven at 100 °C.

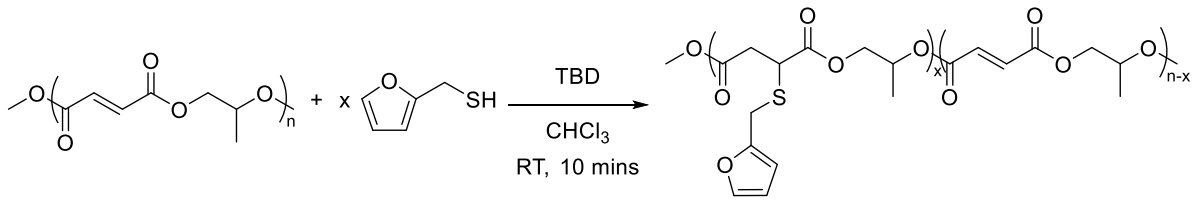

Scheme 6.3 – Addition of furfuryl mercaptan to polypropylene fumarate, where $0 \leq x \leq n$.

Addition was confirmed by ^{1}H NMR spectroscopy and total thiol-ene addition was calculated by integrating the fumarate (δ = 6.85 ppm) and the furan (δ = 6.29-6.24 ppm) resonances and normalising to provide the ratio of furan to alkene (**Figure 6.1**).

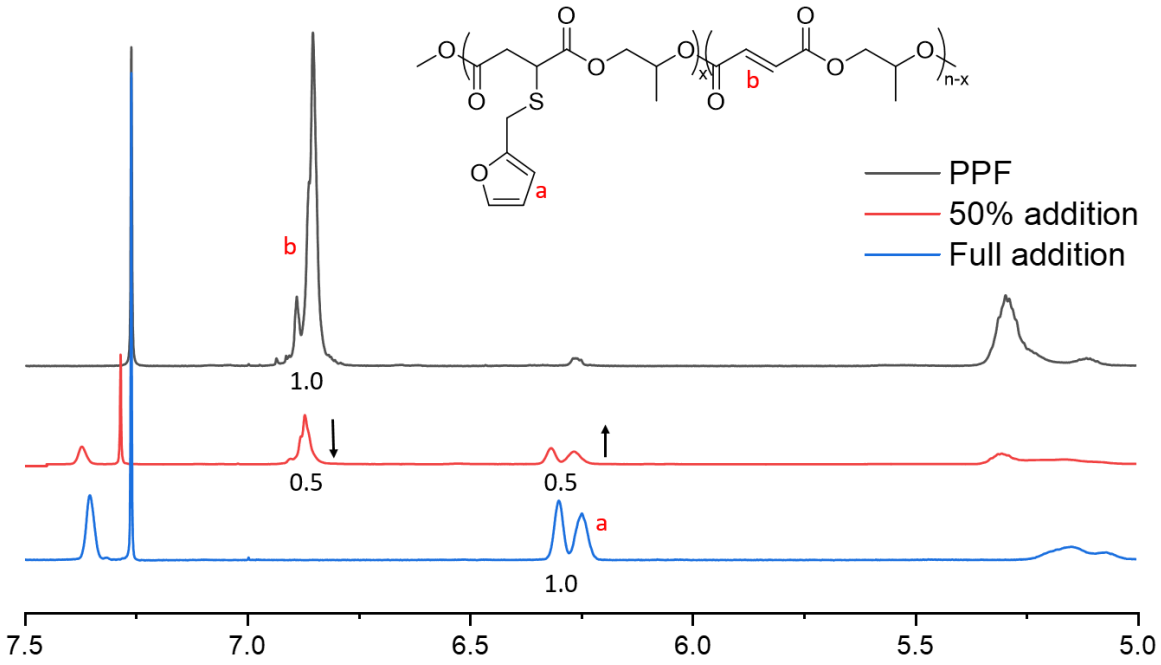

Figure 6.1 - ^{1}H NMR spectra of untreated PPF (top), PPF with 50% of the unsaturated functionalised with furan groups (middle), and PPF with all unsaturation functionalised with furan groups (bottom). (400 MHz, $CDCl_3$, 298 K).

The evolution of multiplet resonances at around δ = 3.65 and 3.00-2.70 ppm are assignable to the main chain CH proton adjacent to the S and its neighbouring CH_2 proton, respectively (**Figure 6.2**). The final product is poly(propylene fumarate-*co*-propylene 2-[(2-furanylmethyl)thio]-succinate) and each product was given a unique identifier according to how much furfuryl mercaptan had been successfully added to the double bond. For example, a chain with furfuryl mercaptan added to 75% of the double bonds would be named 75FM-PPF.

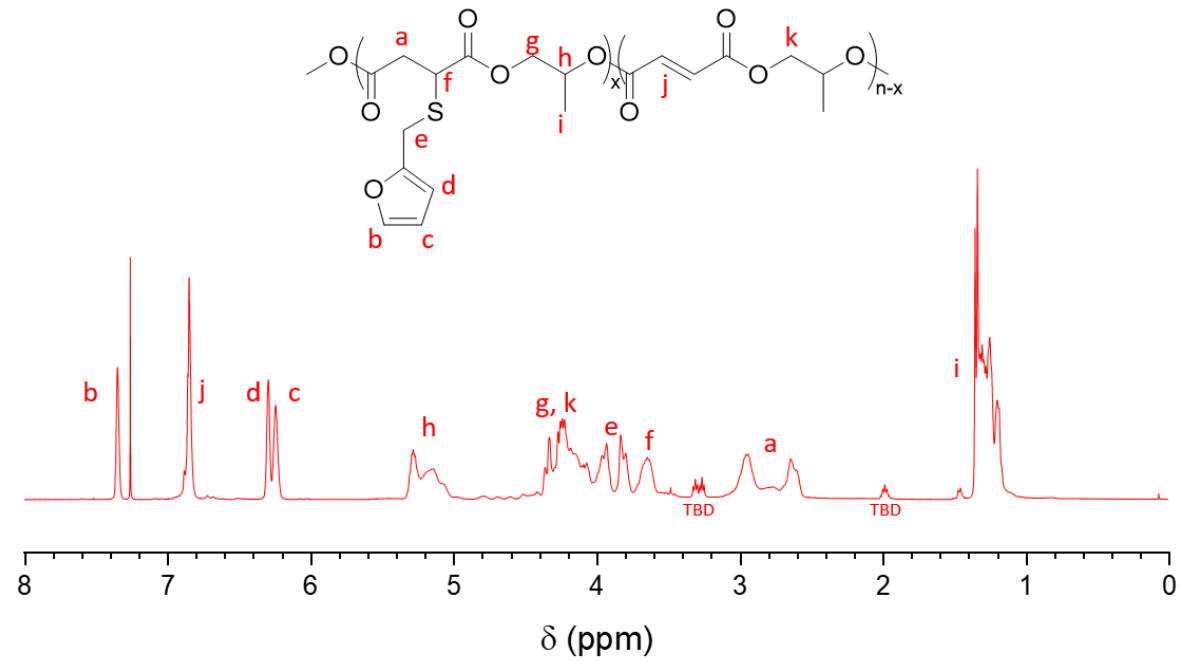

Figure 6.2 - Fully annotated ^{1}H NMR spectra of 50FM-PPF (400 MHz, $CDCl_3$, 298 K).

In total, 9 polymers were synthesised covering a range of functionalisation from 12% to 100%. Complete addition of furfuryl mercaptan to the unsaturation means the final product would contain no fumarate groups to act as a dienophile (**Scheme 6.4**).

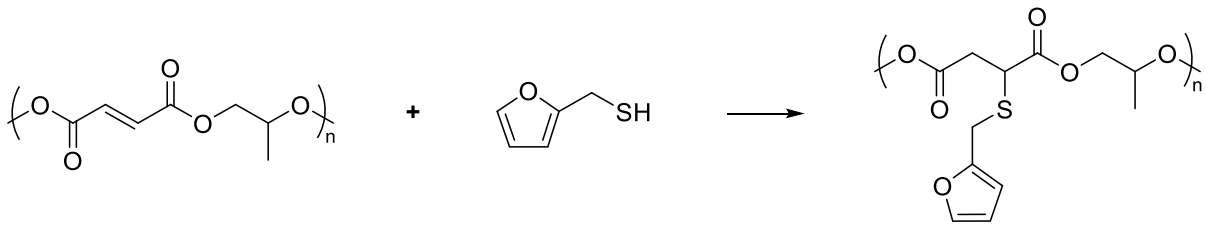

Scheme 6.4 – Complete addition of furfuryl mercaptan to polypropylene fumarate.

A single heat run using differential scanning calorimetry (DSC) was used to determine whether any DA linkages had formed. As there is no potential for any Diels-Alder linkages to form, there are no rDA endotherms in 100FM-PPF or unfunctionalised PPF, as they contain either only diene or dienophile moieties (**Figure 6.3**). The functionalisation lowers the T_g as the pendant groups limit how close the chains can pack, increasing rotational motion.

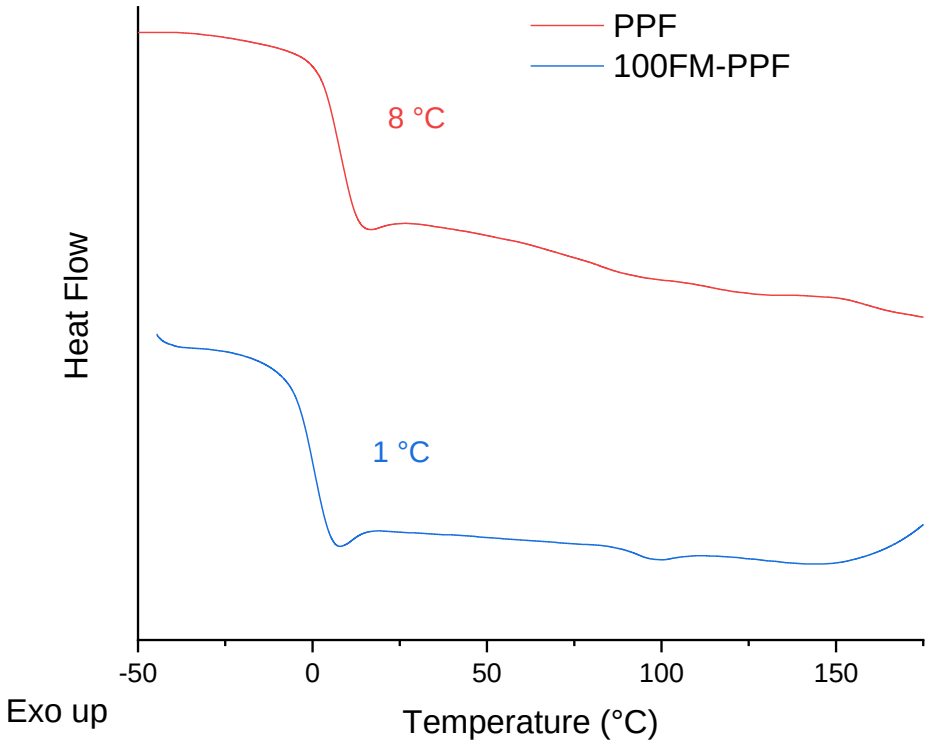

Figure 6.3 – DSC thermogram of the first heating cycle (10 ˚C.min^{-1}) of PPF and 100FM-PPF.

6.2.2 Homogenous Diels-Alder

When a fractional molar equivalent of furfuryl mercaptan w.r.t. to the unsaturation was added, the final polyester will contain both fumarate and furan functionality, i.e. both dienes and dienophiles. This means the chain will be able to form DA linkages between other chains in a one-component "homogenous" system.

50FM-PPF was synthesised and cured at room temperature for 10 days. The material was then evaluated *via* DSC by heating to 165 °C (**Figure 6.4**). The appearance of the endotherm at 91 °C in the first heat ramp is the result of the retro Diels Alder (rDA) reaction between the fumarate and furan, indicating successful cross-linking. The magnitude of this enthalpy change (ΔH) is a good indicator of the degree of cross-linking as a larger number of DA bonds will results in a larger ΔH_{rDA}. After the initial

heat ramp, the sample was cooled back to 0 °C at 10 °C min^{-1} before another heat to 165 °C. On the second heat run there was only a slight endotherm as the chains did not have enough time to fully reassociate after the first heat.

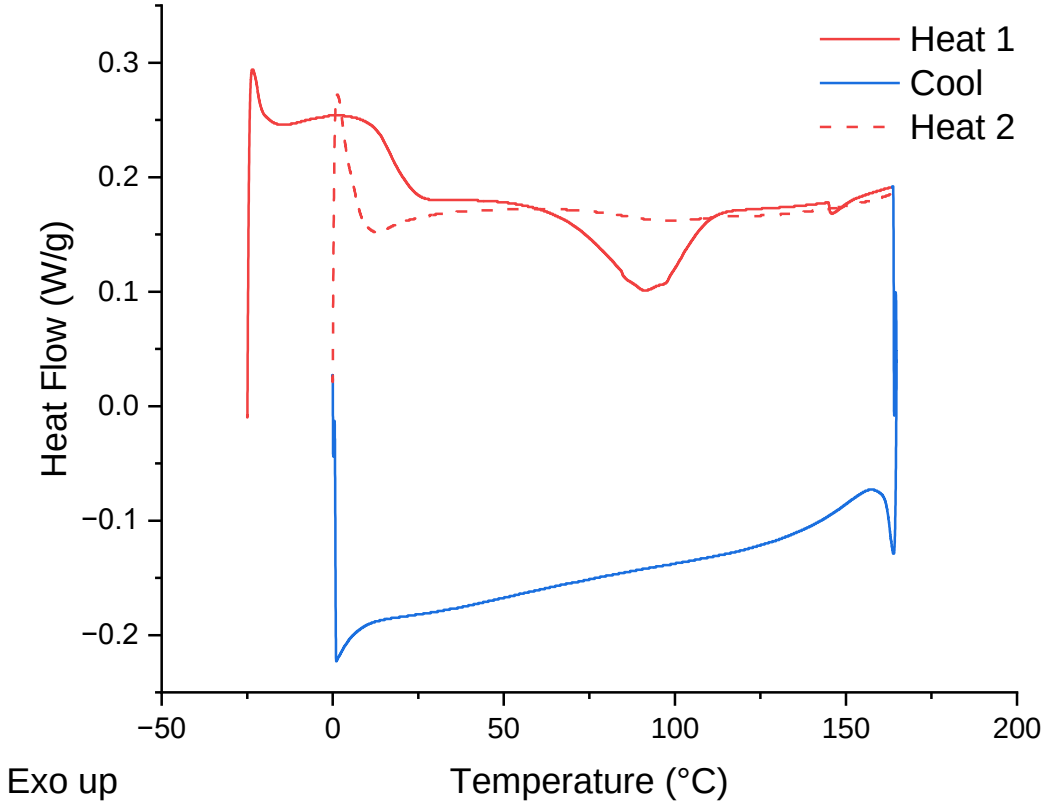

Figure 6.4 – DSC thermogram showing a heat-cool-heat experiment on 50FM-PPF.

The rate of DA bond formation was investigated by following the increase in the ΔH_{rDA} over time. The material was heated to 100 °C for 30 minutes to dissociate the network and unique samples taken from this material were analysed *via* DSC at intervals of 1, 2, 3, 4, 7 and 10 days. The ΔH_{rDA} increases rapidly for the first 4 days, after which the ΔH_{rDA} begins to plateau and reaches equilibrium by 7 days (**Figure 6.5**).

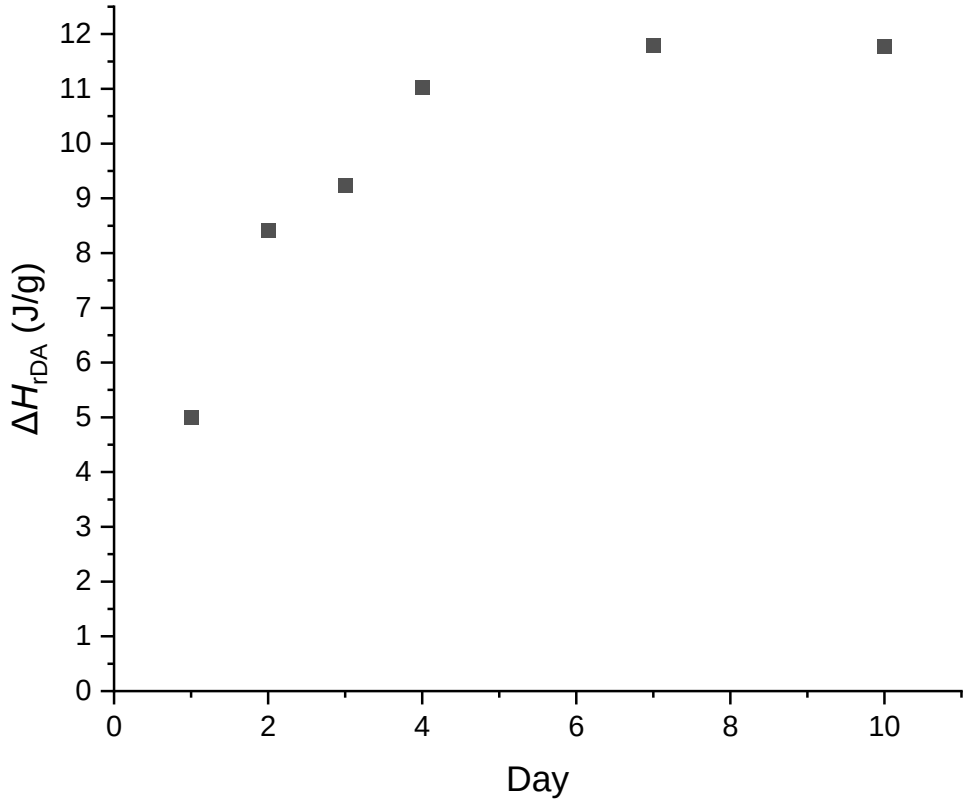

Figure 6.5 – Graph showing how the magnitude of the ΔH_{rDA} of 50FM-PPF increases over the course of 10 days.

In certain cases, the rate of self-healing can be affected by having an excess of diene or dienophile and therefore, the same DSC experiment was conducted on all the synthesised polyesters. The materials that contained an excess of either furan or fumarate showed the same trend of a fast rate of association for the first 4 days before plateauing. However, the lower ΔH_{rDA} of these materials suggests they were unable to reach as high degree of cross-linking as the 50FM-PPF because either the diene or dienophile groups become fully consumed (**Figure 6.6, Table 6.1**).

Table 6.1 - The ΔH_{rDA} of functionalised materials in the days following complete dissociation, as determined by integration of the rDA endotherm found *via* DSC.

Furfuryl mercaptan addition (%)	ΔH_{rDA} (J/g)					
	Day 1	Day 2	Day 3	Day 4	Day 7	Day 10
0	0	0	0	0	0	0
12	0.7	1.3	2.0	3.1	3.1	4.9
18	1.8	3.8	4.7	5.4	6.3	6.8
39	4.5	7.0	6.7	9.0	10.7	10.6
50	5.0	8.4	9.2	11.0	11.8	11.8
60	3.8	5.1	7.8	9.1	10.2	11.0
69	4.0	6.2	7.1	7.0	8.6	8.6
80	2.5	3.5	4.4	6.0	6.1	6.2
92		0.7	2.0	2.5	2.7	3.8
100	0	0	0	0	0	0

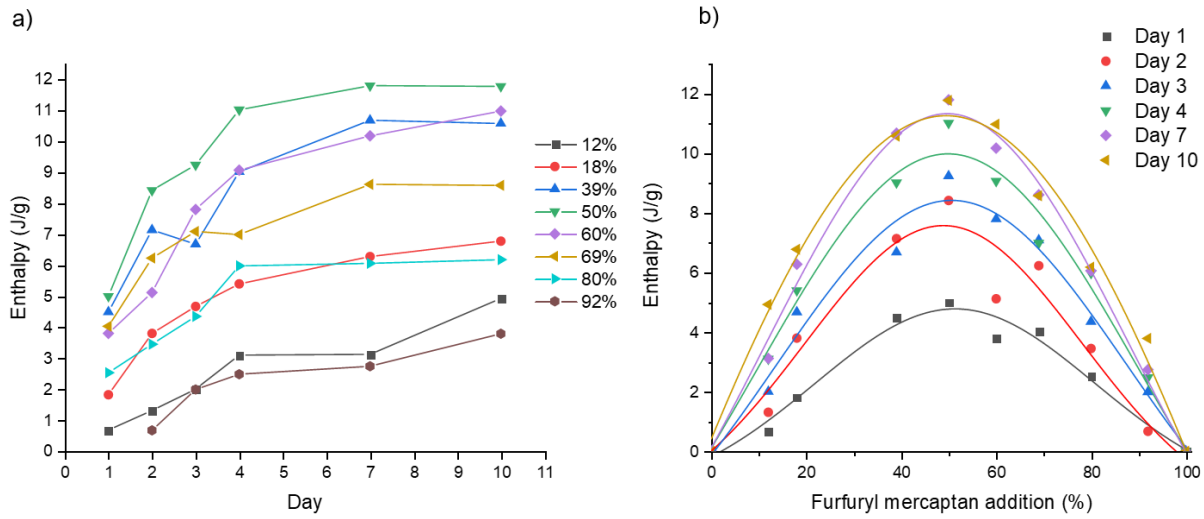

Figure 6.6 – a) Graph showing how the ΔH_{rDA} increases over the course of 7 days, for PPF with varying amounts of functionalisation. b) Graph highlighting maximum ΔH_{rDA} is achieved at 50% furfuryl mercaptan addition.

The T_gs of the materials followed the same trend; for example, the T_g of 50FM-PPF increased from 14 °C to 26 °C over the course of the experiment as the cross-linking formed and restricts rotational

motion (**Table 6.2**). This increase in T_g was less drastic for materials with diene or dienophile excess and the materials with more functionalisation had lower T_gs in general.

Table 6.2 - Changes in T_g over the course of 10 days for the functionalised UPEs.

Furfuryl mercaptan addition (%)	**T_g (°C)**					
	Day 1	Day 2	Day 3	Day 4	Day 7	Day 10
0						
0.12	21.8	23.7	22.1	22.9	26.9	26.9
0.18	21.3	23.5	22.5	22.9	28.3	28.4
0.39	19.5	23.4	23.8	23.5	28.0	28.9
0.5	14.6	18.3	12.3	14.5	25.6	18.0
0.6	16.3	20.2	19.9	19.3	23.8	24.3
0.69	16.3	18.6	18.9	19.9	23.5	23.1
0.8	10.4	12.1	11.7	13.7	15.3	15.1
0.92		9.5	9.1	8.8	9.9	11.5
1						

All of the materials were analysed by SEC (**Table 6.3**). They were first heated for an hour at 100 °C to dissociate any cross-links to allow dissolution into THF. After functionalisation, the materials all showed an increase in molecular weight. Not all of this can be attributed to the addition of furfuryl mercaptan, especially the lower % additions, as its molecular weight is only 114.17 g mol^{-1}. It is possible that most chains are linked to one other and are still soluble, hence giving molecular weights of around double untreated PPF. 100FM-PPF cannot form these links and its M_n is what we'd expect; PPF has roughly 10 repeat units and so the addition of 10 furfuryl mercaptan molecules would give rise to an increase of 1140 g mol^{-1}.

Table 6.3 - Molecular weight distributions of the functionalised UPEs. Determined by size exclusion chromatography (SEC) using THF as an eluent and poly(methyl methacrylate) standards.

Furfuryl mercaptan addition (%)	M_n (g mol^{-1})[a]	M_w (g mol^{-1})[b]	$Đ_M$[c]
0	1700	4700	2.8
0.12	4400	11400	2.6
0.18	4700	14000	3.0
0.39	4400	14700	3.4
0.5	3300	10400	3.1
0.6	3000	10600	3.5
0.69	4200	20400	4.8
0.8	3000	8100	2.8
0.92	2500	6500	2.6
1	3228	7700	2.4

[a] Number average molecular weight. [b] Weight average molecular weight. [c] Dispersity.

6.2.3 Heterogenous Diels-Alder

Factors affecting the thiol-ene reaction, such as reaction time, temperature and concentration of reactants, made it difficult to achieve a specific quantity of furfuryl mercaptan addition to PPF, with the achieved addition of furfuryl mercaptan being up to 10% lower than the theoretical amount. This made the synthesis difficult if targeting a specific cross-link density or T_g. Alternatively, a desired cross-link density can be achieved by combining fully furan-functionalised PPF (100FM-PPF) with a proportional amount of untreated PPF. For example, 25FM-PPF would be analogous to a mixture of 0.25 moles of 100FM-PPF and 0.75 moles of PPF. This two-component mixture forms a “heterogenous” DA system (**Scheme 6.5**).

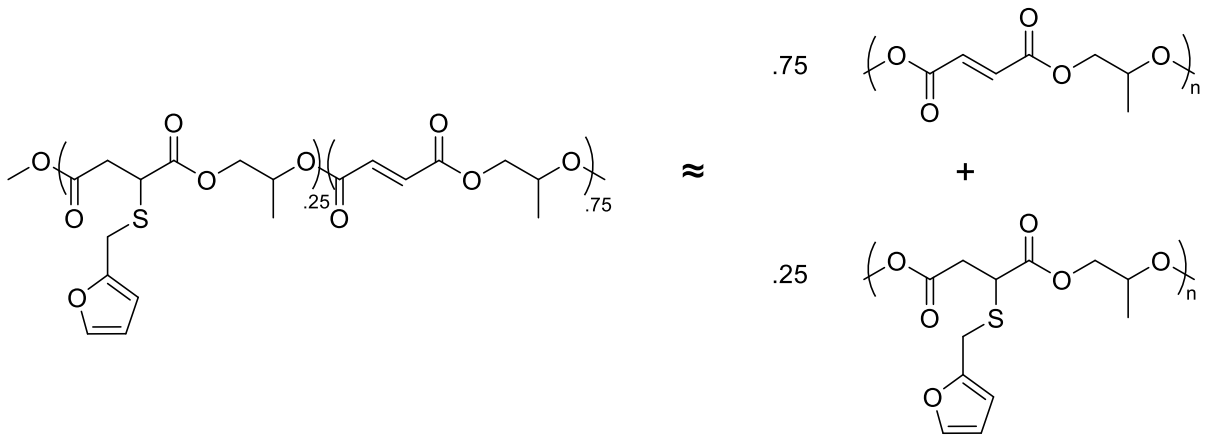

Scheme 6.5 – Comparison between a "homogenous" DA system (left) and a "heterogenous" DA system (right).

The heterogenous system behaved in the same way as the homogenous system, where equimolar equivalents of furan and fumarate functionality yielded the highest amount of DA bonds and both materials had ΔH_{rDA} of 12 J g^{-1} after 7 days (**Figure 6.7**).

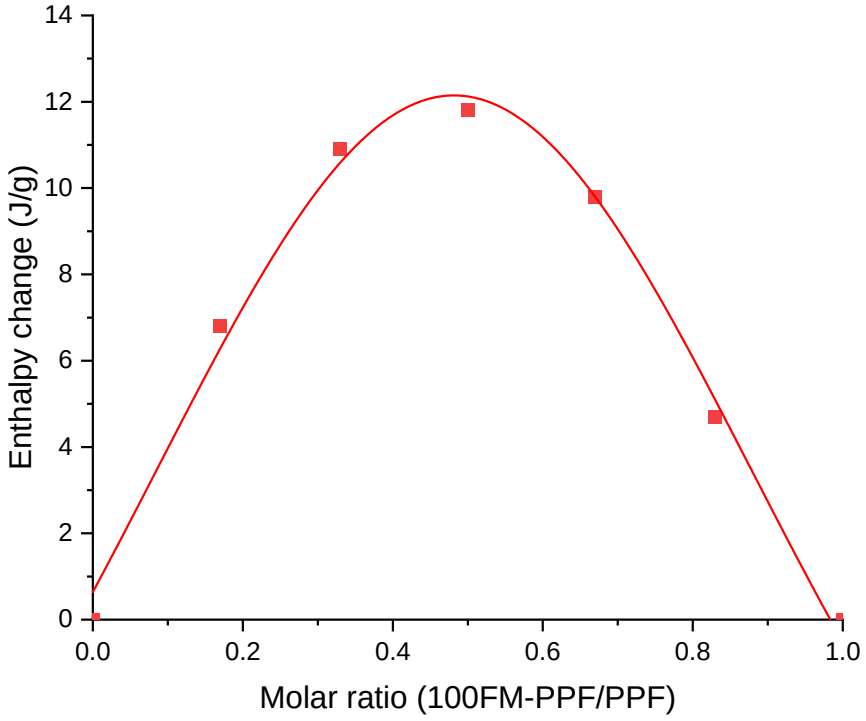

Figure 6.7 – A graph showing how the ratio of functionalised PPF to untreated PPF affects the enthalpy change of the rDA, as determined by integration of the rDA endotherm found *via* DSC.

After 7 days there was a difference in T_gs, with the homogenous material exhibiting a T_g of 26 °C whereas the heterogenous was lower at 17 °C. In the homogenous material the pendant groups are spaced further apart meaning they are more likely to tangle between each other and act like a "fish hook" and raise the T_g.

6.2.4 Network formation

Heterogenous and homogenous DA cross-linking was proven *via* a Soxhlet extraction. Unfunctionalised and fully-functionalised PPF were both soluble in DCM. The two materials with the highest cross-link density underwent a 24 hour Soxhlet extraction in dichloromethane (DCM). The materials with the largest ΔH_{rDA} were 50FM-PPF (homogenous) and the equimolar combination of 100FM-PPF and PPF (heterogenous). After the extraction, the remaining material was dried in an oven

to remove any residual DCM and then weighed to determine the gel fraction of each material. The 50FM-PPF had a gel fraction of 28% and the equimolar combination had a gel fraction of 52%. Despite both materials having a similar cross-link density, these initial results suggest that the heterogenous DA material is more effective at creating a network. This can be explained in a number of ways. Firstly, the homogenous material contains both diene and dienophiles, meaning that the chains cannot only bond to other similar chains, but also to itself intramolecularly, creating DA linkages that are not contributing to network formation. Secondly, the addition of pendant furan groups to the polyester makes the remaining fumarate groups less accessible to incoming furans thus making DA linkages more difficult to form. This also makes chains that are already bonded and hence in close proximity much more likely to bond again, providing no further extension to the network. For these reasons, two-component DA systems that form heterogenous DA bonds are much more effective at generating a network.

6.3 Conclusions

Commercially available polyesters were able to be functionalised with furans that enabled the chains to be cross-linked with Diels-Alder bonds. This could either be done "homogenously," whereby a one-component system of partially functionalised chains interact with each other, or "heterogeneously," whereby a two-component system comprising PPF and 100FM-PPF interact with each other. In both instances, the materials that had equimolar equivalents of furan and fumarate formed the most DA bonds and exhibited the highest enthalpy of retro-Diels-Alder. The network associated rapidly for 4 days before reaching equilibrium after about 7 days. The heterogenous material was more effective at generating a network, as the dissimilar chains were more likely to form linkages between unconnected chains.

Further work includes investigating how the network is affected by using longer chain furan-thiols, using different diene/dienophiles, and altering the composition of the backbone. As seen in other chapters, maleate networks tend to have rDA temperatures around 130 °C, so use of poly(propylene

maleate) is likely to impart more thermal stability on the network. These initial findings also highlight an easy way to impart a variety of other properties onto any commercially available unsaturated polyester. Simple properties, such as the T_g, can be changed by adding bulky or flexible pendant groups, and the solubility influenced by adding polar or non-polar groups. A more specialist application could be the addition of phytochemicals to give the polyester antimicrobial properties.[16] Phytochemicals are used throughout the plant kingdom as they provide antibacterial, antiviral and antifungal activities and even protection against ultraviolet radiation. Antifouling properties are also a point of interest within the polymer industry as it has many applications in the medical and marine sectors.[17] Unwanted adhesion can be prevented by tweaking the surface chemistry by introducing hydrophobic surfaces or grafting polyethylene glycol can resist the adsorption of numerous protein molecules due to the formation of an extensive hydration layer, rapid conformational changes and steric repulsion.[18] In addition to fouling-resistant coatings, fouling-degrading compounds can also be used. Quaternary ammonium compounds are a popular functional group for contact-killing coatings that work by attracting negatively charged cell membranes to the positively charged surface, where the strong electrostatic interaction destroys the cell structure.[19] The thiol-ene addition demonstrated here provides a facile route to attaching these groups to unsaturated polyesters and furnishing them with these desired properties.

6.4 Bibliography

1 M. H. Irfan, in *Chemistry and Technology of Thermosetting Polymers in Construction Applications*, Springer Netherlands, Dordrecht, 1998, pp. 230–239.

2 Y. Gao, P. Romero, H. Zhang, M. Huang and F. Lai, *Constr Build Mater*, 2019, **228**, 116709.

3 A. Buketov, M. Brailo, S. Yakushchenko and A. Sapronova, *Advances in Materials Science and Engineering*, 2018, **2018**, 1–6.

4 T. A. Eggelte, H. de Koning and H. O. Huisman, *Tetrahedron*, 1973, **29**, 2491–2493.

5 X. Liu, P. Du, L. Liu, Z. Zheng, X. Wang, T. Joncheray and Y. Zhang, *Polymer Bulletin*, 2013, **70**, 2319–2335.

6 T. T. Truong, H. T. Nguyen, M. N. Phan and L.-T. T. Nguyen, *J Polym Sci A Polym Chem*, 2018, **56**, 1806–1814.

7 V. Froidevaux, M. Borne, E. Laborbe, R. Auvergne, A. Gandini and B. Boutevin, *RSC Adv*, 2015, **5**, 37742–37754.

8 A. Gandini, *Prog Polym Sci*, 2013, **38**, 1–29.

9 A. Gandini, A. J. D. Silvestre and D. Coelho, *J Polym Sci A Polym Chem*, 2010, **48**, 2053–2056.

10 C. E. Hoyle and C. N. Bowman, *Angewandte Chemie International Edition*, 2010, **49**, 1540–1573.

11 H. C. Kolb, M. G. Finn and K. B. Sharpless, *Angewandte Chemie*, 2001, **113**, 2056–2075.

12 T. Posner, *Berichte der deutschen chemischen Gesellschaft*, 1905, **38**, 646–657.

13 C. E. Hoyle, T. Y. Lee and T. Roper, *J Polym Sci A Polym Chem*, 2004, **42**, 5301–5338.

14 D. P. Nair, M. Podgórski, S. Chatani, T. Gong, W. Xi, C. R. Fenoli and C. N. Bowman, *Chemistry of Materials*, 2014, **26**, 724–744.

15 O. Daglar, B. Ozcan, U. S. Gunay, G. Hizal, U. Tunca and H. Durmaz, *Polymer (Guildf)*, 2019, **182**, 121844.

16 A. K. Patra, in *Dietary Phytochemicals and Microbes*, Springer Netherlands, Dordrecht, 2012, pp. 1–32.

17 A. M. C. Maan, A. H. Hofman, W. M. Vos and M. Kamperman, *Adv Funct Mater*, 2020, **30**, 2000936.

18 G. W. Greene, L. L. Martin, R. F. Tabor, A. Michalczyk, L. M. Ackland and R. Horn, *Biomaterials*, 2015, **53**, 127–136.

19 E. Obłąk, A. Piecuch, A. Krasowska and J. Łuczyński, *Microbiol Res*, 2013, **168**, 630–638.

7 Conclusions and future work

7.1 Conclusions

The aim of this doctoral work was to develop a sustainable adhesive that enables a circular economy through two key routes. The first is that the adhesive should be able to debond on demand, in response to an external stimulus, such as heat. This allows for composite materials to be separated and allow for easy recycling. The second would be that the adhesive regains its mechanical properties upon reassociation of the network, allowing it to be used again with no loss of performance compared to virgin material.

Firstly, the well-known Diels-Alder system comprising maleimides and furans was explored. A long chain bismaleimide and trifunctional furan were combined to create a dissociative covalent adaptable network. The ability of the network to reassociate was proven by the devolution of the furan infrared absorbance resonance, which happened consistently after 5 heat cycles. These findings correlated with the tensile strength of the material; it was able to rebond aluminium coupons 5 times with concordant bond strengths of around 10 MPa each time.

The findings from this preliminary research on the maleimide and furan system was introduced into a novel architecture. Moisture-curing adhesives are commonplace in the industry but are yet to be utilised in a sustainable way. In contrast to the traditional route of curing these materials by forming irreversible urea cross-links, chain extenders with dynamic bonds were integrated into the system, allowing the material to be transformed into a covalent adaptable network (CAN). This enabled the cured material to revert back to its lower molecular weight prepolymers at the retro Diels-Alder temperature (>130 °C).

Striving to be even ‘greener,’ other dienophiles were considered to replace the maleimide, which comes from non-renewable sources. Unsaturated polyesters are already available on a large scale and increasingly more of them are synthesised from bioresources. The potential for the alkene groups in

the backbone of unsaturated polyesters (UPEs) to act as the dienophile in Diels-Alder reactions was examined. It was shown that the ability to form networks with furan cross-linkers was possible, and some of these materials displayed good tensile properties. The stereochemistry of the unsaturation affects the thermal stability of the networks, with maleates dissociating at 130 °C and fumarates dissociating at 90 °C. For certain applications, a higher dissociation temperature is desired, yet the vast majority of UPEs on the market are fumarates. An investigation was launched on how to retain maleate content. Ring-opening copolymerisation provided absolute maleate stereochemistry, but would be difficult to perform on a large scale. The high temperatures of the industrial method of UPE synthesis facilitates the isomerisation of maleate to fumarate, but careful consideration of glycol and reaction conditions can retain the maleate isomer by up to 86%.

An alternate way to create CANs from UPEs was discovered. The unsaturation is easily functionalised with a diene *via* the Michael thiol-ene addition. This means the UPE can be furnished with either diene or dienophile functionality or both, enabling it to participate in Diels-Alder reactions to form cross-links between chains. The appearance of a retro Diels-Alder endotherm and increases solvent resistance suggests that there was enough successful cross-linking to generate a covalent adaptable network.

7.2 Future work

The research performed in this project has proven that covalent adaptable networks bearing Diels-Alder bonds are a viable option for use as structural adhesives. Utilising unsaturated polyesters in this way is relatively unexplored yet the initial findings from their use in CANs shows promise. Only the lap shear strength was tested in this thesis, but there is a multitude of other performance tests such as peel, shear modulus, flexural, impact, cleavage strength, environmental resistance, and mechanical properties (e.g., creep, fracture, and fatigue) that can highlight how durable these materials can be. It was shown in Chapter 4 that the materials' properties can be significantly altered by a simple change in composition, and the huge variety of glycols and anhydrides at our disposal means that there are

many avenues that can be explored in order to fine tune a material to achieve a desired property. Any material can be tuned even further, by post-functionalisation *via* the Michael thiol-ene addition. Finally, there is always work to be done to achieve a more circular economy, and any synthesis can be improved by making the process more efficient and using more sustainable raw materials.

8 Experimental

8.1 Materials

Chapter 2 - Maleimide and furan-based networks

Furan and maleimide functionalised monomers were provided by Henkel Corporation. Toluene was obtained from Sigma Alrich. THF was obtained from VWR chemicals. Ethyl actetate was obtained from Fisher Chemicals. Isopropyl acetate was obtained from Honeywell.

Chapter 3 - Diels-Alder cycloadducts as chain extenders in reversible polyurethane adhesives

The following materials were used as supplied. Furan, furfuryl alcohol, toluene, ethanolamine, trimethylamine, methylene diisocyanate, and diethyl ether were obtained from Sigma Aldrich. Maleic anhydride and 2,5-bis(hydroxymethyl)furan was obtained from Fluorochem. Methanol was obtained from Fisher Chemical. Priplast™ 1838 was provided by Croda International.

Chapter 4 - Covalent adaptable networks using unsaturated polyesters

The following materials were used as supplied. Furfuryl alcohol and dibutyltin dilaurate (DBTL) were obtained from Sigma-Aldrich. 4,4'-methylene-diphenyl diisocyanate (MDI, Desmodur® 44M), isophorone diisocyanate (IPDI) (Desmodur® Z4470) and hexane diisocyanate (HDI) trimer (Desmodur® N3300) were obtained from Covestro, Germany. Poly(propylene fumarate) was provided by Scott Bader. Poly(propylene maleate) was kindly provided by the Becker Laboratory for Functional Biomaterials at Duke University.

Chapter 5 - Synthesis and characterisation of unsaturated polyesters from short-chain diacids and diols

Propylene oxide was obtained from Acros organics and dried over calcium hydride. Maleic anhydride was obtained from Fluorochem and recrystallised and dried in a vacuum desiccator over phosphorus

pentoxide. The following materials were used as supplied. Propylene glycol was provided by Scott Bader. Monobutyltin oxide (FASCAT® 4100) was obtained from PMC Organometallix. Calcium hydroxide and phosphorus pentoxide was obtained from Thermo Scientific. Magnesium ethoxide was obtained from Fluorochem. Diethyl ether was obtained from Sigma Aldrich.

Chapter 6 - Thiol-ene addition to unsaturated polyesters to form covalent adaptable networks

The following materials were used as supplied. Furfuryl mercaptan was obtained from Alfa Aesar. Chloroform and methanol were obtained from Fisher Chemical. Dichloromethane and 1,5,7-triazabicyclo[4.4.0]dec-5-ene was obtained from Sigma Aldrich. PPF was provided by Scott Bader.

8.2 Instrumental methods

^{1}H and ^{13}C nuclear magnetic resonance (NMR) spectroscopy measurements of monomers and prepolymers were recorded on a Bruker AV or AVIIIHD 400 MHz spectrometer at room temperature with the sample fully dissolved in deuterated chloroform ($CDCl_3$). ^{13}C NMR spectra were recorded at 125 MHz. Chemical shifts were recorded in parts per million (ppm) relative to a reference peak of chloroform solvent at δ = 7.26 (^{1}H) and 77.16 (^{13}C) ppm or DMSO solvent at δ = 2.50 (^{1}H) and 39.51 (^{13}C) ppm.

Fourier transform infrared (FTIR) measurements were recorded using a PerkinElmer FT-infrared spectrometer equipped with a UATR Two accessory. Eight scans were taken in the range of 4000 – 500 cm^{-1}. Gel permeation chromatography (GPC) was performed using an Agilent Technologies 1260 Infinity II system equipped with a refractive index detector. Two Agilent PLgel 5 µm Mixed-D columns and a guard column were connected in series and maintained at 35 °C. HPLC grade THF was used as the eluent and the flow rate was set at 1.0 mL min^{-1}. The refractive index detector was used for calculation of molecular weights and dispersity by calibration using a series of near-monodisperse poly(methyl methacrylate) standards.

Differential scanning calorimetry (DSC) was performed using a TA instruments Discovery DSC 25. 5-8 mg of sample was accurately weighed and loaded into a Tzero aluminium pan, with heating and cooling ramps conducted under a nitrogen atmosphere at a standard rate of 10 °C.min^{-1} unless otherwise stated.

The lap shear strength was measured using an Instron tensometer with a 30 kN load cell and a displacement speed of 1.27 mm min^{-1}. Samples were used to bond grit-blasted aluminium coupons with a bond overlap of 25 × 16.5 mm^2 and a bondline thickness of 0.1 mm.

Viscosity measurements were made on a Brookfield CAP 1000+ viscometer at 750 RPM.

Matrix assisted laser desorption/ionisation – time of flight (MALDI-TOF) spectra were recorded using a Waters G2 Synapt Q-TOF mass spectrometer, equipped with a solid-state laser delivering laser pulses at 355 nm with a positive ion ToF detection performed using an accelerating voltage of 10 kV. Samples were spotted onto analytical plates through application of 1 µL of a solution containing 2,5-dihydroxybenzoic acid (DHB) (10 mg/ml in THF) as a matrix and analyte (10 mg/ml in THF) followed by solvent evaporation. The samples were measured in reflectron ion mode.

Thermogravimetric analysis was performed on a Perkin Elmer Pyris 1 instrument in a temperature range of 20-500 °C at a heating rate of 10 °C min^{-1} under a nitrogen atmosphere.

8.3 Generic experimental procedures

8.3.1 Lap shear testing – hot melt

Aluminium coupons were grit-blasted to remove the surface layer and cleaned with an acetone wipe. The networks were melted and a thin layer was spread on the end of the substrate, covering a 25 × 16.5 mm^2 area. A small amount of 0.1 mm spacer beads was sprinkled on the material to ensure constant bondline thickness across samples. The second aluminium coupon was placed over the first to give an overlap area of 25 × 16.5 mm^2 and secured with a Hoffman clamp. The lap shear joints then re-entered the oven for 20 minutes to ensure maximum wetting of the material to the second

substrate. The joints were then left to cure for 7 days in a climate-controlled room at 23 °C and 50% relative humidity. The lap shear strength was measured using an Instron tensometer with a 30 kN load cell and a displacement speed of 1.27 mm min^{-1}.

8.3.2 Lap shear testing – film

The adhesive was applied to the substrate either as a film (25 mm × 12.5 mm) or a hot melt and secured in place with bulldog clips. Glass beads were embedded in the film to ensure consistent bond line thickness. The specimens were heated in an oven at 150 °C for one hour, in order to allow the film to melt and wet onto the substrate surface. Upon removal from the oven, the specimens were cured for 8 days at 23 °C and 50% humidity.

8.3.3 Soxhlet extraction

An accurately measured mass of polyurethane film (200 mg) was placed inside a cellulose extraction thimble and inserted into a 250 mL Soxhlet extractor on top of a 500 mL round-bottom flask containing an appropriate solvent (300 mL) and a reflux condenser was attached above (**Figure 8.1**). The solvent was heated to reflux for 24 hours. Mass of the film was recorded before and after extraction.

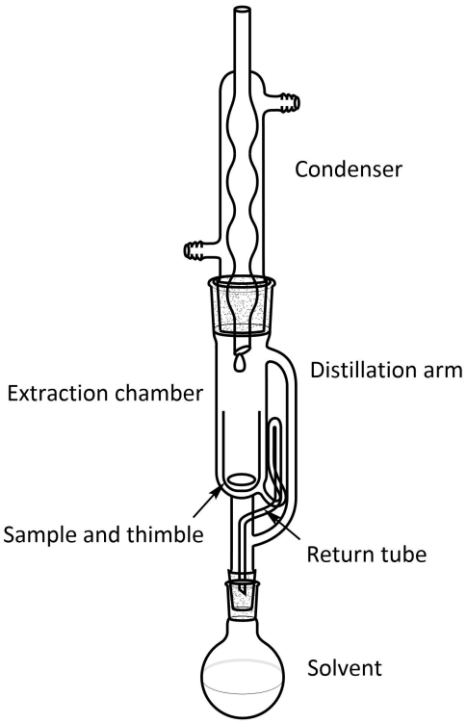

Figure 8.1 – A Soxhlet extraction setup.

The mass difference is used to calculate the gel fraction of the material, which provides insight into how successfully it has cross-linked. The gel fraction is defined as the weight ratio of dried network polymer (W_2) after extraction to that of the polymer before (W_1).

$[W_2 / W_1] \times 100\%$ = Gel fraction, % (or cross-linked material) (Equation 1)

8.4 Experimental procedures for Chapter 2 - Maleimide and furan-based networks

8.4.1 Synthesis of a network *via* copolymerization of multifunctional furan and bifunctional maleimide

The cross-linked network composition DA1 was made by combining trifurfuryl 1,3,5-benzenetricarboxylate (F1), and bismaleimidocaproyl C_{36} dimerate (M1) in an equimolar ratio of maleimide to furan functional groups. F1 (4.8 g) and M1 (15.2 g) were weighed in a glass container and heated in an oven at 120-150 °C for 30 minutes with occasional manual stirring until a

homogeneous mixture was obtained. Materials were coated directly onto silicone release paper to produce films with a thickness of 250 µm using a metal applicator and allowed to copolymerise at room temperature.

8.5 Experimental procedures for Chapter 3 - Diels-Alder cycloadducts as chain extenders in reversible polyurethane adhesives

8.5.1 Synthesis of *N*-(2-hydroxyethyl)maleimide (HEMI)

This method was modified from reported methods in literature.[1,2]

Synthesis of 3a,4,7,7a-Tetrahydro-4,7-epoxyisobenzofuran-1,3-dione (1)

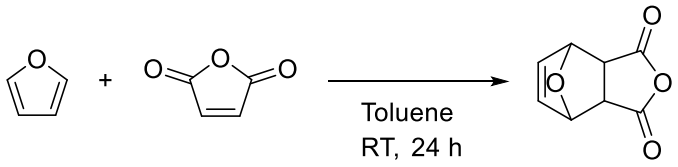

1

Scheme 8.1 – Cycloaddition of furan to maleic anhydride.

Maleic anhydride (100 g, 1.02 mol) was mixed with furan (75 mL, 1.03 mol) in toluene (250 mL) (**Scheme 8.1**). The flask was sealed and stirred at room temperature for 24 hours. The product **1** appeared as white precipitate and was washed with diethyl ether, filtered, and vacuum-dried for 24 hours at 40 °C. Yield = 61%

^{1}H NMR (400 MHz, $CDCl_3$, 298 K): δ = 6.58 (t, *J* = 1.0 Hz, 2H, C*H*=C*H*), 5.46 (t, *J* = 1.0 Hz, 2H, C-C*H*(O)-C), 3.17 (s, 2H) ppm.

Synthesis of 3a,4,7,7a-Tetrahydro-2-(2-hydroxyethyl)-4,7-epoxy-1H-isoindole-1,3(2H)-dione (2)

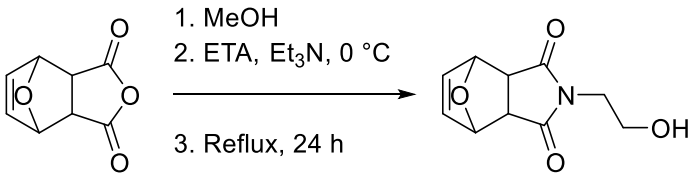

1 **2**

Scheme 8.2 – Addition of ethanolamine to maleic anhydride.

The product **1** (103.9 g, 0.625 mol) was solubilized in methanol (360 mL) and cooled to 0 °C in an ice bath (**Scheme 8.2**). Ethanolamine (42.0 mL, 0.69 mol) and triethylamine (69.6 g, 95.8 mL, 0.33 mol) were added drop-wise through a dripping funnel over 30 minutes. The solution was then refluxed for 24 hours, and an orange colour was observed. The flask was cooled to room temperature and stored in a refrigerator for crystallization for 48 hours. The recrystallized product **2** was filtered and vacuumed dried overnight at 40 °C. Yield = 61%

Synthesis of N-(2-hydroxyethyl)maleimide (HEMI)

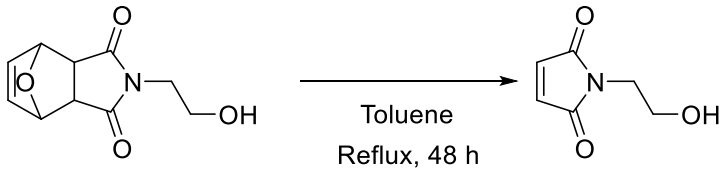

2 **HEMI**

Scheme 8.3 – Removal of furan.

A 500 mL dried round bottom flask was charged with toluene (500 mL) and **2** (79.4 g, 0.38 mol), and the reaction was heated to reflux conditions for 48 hours under atmospheric pressure (**Scheme 8.3**). The *N*-(2-hydroxyethyl)maleimide (HEMI) product was allowed to slowly cool to room temperature where it precipitated out of solution and was washed with diethyl ether. Final mass 32.7 g. Yield = 61%

^{1}H NMR (400 MHz, $CDCl_3$, 298 K): δ = 6.74 (s, 2H, CH=CH), 3.80-3.71 (m, 4H, N-C*H*$_2$-C*H*$_2$-OH), 2.05 (s, 1H, CH_2-O*H*) ppm.

^{13}C NMR (125 MHz, $CDCl_3$, 298 K): δ = 171.20 (C=O), 134.88 (C=C), 60.76 (HO-CH_2), 40.71 (N-CH_2) ppm.

ν_{max} = 3260 (OH), 1710 (C=O) cm^{-1}

8.5.2 Synthesis of 4,7-Epoxy-1*H*-isoindole-1,3(2*H*)-dione, 3a,4,7,7a-tetrahydro-2-(2-hydroxyethyl)-4-(hydroxymethyl) or bifunctional chain extender (BFCE)

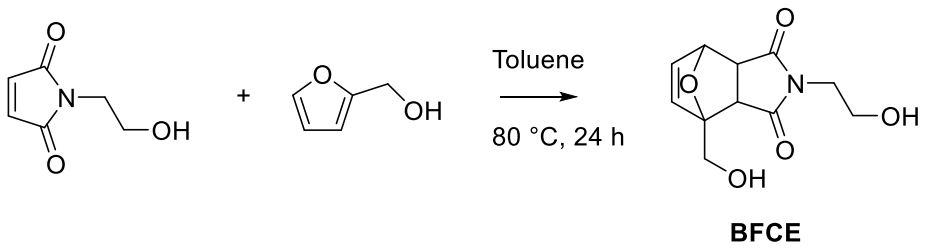

BFCE

Scheme 8.4 – Addition of furfuryl alcohol to HEMI to form the bifunctional chain extender.

This material was synthesised according to literature.[3] To an oven dried 250 mL three-neck round-bottom flask equipped with a magnetic stir bar and fitted with a reflux condenser was added HEMI (7.06 g, 0.05 mol), toluene (100 mL) and furfuryl alcohol (5.00 g, 0.051 mol) (**Scheme 8.4**). The reaction was refluxed at 80 °C for 24 h, during which the product precipitated. The resulting mixture was cooled to room temperature. Then the product was collected *via* vacuum filtration, washed with diethyl ether and was further dried under vacuum to produce a crystalline solid.

^{1}H NMR (400 MHz, d_6-DMSO, 298 K) δ = 6.52 (m, 2H, CH_2=CH_2), 5.07 (d, J = 1.6 Hz, 1H), 4.94 (t, J = 5.7 Hz, 1H, OH), 4.80 – 4.71 (m, 1H, OH), 4.03 (dd, J = 12.5, 6.0 Hz, 1H), 3.68 (dd, J = 12.5 Hz, 5.4 Hz, 1H), 3.40 (d, J = 2.6 Hz, 4H), 3.04 (d, J = 6.5 Hz, 1H), 2.87 (d, J = 6.5 Hz, 1H) ppm.

^{13}C NMR (125 MHz, d_6-DMSO, 298 K): δ = 176.40, 174.95 (C=O), 138.12, 136.46 (C=C), 91.65 (HO-CH_2-*C*), 80.18 (CH-*C*H(-O)-C), 58.94 (HO-*C*H_2-C), 57.27 (HO-*C*H_2-CH_2-N), 49.97, 47.78 (O=C-*C*H-CH), 40.55 (HO-CH_2-*C*H_2-N) ppm.

ν_{max} = 3440 (OH), 1680 (C=O) cm^{-1}

8.5.3 Synthesis of 4,7-Epoxy-1*H*-isoindole-1,3(2*H*)-dione, 3a,4,7,7a-tetrahydro-2-[2-hydroxyethyl]-4,7-bis(hydroxymethyl) or trifunctional chain extender (TFCE)

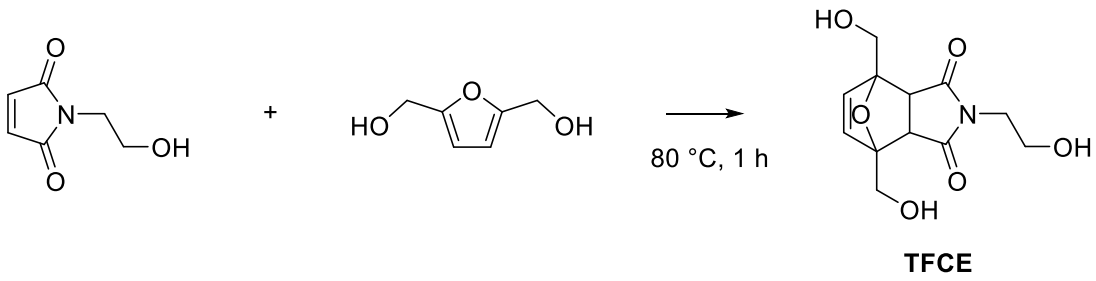

TFCE

Scheme 8.5 – Addition of furfuryl alcohol to HEMI to form the trifunctional chain extender.

HEMI and bishydroxymethylfuran (BHMF) were melt blended at 85 °C in an equimolar ratio whilst stirring (**Scheme 8.5**). After 1 hour they had become homogenous and the mixture was allowed to cool.

^{1}H NMR (400 MHz, d_6-DMSO, 298 K) δ = 6.52,* 6.28 (s, 2H, CH_2=CH_2), 5.14, 4.92* (t, J = 5.82 Hz, 2H, OH), 4.72 (m, 1H, OH), 4.05-3.65 (m, 4H, OH-CH_2-C), 3.48, 2.99* (s, 2H, CH), 3.40 (d, J = 3.11 Hz, 2H, N-CH_2), 3.32-3.22 (m, 2H, CH2-CH_2-OH) ppm.

^{13}C NMR (125 MHz, d_6-DMSO, 298 K): δ = 175.37, 174.78* (C=O), 138.07,* 135.86 (C=C), 92.14, 91.34* (HO-CH_2-*C*-), 59.76, 59.06* (HO-*C*H_2-C), 57.29 (HO-*C*H_2-CH_2-N), 50.42,* 47.22 (O=C-*C*H-CH), 40.49 (HO-*C*H_2-CH_2-N) ppm.

* = resonance from *exo* isomer

ν_{max} = 3380 (OH), 1680 (C=O) cm^{-1}

8.5.4 Synthesis of the moisture-curing prepolymer

Bulk

The moisture-curing prepolymer was synthesised through a step-growth polymerisation. The polyol (41.36 g, 20.9 mmol) was heated to 110 °C under vacuum for an hour in oven-dried glassware to

remove any residual moisture. 2 equivalents of MDI (10.46 g, 41.8 mmol) were then added to the mixture and the vacuum reapplied to yield the isocyanate-terminated prepolymer. 1.3 equivalents of the bifunctional linker (6.5 g, 27.2 mmol) was then added to end-cap the prepolymer. The reaction mixture was monitored periodically *via* IR spectroscopy and the reaction ended when the NCO resonance at 2200 cm^{-1} stopped decreasing.

Solution

Priplast™ 1838 (25.00 g, 12.6 mmol) was heated to 90 °C under vacuum to remove moisture. After one hour, the atmosphere was switched to nitrogen and anhydrous toluene (approx. 20 mL) was added. The temperature was increased to 110 °C and then MDI (6.32 g, 25.3 mmol) was added. After one hour, a further 100 mL of toluene was added and the reaction mixture was allowed to return to 110 °C. TFCE (2.27 g, 8.4 mmol) was added and the reaction was stirred overnight to fully react, which was confirmed *via* FTIR analysis of the NCO bond. The product was cooled to room temperature and then precipitated in chilled diethyl ether (1000 mL). Excess solvent was decanted off and then the product left to dry overnight in a fumehood before a complete dry in a vacuum oven.

8.6 Experimental procedures for Chapter 4 - Covalent adaptable networks using unsaturated polyesters

8.6.1 Synthesis of difuran methylene diphenyl carbamate (MDF)

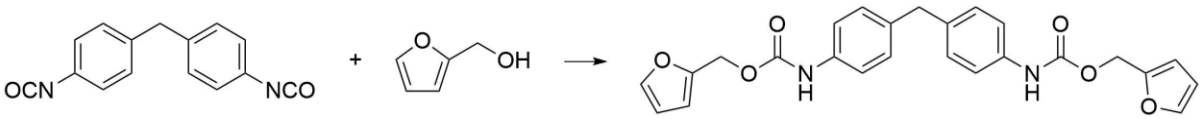

Scheme 8.6 – Addition of MDI and furfuryl alcohol to form MDF

Furfuryl alcohol (7.87 g, 0.08 mol), toluene (90 mL) and dibutyltin dilaureate (0.1 mL) was added to a round-bottom flask (**Scheme 8.6**). The solution was heated to 80 °C and methylene diphenyl diisocyanate (MDI) (10.03 g, 0.04 mol) was slowly added. Completion of the addition was confirmed

by the disappearance of the NCO resonance (λ = 2200 cm^{-1}) in the IR spectrum. The solvent was removed by rotary evaporation to produce a white solid. Yield = 99%.

^{1}H NMR (400 MHz, $CDCl_3$, 298 K): δ = 7.43 (dd, *J* = 2.0, 0.8 Hz, 2H, OC*H*=CH-CH), 7.27 (s, 4H, aromatic C*H*), 7.14-7.04 (m, 4H, aromatic C*H*) 6.59 (s, 2H, N*H*), 6.45 (dd, *J* = 3.1, 0.8 Hz, 2H, OCH=CH-C*H*), 6.37 (dd, *J* = 3.3, 1.8 Hz, 2H, OCH=C*H*-CH), 5.14 (s, 4H, COOCH_2C(O)=CH) and 3.88 (s, 2H, CH_2(C_6H_4)$_2$) ppm.

^{13}C NMR (125 MHz, $CDCl_3$, 298 K): δ = 153.18 (C=O), 149.74 (furfuryl C-O), 143.46 (furfuryl CH-O), 136.59 (Ar-N), 135.84 (*Ar*-CH_2), 129.56 (Aromatic *C*H-C-N), 119.08 (Aromatic *C*H-C-CH_2), 110.86 (CH=*C*H-CH), 110.75 (CH-*C*H=C), 58.78 (C-*C*H_2-O), 40.66 (Ar-*C*H_2-Ar) ppm.

ν_{max} = 3330 (NH), 1700 (C=O) cm^{-1}.

8.6.2 Synthesis of difuran isophorone carbamate (IPDF)

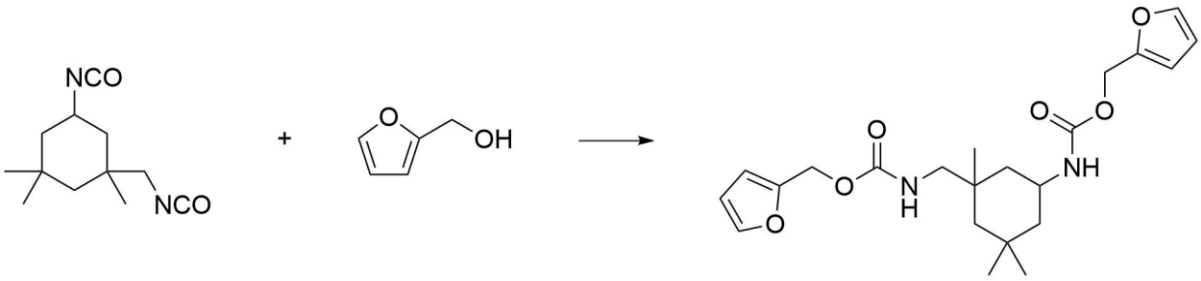

Scheme 8.7 – Addition of IPDI and furfuryl alcohol to form IPDF

Furfuryl alcohol (18.27 g, 0.19 mol) and dibutyltin dilaureate (0.1 mL) was added to a round-bottom flask and the mixture was heated to 80 °C (**Scheme 8.7**). Isophorone diisocyanate (IPDI) (20.70 g, 0.09 mol) was slowly added. Completion of the addition was confirmed by the disappearance of the NCO resonance (λ = 2200 cm^{-1}) in the IR spectrum. Yield = 99%.

^{1}H NMR (400 MHz, $CDCl_3$, 298 K): δ = 7.40 (mi, 2H, OC*H*=CH-CH), 6.39 (m, 2H, OCH=C*H*-CH), 6.34 (m, 2H, OCH=CH-C*H*), 5.03 (t, *J* = 5.2 Hz, 4H, COOCH_2C(O)=CH), 4.83 (t, *J* = 6.8 Hz, 1H, N*H*-CH_2), 4.55 (d, *J* = 5.9 Hz, 1H, N*H*), 3.8 (m, 1H, C*H*), 2.91 (d, *J* = 6.7 Hz, 2H, CH_2NH), 1.69 (t, *J* = 14.5 Hz, 2H, CH_2C(CH_3)CH_2), 1.39-1.19 (m, CH_2CHNH), 1.04-0.91 (m, 9H, CH_3) ppm.

^{13}C NMR (125 MHz, $CDCl_3$, 298 K): δ = 156.54 (C=O), 150.11 (furfuryl C-O), 143.29 (furfuryl CH-O), 110.67 (CH=*C*H-CH), 110.64 (CH-*C*H=C), 58.71 (C-*C*H_2-O), 55.04 (NH-*C*H_2-C) ppm.

ν_{max} = 3330 (NH), 2950 (alkane CH), 1690 (C=O) cm^{-1}.

8.6.3 Synthesis of trifuran hexamethylene trimer carbamate (HMTF)

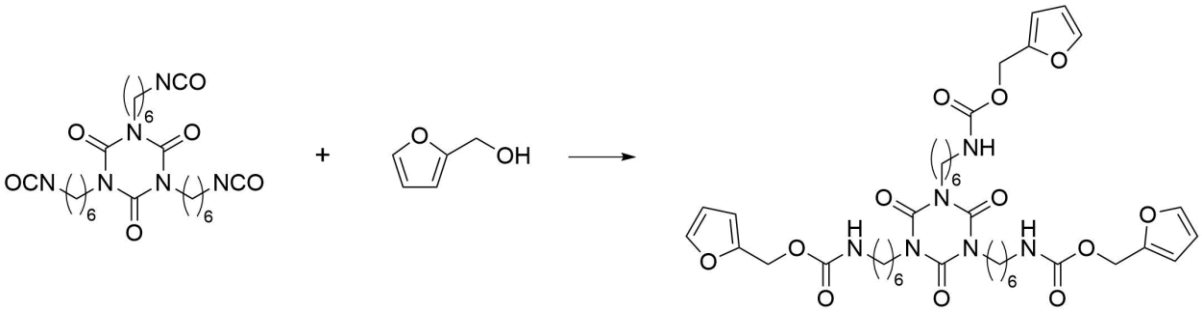

Scheme 8.8 – Addition of HDIT and furfuryl alcohol to form HMTF

In a 4-necked flask equipped with a mechanical stirrer, reflux condenser and nitrogen inlet, HDI trimer Desmodur N3300 (100 g, 518 mmol isocyanate) was mixed with toluene (60 mL) and dibutyltin dilaurate (0.1 mL) and the mixture was stirred with a mechanical stirrer and heated to 85 °C (**Scheme 8.8**). Furfuryl alcohol (50.8 g, 518 mmol) was added dropwise with mechanical stirring and heated for 3 hours. Completion of the addition was confirmed by the disappearance of the NCO resonance (λ = 2200 cm^{-1}) in the IR spectrum. Toluene was removed under vacuum using a rotary evaporation. The product was further dried in a vacuum oven overnight at 40 °C. Yield = 99%.

^{1}H NMR (400 MHz, $CDCl_3$, 298 K): δ = 7.41 (d, *J* = 2.2 Hz, 3H, OC*H*=CH-CH), 6.39 (d, *J* = 3.3 Hz, 3H, OCH=CH-C*H*), 6.34 (dd, *J* = 3.3, 1.8 Hz, 3H, OCH=C*H*-CH), 5.03 (s, 6H, COOCH_2C(O)=CH), 4.79 (s, 3H, N*H*), 3.85 (m, 6H, NC*H*), 3.17 (m, 6H, CH_2NH), 1.75-1.25 (m, 24H, CH_2) ppm.

^{13}C NMR (125 MHz, $CDCl_3$, 298 K): δ = 156.14 (O-*C*(=O)-NH), 150.27 (N-C(=O)-N), 149.11 (furfuryl C-O), 143.29 (furfuryl CH-O), 110.65 (CH=*C*H-CH), 110.39 (CH-*C*H=C), 58.51 (C-*C*H_2-O), 42.93 (NH-*C*H_2-CH_2), 41.03 (N-*C*H_2-CH_2), 29.86 (NH-CH_2-*C*H_2), 27.80 (N-CH_2-*C*H_2), 26.35 (CH_2-*C*H_2-CH_2) ppm.

ν_{max} = 3320 (NH), 2930 and 2860 (alkane CH), 1680 (C=O) cm^{-1}.

8.6.4 Synthesis of networks

The unsaturated polyester and furan-functionalised linker was heated to a fluid in a 100 °C oven. The two components were then combined in a 1:1 molar ratio with respect to furan and alkene groups. The hot melt was left in the oven for a further hour, with periodic manual stirring to ensure homogeneity. Using a casting block, the hot melt was then spread on release paper as a 100 µm thick film.

8.7 Experimental procedures for Chapter 5 - Synthesis and characterisation of unsaturated polyesters from short-chain diacids and diols

8.7.1 Drying of propylene oxide

All glassware was dried overnight at 150 °C. The apparatus was then assembled whilst hot in an order that minimised introducing argon (condenser attached to Schlenk line, then 50 mL ampoule, then stopped and finally the 50 mL round-bottom flask. Once cooled to room temperature, the argon flow was increased, and the round-bottom flask removed. Propylene oxide (35 mL) and 7 scoops of calcium hydride was added to the flask quickly before returning to the apparatus. The argon flow was reduced, and the mixture left to stir overnight. The water flow to the condenser was then turned on, the argon flow was increased, and the hotplate set to just above the boiling point of the propylene oxide (40 °C).

8.7.2 Synthesis of unsaturated polyesters *via* ring opening copolymerisation

Prior to polymerisation, maleic anhydride was recrystallised and dried over phosphorus pentoxide in a vacuum desiccator. All glassware was dried overnight at 150 °C and kept air and moisture-free throughout the polymerisation. The mass of initiator was calculated to give a degree of polymerisation (DP) of 40. $DP = \frac{[monomer]}{[initiator]}$. The volume of toluene was calculated to give a 4M solution.

Magnesium ethoxide (0.3066 g, 2.6 mmol) and maleic anhydride (10.51 g, 0.11 mol) was added to a 100 mL Schlenk flask by removing the stopper under positive pressure and pouring through a funnelled filter paper and quickly replacing the stopper. The stopper was replaced with a rubber septum and propylene oxide (7.5 mL, 0.11 mol) and toluene (36 mL) was added *via* a degassed syringe before replacing the stopper. The Schlenk was stirred was 72 hours at 100 °C. The mixture was precipitated into diethyl ether and the solvent decanted off. The product was dissolved in chloroform and reprecipitated in diethyl ether. The solvent was decanted off again and the final product dried overnight in a vacuum oven. Yield = 76%.

^{1}H NMR (400 MHz, $CDCl_3$, 298 K): δ = 6.25 (t, J = 7.6 Hz, 2H, C*H*=C*H*), 5.33-5.17 (m, 1H, O-CH_2-C*H*(-CH_3)-O)), 4.33-4.16 (m, 2H, O-C*H*$_2$-CH(-CH_3)-O), 1.32 (dd, J = 6.5, 1.4 Hz, 3H, O-CH_2-CH(-C*H*$_3$)-O) ppm.

^{13}C NMR (125 MHz, $CDCl_3$, 298 K): δ = 164.79 (C=O), 129.92 (C=C), 69.27 (CHO), 66.49 (CH_2O), 29.11 (CH_2-CH_2), 16.32 (CH_3) ppm.

ν_{max} = 1720 (C=O), 1650 (C=C) cm^{-1}

8.7.3 Synthesis of unsaturated polyesters *via* step growth

Maleic anhydride (446.2 g, 4.55 mol), propylene glycol (380.6g, 5 mol) and monobutyltin oxide (FASCAT® 4100) (0.05 g) was added to a 1 L flange flask. The flask was equipped with a mechanical stirrer, a heated glycol column, thermocouple, and nitrogen inlet. Above the column was attached a still head with thermocouple, then a water-cooled condenser. Underneath this condenser was a measuring cylinder to monitor the distillate volume. The glycol column was set to 105 °C and the water condenser to 6 °C and the nitrogen flow set to 1 L min^{-1}. The mixture was heated to 220 °C and the flask was insulated. When the volume of the distillate began to reach the calculated expected amount, small samples of the reaction mixture (≈1 g) were taken for an acid value calculation. Once the reaction had reached desired completion indicated by an acid value below 30 mg KOH/g, the mixture was transferred to a large tin. Yield = 99%.

^{1}H NMR (400 MHz, $CDCl_3$, 298 K): δ = 6.85 (2H, s, C*H*=C*H*), 5.29 (s, O-CH_2-C*H*(-CH_3)-O)), 4.29 (m, 2H, O-C*H*$_2$-CH(-CH_3)-O), 1.33 (s, 3H, O-CH_2-CH(-C*H*$_3$)-O) ppm.

^{13}C NMR (125 MHz, $CDCl_3$, 298 K): δ = 164.13 (C=O), 133.57 (C=C), 69.31 (CHO), 66.63 (CH_2O), 16.37 (CH_3) ppm.

ν_{max} = 1720 (C=O), 1650 (C=C) cm^{-1}

8.7.4 Calculation of the acid value

An accurately measured sample (≈1 g) was dissolved in 30 mL of a 2:1 ethyl acetate/ethanol solution. A few drops of phenolphthalein indicator solution was added. The solution was titrated against 0.1M potassium hydroxide solution until the pink phenolphthalein colour persisted for 5 seconds. The acid value was determined by the equation: $Acid\ value\ \left(\frac{mg}{g}\right) = \frac{Titre \times KOH\ factor}{Sample\ mass}$.

8.8 Experimental procedures for Chapter 6 - Thiol-ene addition to unsaturated polyesters to form covalent adaptable networks

8.8.1 Thiol-ene addition

The masses of each reactant was calculated prior to beginning the experiment (**Table 8.1**). The mass of furfuryl mercaptan was calculated to give a specific percentage of addition to the unsaturation on the poly(propylene fumarate) (PPF), therefore, the equivalent weight* of the polyester is used instead of molecular weight. 10 mol % (w.r.t. to alkene) of 1,5,7-triazabicyclo[4.4.0]dec-5-ene (TBD) was used. The volume of chloroform was calculated to give a final concentration of 2.65 mol dm^{-3}.

*The equivalent weight of a reactive polymer is the mass of polymer that has one equivalent of reactivity.

Table 8.1 – Example masses of reactants for typical thiol-ene additions

PPF		**Furfuryl mercaptan**				**TBD**		**$CHCl_3$**
Mass (g)	Moles	Fraction	Moles	Mass (g)	Volume (mL)	Moles	Mass (g)	Volume (mL)
3	0.018	1.00	0.018	2.09	1.85	0.0018	0.255	9.40
3	0.018	0.83	0.015	1.73	1.53	0.0015	0.211	8.47
3	0.018	0.67	0.012	1.40	1.24	0.0012	0.171	7.59
3	0.018	0.50	0.009	1.04	0.92	0.0009	0.127	6.66
3	0.018	0.33	0.006	0.69	0.61	0.0006	0.084	5.72
3	0.018	0.17	0.003	0.36	0.31	0.0003	0.043	4.84

PPF (≈3 g) was added to a round-bottom flask and dissolved in chloroform. The calculated amount of furfuryl mercaptan was then added to the solution with a syringe. The solution was stirred and warmed on a hotplate to 30 °C. TBD was added slowly to control the exotherm. Once all of the TBD was added, a timer was started. After 10 minutes, the mixture was then precipitated in 300 mL of chilled methanol. The mixture was centrifuged at 4000 RPM for 5 minutes and excess solvent decanted off. The product was left to dry overnight at the back of a fume hood before a complete dry in an oven at 100 °C.

^{1}H NMR (400 MHz, $CDCl_3$, 298 K): δ = 7.36 (s, 1H, O-C*H*=CH), 6.85 (s, 2H, -C*H*=CH), 6.30 (s, 1H, C=C*H*-CH), 6.25 (s, 1H, CH=C*H*-CH), 5.29 (m, 2H, CH_3-C*H*), 4.37-4.15 (m, 4H, O-CH_2), 3.94 (m, 2H, S-CH_2), 3.65 (s, 1H, S-CH), 2.95 (s, 2H, S-CH-CH_2), 1.34 (m, 6H, CH_3) ppm.

^{13}C NMR (125 MHz, d_6-DMSO, 298 K): δ = 171.33 (C=O), 150.35 (O-*C*-CH_2-S), 142.68, 110.73 (O-CH=*C*H-CH), 108.65 (O-C=*C*H_2), 68.96 (CHO), 66.61 (CH_2O), 41.08 (S-CH), 21.06 (S-*C*H_2-C), 16.39 (CH_3) ppm.

ν_{max} = 1720 (C=O), 1650 (C=C) cm^{-1}

8.9 Bibliography

1 Y. Jiang, S. Wong, F. Chen, T. Chang, H. Lu and M. H. Stenzel, *Bioconjug Chem*, 2017, **28**, 979–985.

2 D. Pratchayanan, J.-C. Yang, C. L. Lewis, N. Thoppey and M. Anthamatten, *J Rheol (N Y N Y)*, 2017, **61**, 1359–1367.

3 X. Ke, H. Liang, L. Xiong, S. Huang and M. Zhu, *Prog Org Coat*, 2016, **100**, 63–69.